Title
Fast Solvers for Numerical Schemes Based On Finite Element Exterior Calculus

Author
Zhong, Lin

Publication Date
2015

UNIVERSITY OF CALIFORNIA,
IRVINE

Fast Solvers for Numerical Schemes Based On Finite Element Exterior Calculus

DISSERTATION

submitted in partial satisfaction of the requirements
for the degree of

DOCTOR OF PHILOSOPHY

in Mathematics

by

Lin Zhong

Dissertation Committee:
Long Chen, Chair
Qing Nie
Hongkai Zhao

2015

DEDICATION

To my parents

TABLE OF CONTENTS

LIST OF FIGURES

Page

LIST OF TABLES

ACKNOWLEDGMENTS

I would like to express my sincere gratitude to my advisor Prof. Long Chen for his continuous support of my Ph.D study and research. His motivation, enthusiasm, guidance, knowledge, and patience make this thesis a reality. It was a pleasure working with him for the past years.

I express my appreciation to Prof. Qing Nie, Prof. Hongkai Zhao, Prof. Zhiqin Lu and Prof. Yun Wang for being my committee members and sharing their insights. I am grateful to my collaborators Dr. Bin Zheng, Dr. Yongke Wu, Dr. Jie Zhou and Dr. Ming Wang for all enlightening discussions and the efforts made to finish our projects together. I would also like to thank my friends at Mathematics department, especially Dr. Deliang Yin, for their help during my graduate life.

Finally, I would like to thank my husband Zhimin Xiang, my parents and son for their unconditional love and support, which make my graduate life a wonderful journey.

CURRICULUM VITAE

Lin Zhong

EDUCATION

Doctor of Philosophy in Mathematics **2015**
University of California, Irvine *Irvine, CA*

Bachelor of Mathematics **2010**
University of Science and Technology of China *Hefei, China*

ABSTRACT OF THE DISSERTATION

Fast Solvers for Numerical Schemes Based On Finite Element Exterior Calculus

By

Lin Zhong

Doctor of Philosophy in Mathematics

University of California, Irvine, 2015

Long Chen, Chair

Finite element exterior calculus (FEEC) is a framework to design and understand finite element discretizations for a wide variety of systems of partial differential equations. The applications are already made to the Hodge Laplacian, Maxwell's equations, the equations of elasticity, elliptic eigenvalue problems [2][3][4][5][6] and etc.. In this thesis, we propose fast solvers for several numerical schemes based on the discretization of this approach and present theoretical analysis. Specifically, in the first part, we propose efficient block diagonal and block triangular preconditioners for solving the discretized linear system of the vector Laplacian by mixed finite element methods. A variable V-cycle multigrid method with the standard point-wise Gauss-Seidel smoother is proved to be a good preconditioner for the Schur complement. The major benefit of our approach is that the point-wise Gauss-Seidel smoother is more algebraic and can be easily implemented as a 'black-box' smoother. The multigrid solver for the Schur complement will be further used to build preconditioners for the original saddle point systems. In the second part, we propose a discretization method for the Darcy-Stokes equations under the framework of FEEC. The discretization is shown to be uniform with respect to the perturbation parameter. A preconditioner for the discrete system is also proposed and shown to be efficient. In the last part, we focus on the stochastic Stokes equations. The stochastic saddle-point linear systems are obtained by using finite element discretization under the framework of FEEC in physical space and generalized polynomial chaos expansion in random space. We prove the existence and uniqueness of the solutions to the continuous problem and its corresponding stochastic Galerkin discretization. Optimal error estimates are also derived. We construct block-diagonal/triangular preconditioners for use with the generalized minimum residual method and the bi-conjugate gradient stabilized method. An optimal multigrid solver is applied to efficiently solve the diagonal blocks that correspond to deterministic discrete Stokes systems. To demonstrate the efficiency and robustness of the discretization methods and proposed preconditioners, various numerical examples also are provided.

Introduction

Partial differential equations (PDEs), which can be used to describe a wide variety of phenomena such as fluid flow, electrostatics, elasticity or quantum mechanics, are applied in countless ways to solve real world problems. While most PDEs cannot be explicitly solved, numerical algorithms play as an essential tool to PDE models. The finite element method (FEM), which began over half century ago, is proven to be a most important technology in numerically solving PDEs. Finite element exterior calculus (FEEC), which is developed by Arnold, Falk, Winther in 2006 [2], is a framework to design and understand finite element discretizations for a wide variety of systems of PDEs.

This dissertation is on proposing fast solvers for the discrete numerical schemes based on FEEC, and theoretically analyzing the efficiency and robustness of the discretization methods and proposed solvers. Specifically, we study in deepth the numerical schemes for three different PDEs, i.e., the vector Laplacian equations, the Darcy-Stokes equations, the Stokes equations with random viscosity.

0.1 Multigrid Preconditioners for Mixed Finite Element Methods of Vector Laplacian

Discretization of the vector Laplacian in spaces $\boldsymbol{H}_0(\mathrm{curl})$ and $\boldsymbol{H}_0(\mathrm{div})$ by mixed finite element methods is well-studied in [2]. The discretized linear algebraic system is ill-conditioned and in the saddle point form which leads to the slow convergence of classical iterative methods as the size of the system becomes large. In [2], a block diagonal preconditioner has been developed and shown to be an effective preconditioner. The purpose of this paper is to present alternative and effective block diagonal and triangular preconditioner for solving these saddle point systems.

Due to the similarity of the problems arising from spaces $\boldsymbol{H}_0(\mathrm{curl})$ and $\boldsymbol{H}_0(\mathrm{div})$, we use the mixed formulation of vector Laplacian in $\boldsymbol{H}_0(\mathrm{curl})$ as an example to illustrate our approach. Choosing appropriate finite element spaces $S_h \subset H_0^1$ (vertex element) and $\boldsymbol{U}_h \subset \boldsymbol{H}_0(\mathrm{curl})$ (edge element), the mixed formulation is: Find $\sigma_h \in S_h, \boldsymbol{u}_h \in \boldsymbol{U}_h$ such that

$$\begin{cases} -(\sigma_h, \tau_h) + (\boldsymbol{u}_h, \mathrm{grad}\,\tau_h) = 0 & \text{for all } \tau_h \in S_h, \\ (\mathrm{grad}\,\sigma_h, \boldsymbol{v}_h) + (\mathrm{curl}\,\boldsymbol{u}_h, \mathrm{curl}\,\boldsymbol{v}_h) = (\boldsymbol{f}, \boldsymbol{v}_h) & \text{for all } \boldsymbol{v}_h \in \boldsymbol{U}_h. \end{cases}$$

The corresponding matrix formulation is

$$\begin{pmatrix} -M_v & B \\ B^T & C^T M_f C \end{pmatrix} \begin{pmatrix} \sigma_h \\ \boldsymbol{u}_h \end{pmatrix} = \begin{pmatrix} 0 \\ \boldsymbol{f} \end{pmatrix}. \tag{0.1.1}$$

Here M_v and M_f are mass matrices of the vertex element and the face element, respectively, B^T corresponds to the grad operator, and C corresponds to the curl operator.

Based on the stability of (0.1.1) in $H_0^1 \times \boldsymbol{H}_0(\mathrm{curl})$ norm, in [2], a block diagonal preconditioner in the form

$$\begin{pmatrix} (I + BM_e^{-1}B^T)^{-1} & O \\ O & (I + C^T M_f C)^{-1} \end{pmatrix}$$

is proposed and the preconditioned Krylov space method is shown to converge with optimal complexity. To compute the inverse operators in the diagonal, multigrid methods based on additive or multiplicative overlapping Schwarz smoothers (each smoothing need to invert a small system of degree of freedoms surrounding a vertex) [3], multigrid methods based on Hiptimair smoothers [20, 21], or auxiliary space preconditioner [23] can be used. In all these methods, to achieve a mesh independent condition number, a special smoother taking care of the large kernel of the curl or div differential operators is needed.

In contrast, we shall use multigrid methods with standard point-wise Gauss-Seidel (G-S) smoother to the Schur complement of (0.1.1)

$$A = B^T M_v^{-1} B + C^T M_f C \tag{0.1.2}$$

which is a matrix representation of the identity of the vector Laplacian

$$-\Delta \boldsymbol{u} = -\operatorname{grad}\operatorname{div}\boldsymbol{u} + \operatorname{curl}\operatorname{curl}\boldsymbol{u}.$$

In (0.1.2), the inverse of the mass matrix, i.e., M_v^{-1} is dense. To be practical, the exact Schur complement can be replaced by an approximation

$$\tilde{A} = B^T \tilde{M}_v^{-1} B + C^T M_f C,$$

with $\tilde{M}_v$ an easy-to-invert matrix, e.g., diagonal or mass lumping of M_v.

A variable V-cycle multigrid method with the standard point-wise Gauss-Seidel smoother is proved to be a good preconditioner for the Schur complement A or its approximation $\tilde{A}$. The major benefit of our approach is that the point-wise Gauss-Seidel smoother is more algebraic and can be easily implemented as a 'black-box' smoother. The block smoothers proposed in [3] for the $\boldsymbol{H}(\mathrm{curl})$ and $\boldsymbol{H}(\mathrm{div})$ problems, however, requires more geometric information and solving local problems in small patches.

Although the finite element spaces are nested and A (or $\tilde{A}$) is symmetric positive definite, due to the inverse of the mass matrix, the bilinear forms in the coarse grid is non-inherited from the fine one. To overcome this difficulty, we shall follow the multigrid framework developed by Bramble, Pasciak, and Xu [8]. In this framework, we only need to verify two conditions: (1) Regularity and approximation assumption; (2) Smoothing property. Since A is SPD, the smoothing property of the Gauss-Seidel smoother is well known, see e.g. [9]. To prove the approximation property, we make use of error estimates of mixed methods established in [3] and thus have to assume the full regularity of elliptic equations. Numerically our method works well for the case when the full regularity does not hold. With the approximation and smoothing properties, we show that one V-cycle is an effective preconditioner. As noticed in [9], W-cycle or two V-cycles may not be a valid preconditioner as the corresponding operator may not be positive definite. In other words, the proposed multigrid method for the Schur complement cannot be used as an iterative method but one V-cycle can be used as an effective preconditioner.

The multigrid preconditioner for $\tilde{A}$ will be used to build preconditioners for (0.1.1). We prove that the preconditioned system with the block diagonal preconditioner

$$\begin{pmatrix} M_v^{-1} & O \\ O & \tilde{A}^{-1} \end{pmatrix} \tag{0.1.3}$$

has a uniformly bounded conditional number. Following the framework of [24], we verify this by establishing a new stability result of the saddle system (0.1.1) in the $\|\cdot\| \times \|\cdot\|_A$ norm. The action M_v^{-1} can be further approximated by just one symmetric Gauss-Seidel iteration or by $\tilde{M}_v^{-1}$ and $\tilde{A}^{-1}$ by one V-cycle.

0.2 Robust Error Estimate and Uniform Preconditioners of TMAC Discretization of Darcy-Stokes Equations

[66]We consider the following singular perturbation problem

$$\begin{cases} (I - \epsilon^2 \Delta)\boldsymbol{u} + \operatorname{grad} p = & \boldsymbol{f} \quad \text{in } \Omega, \\ -\operatorname{div} \boldsymbol{u} = & 0 \quad \text{in } \Omega, \\ \boldsymbol{u} = & 0 \quad \text{on } \partial\Omega, \end{cases} \tag{0.2.1}$$

where $\epsilon \in (0, 1]$ is a parameter and Δ is the Laplacian operator applied to vector functions. The system (0.2.1) is a steady state generalized Stokes equation when the perturbation parameter is large, and it degenerates to the mixed formulation of the Darcy equation when the parameter goes to zero. It can also be derived from time discretization of the transient Stokes equations, where the parameter corresponds to the square roof of the time step.

We shall consider numerical methods which are robust to the parameter ϵ. It is numerically verified that most of the proposed finite element methods for Stokes problem or the Darcy problem are not well behaved uniformly in the perturbation parameter [78]. Design a finite element method robust to both Darcy and Stokes equations is an active research topic and successful examples can be found in [78, 84, 76].

Another related topic is a fast solver robust to the paraemeter ϵ. For the generalized Stokes equations discretized from time discretization of transient Stokes equations, a robust multigrid method using distributive or Uzawa smoothers has been developed and analyzed in [83]. Block-diagonal preconditioners with uniformly bounded conditioners are considered in [79, 82].

We shall apply the triangular MAC (TMAC) developed in [66] for Stokes equations to Darcy-Stokes equations. We show TMAC has both merits: uniformly convergent rates and a uniform preconditioner can be easily construct.

The idea of TMAC scheme is to use H(div) elements for the velocity and discontinuous polynomial for pressure. It retains all the desirable properties of the MAC scheme: exact divergence-free, solver-friendly, and local conservation of physical quantities. For Darcy-Stokes system, the most relevant work is [76]. The difference of our approach and that in [76] is the discretization of vector Laplacian operator. In [76], DG formulation is used while in [66], a weak rot_h differential operator is introduced. It can be shown that in the simplest form (uniform rectangular grids), both are equivalent to the classical MAC scheme.

The lowest order element is the RT_0-P_0 element. Use the superconvergence results of the Lagrange interpolation of the linear element in [7], we can obtain a uniform error estimate

$$\|\boldsymbol{u}_h - \boldsymbol{u}_I\|_A + \|p_h - p_I\| \lesssim h^{\min(1,\sigma)} |\log h|^{1/2} \left(\|\boldsymbol{u}\|_{2,\infty} + \|\operatorname{rot} \boldsymbol{u}\|_2 \right). \tag{0.2.2}$$

where $\boldsymbol{u}_I$ is the canonical interpolation of $\boldsymbol{u}$ on to the space RT_0, p_I is the L^2-projection of p to the piecewise constant space, $\boldsymbol{u}_h$ and p_h are the RT_0-P_0 approximation of (0.2.1), and $\|\cdot\|_{A^\epsilon}$ is the energy norm defined by the SPD operator $I - \epsilon^2\Delta$. The convergence rate depends crucially on the symmetry of the mesh through the parameter σ (see Section 3 for a detailed definition). Roughly speaking to obtain a first order scheme, two triangles sharing an edge should form a parallelogram. For a class of grids violating this symmetry requirement, non-convergence is observed for Stokes equations [66].

To relax the constraint of the mesh condition, we enrich the velocity space to BDM_1 plus a bubble function and obtain another velocity-pressure discretization $\mathrm{BDM}_1^{\mathrm{b}}$-$\mathrm{P}_0$. The bubble function is introduced such that a mass lumping can be applied to quadratic Lagrange elements. Now the convergence rate is independent of the mesh symmetry and for a general quasi-uniform mesh:

$$\|\boldsymbol{u}_h - \boldsymbol{u}_I\|_A + \|p_h - p_I\| \lesssim h \left(\|\boldsymbol{u}\|_2 + \|\operatorname{rot} \boldsymbol{u}\|_2 \right).$$

For general quasi-uniform grids, the $\mathrm{BDM}_1^{\mathrm{b}}$-$\mathrm{P}_0$ scheme will produce an optimal first-order approximation for $\boldsymbol{u}$ and p. It is both robust and more accurate than the RT_0-P_0 element.

We then consider a uniform preconditioner for TMAC discretization of Darcy-Stokes equations.

Let us write the operator for the Darcy-Stokes equations as

$$\mathcal{A}^\epsilon = \begin{pmatrix} I - \epsilon^2 \Delta & \mathrm{grad} \\ -\operatorname{div} & 0 \end{pmatrix}.$$

Let Δ_p be the Laplacian operator with Neumann boundary condition defined on L_0^2. Mardal and Winther [79] show that the block-diagonal preconditioner

$$\mathcal{B}^\epsilon = \begin{pmatrix} (I - \epsilon^2 \Delta)^{-1} & 0 \\ 0 & (-\triangle_p)^{-1} + \epsilon^2 I \end{pmatrix} \tag{0.2.3}$$

is a uniformly effective preconditioner of $\mathcal{A}^\epsilon$, i.e., $\kappa(\mathcal{B}^\epsilon \mathcal{A}^\epsilon) \leq C$ with a constant independent of ϵ. When move to the discrete level, $\kappa(\mathcal{B}_h^\epsilon \mathcal{A}_h^\epsilon) \leq C$ with a constant independent of both h and ϵ will be hold if a uniformly stable Fortin operator can be constructed [81]. In practice, a V-cycle multigrid for the vector Laplacian developed in [15] can be used to approximate the $(1,1)$ block and an auxiliary space preconditioner [8] can be used to approximate $(-\triangle_p)^{-1}$ in the $(2,2)$ block.

0.3 Block Triangular Preconditioner for Stochastic Stokes Equations

In the past decade, there has been growing interest in the study of numerical methods for solving stochastic partial differential equations (SPDEs). SPDEs are partial differential equations with random input data (e.g., coefficient, boundary conditions, initial conditions, source terms, computational domain, etc.) and have been widely used to model uncertainty propagation and quantification in complex physical and engineering applications, including flows in random porous media [31, 32, 33], thermo-fluid processes [34, 35], flow-structure interactions [36], etc.

Usually, numerical methods for solving SPDEs are characterized as either non-intrusive type (e.g., Monte Carlo method [37] or stochastic collocation method [38, 39, 40]) or intrusive type (e.g., stochastic Galerkin method based on the generalized polynomial chaos (gPC) expansion

[41, 42, 43, 44]). In [45, 46], the authors show that the stochastic Galerkin method is computationally more efficient than the stochastic collocation method. However, this conclusion relies on the assumption that specialized iterative solvers are available for solving the fully coupled linear systems arising from the stochastic Galerkin discretization. Many studies have centered on iterative solvers for the stochastic Galerkin discretization of elliptic equations with random input data [47, 48, 49, 50, 51, 52]. For example, in [48], an efficient multigrid solver is proposed. In [53], they suggested a preconditioned conjugate gradient (PCG) method with a block-diagonal preconditioner. When the random input variance is large, [54] demonstrates that a block triangular preconditioner used with either generalized minimum residual (GMRes) method or generalized preconditioned conjugate gradient (GPCG) method is more efficient and robust than PCG with a block-diagonal preconditioner.

In the literature, there are several studies on stochastic Galerkin methods for Stokes equations and Navier-Stokes equations with random input data [55, 56, 34, 35, 57, 58, 59, 60, 61]. Conversely, little work has been done involving efficient iterative solvers for the resulting saddle-point linear systems with tensor product structure [62, 61]. Efficient block triangular preconditioners for discrete stochastic Navier-Stokes systems are developed in [62]. In [63, 64, 65], the minimum residual (MINRES) method preconditioned by block-diagonal preconditioners are investigated for solving the saddle-point systems resulting from the stochastic Galerkin mixed formulation of elliptic problems with random diffusion coefficients.

In this work, we focus on the design of iterative solvers for saddle-point systems resulting from the stochastic Galerkin discretizations of Stokes equations with random viscosity. In particular, we use the H(div) conforming finite element discretization in physical space, which is a generalization of the Marker and Cell (MAC) scheme to triangular meshes (TMAC) [66]. The TMAC scheme retains all of the MAC scheme's desirable properties: pointwise divergence free, solver friendly, and local conservation of physical quantities. In probability space, we use gPC expansion [67]. The resulting block-structured linear systems can be reformulated so each diagonal block corresponds to a deterministic discrete Stokes system. Hence, we can take advantage of the optimal multigrid solver developed in [68] for these deterministic systems and construct block-diagonal/triangular preconditioners for use with the GMRes and bi-conjugate gradient stabilized (BiCGStab) methods to solve the discrete stochastic Stokes systems. The efficiency and robustness of the proposed preconditioners with respect to all the dicretization parameters are tested on Stokes equations with random viscosity satisfying uniform or lognormal distribution. We also develop multigrid methods with block Jacobi or block Gauss-Seidel methods as the smoother for solving the discrete stochastic Stokes systems.

Chapter 1

Finite Elements, Exterior Calculus, and Stochastic Finite Elements

In this chapter, we first recall the function spaces and finite element spaces which we are going to work on, and then present preliminaries about finite element exterior calculus and general polynomial chaos.

We assume that Ω is a bounded and convex polyhedron in $\mathbb{R}^2$ or $\mathbb{R}^3$ with a simple topology (homomorphism to a disk or ball), and it is triangulated into a mesh $\mathcal{T}_h$ with size h. We assume that the mesh belongs to a shape regular and quasi-uniform family.

1.1 Function Spaces

Let us introduce notations of the differential operators we are going to work on. In $\mathbb{R}^2$, we will use the curl operator acting on the scalar function and rot, div operators acting on vector function respectively. For any scalar function τ, and vector function $\boldsymbol{u} = [u, v]^t$, we have:

- $\operatorname{curl} \tau = \Big(\partial_y \tau, -\partial_x \tau\Big)$

- $\operatorname{rot} \boldsymbol{u} = \partial_x v - \partial_y u$

- $\operatorname{div} \boldsymbol{u} = \partial_x u + \partial_y v$

In $\mathbb{R}^3$, we will use the grad operator acting on the scalar function and curl, div operators acting on vector function respectively. For any scalar function τ, and vector function $\boldsymbol{u} = [u, v, w]^t$, we have:

- $\operatorname{grad} \tau = \Big(\partial_x \tau, \partial_y \tau, \partial_z \tau\Big)$
- $\operatorname{curl} \boldsymbol{u} = \Big(\partial_y w - \partial_z v, \partial_z u - \partial_x w, \partial_x v - \partial_y u\Big)$
- $\operatorname{div} \boldsymbol{u} = \partial_x u + \partial_y v + \partial_z w$

We use $L^2(\Omega)$ to denote the space of all square integrable scalar or vector functions on Ω. Given a differential operator $d = \operatorname{grad}, \operatorname{curl}, \operatorname{rot}$ or div, we introduce the Sobolev space $H(d, \Omega) = \{v \in L^2(\Omega), dv \in L^2(\Omega)\}$. For $d = \operatorname{grad}$, $H(\operatorname{grad}, \Omega)$ is the standard $H^1(\Omega)$ space. For simplicity, we will suppress the domain Ω in the notation. We further introduce the following Sobolev spaces on domain Ω with homogenous traces:

- $H_0^1 = \{\boldsymbol{u} \in H^1(\Omega) : \boldsymbol{u} = 0 \text{ on } \partial\Omega\}$

- $H_0(\operatorname{curl}) = \{\boldsymbol{u} \in H(\operatorname{curl}) : \boldsymbol{u} \times \boldsymbol{n} = 0 \text{ on } \partial\Omega\}$

- $H_0(\operatorname{div}) = \{\boldsymbol{u} \in H(\operatorname{div}) : \boldsymbol{u} \cdot \boldsymbol{n} = 0 \text{ on } \partial\Omega\}$

- $L_0^2 = \{u \in L^2(\Omega) : \int_\Omega u \, dx = 0\}$

In $\mathbb{R}^2$, as curl is a rotation of grad, $H(\operatorname{curl}) \cong H^1$ and $H_0(\operatorname{curl}) \cong H_0^1$. The inner product for L^2 or $\boldsymbol{L}^2$ is denoted by $(\cdot, \cdot)$.

1.2 Finite Elements

To discretize partial differential equations, it is critical to choose appropriate discrete subspaces of function spaces. Let us recall the following finite element spaces in $\mathbb{R}^3$:

- $S_0^h \subset H_0^1$ is the well-known Lagrange elements, i.e., continuous and piecewise polynomials,
- $\boldsymbol{U}_0^h \subset \boldsymbol{H}_0(\mathrm{curl})$ is the edge element space [26, 27],
- $\boldsymbol{V}_0^h \subset \boldsymbol{H}_0(\mathrm{div})$ is the face element space [28, 26, 11, 27, 10, 12],
- $W_0^h \subset L_0^2$ is discontinuous and piecewise polynomial space.

We will use the notations without subscript to denote the discrete subspaces without homogenous traces, i.e., $S^h \subset H^1$, $\boldsymbol{U}^h \subset \boldsymbol{H}(\mathrm{curl})$, $\boldsymbol{V}^h \subset \boldsymbol{H}(\mathrm{div})$ and $W^h \subset L^2$.

In $\mathbb{R}^2$, the elements are similar, and we keep the notation as $S_0^h \subset H_0(\mathrm{curl})$ for Lagrange element, $\boldsymbol{V}_0^h \subset \boldsymbol{H}_0(\mathrm{div})$ for edge element and $W_0^h \subset L_0^2$ for discontinuous piecewise polynomial space. We will discuss more about how to choose proper finite elements in each Sobolev spaces in the next section.

1.3 Finite Elements Exterior Calculus

1.3.1 The de Rham Complex

To discretize the partial differential equations, we start from the following de Rham complex and corresponding co-chain exact sequence:

- $\mathbb{R}^2$: $0 \longrightarrow H^1 \xrightarrow{\mathrm{curl}} \boldsymbol{H}(\mathrm{div}) \xrightarrow{\mathrm{div}} L^2 \longrightarrow 0$

  $0 \longleftarrow L_0^2 \xleftarrow{\mathrm{rot}} \boldsymbol{H}_0(\mathrm{rot}) \xleftarrow{\text{-grad}} H_0^1 \longleftarrow 0$

- $\mathbb{R}^3$: $0 \longrightarrow H^1 \xrightarrow{\text{grad}} \boldsymbol{H}(\text{curl}) \xrightarrow{\text{curl}} \boldsymbol{H}(\text{div}) \xrightarrow{\text{div}} L^2 \longrightarrow 0$

  $0 \longleftarrow L^2_0 \xleftarrow{\text{-div}} \boldsymbol{H}_0(\text{div}) \xleftarrow{\text{curl}} \boldsymbol{H}_0(\text{curl}) \xleftarrow{\text{-grad}} H^1_0 \longleftarrow 0$

We choose appropriate degrees and types of finite element spaces such that the discrete de Rham complex holds

- $\mathbb{R}^2$: $0 \longrightarrow S^h \xrightarrow{\text{curl}} \boldsymbol{V}^h \xrightarrow{\text{div}} W^h \longrightarrow 0$

- $\mathbb{R}^3$: $0 \longrightarrow S^h \xrightarrow{\text{grad}} \boldsymbol{U}^h \xrightarrow{\text{curl}} \boldsymbol{V}^h \xrightarrow{\text{div}} W^h \longrightarrow 0$

In $\mathbb{R}^2$, given an integer $r \geq 1$, a stable method is achieved by choosing S^h_0 as the Lagrange element of order r, $\boldsymbol{V}^h_0$ as the Raviart-Thomas element $\mathrm{RT_{r-1}}$, and W^h_0 as the discontinuous piecewise polynomial function space of order $r-1$. The case $r=1$ corresponds to the lowest-order elements discretization, i.e., $\mathrm{P_1}$-$\mathrm{RT_0}$-$\mathrm{P_0}$, see Fig. 1.1. Another method relies on choosing S^h_0 as the Lagrange elements of order $r+1$, $\boldsymbol{V}^h_0$ as the Brezzi-Douglas-Marini elements $\mathrm{BDM_r}$, and W^h_0 as the discontinuous piecewise polynomial function space of order $r-1$. The case $r=1$ corresponds to the lowest-order element in this sequence, i.e., $\mathrm{P_2}$-$\mathrm{BDM_1}$-$\mathrm{P_0}$, see Fig. 1.2. In $\mathbb{R}^3$, given an integer $r \geq 1$, a stable method is achieved by choosing S^h_0 as the Lagrange element of order r, $\boldsymbol{U}^h_0$ is the Nedelec edge element $\mathrm{ND_r}$, $\boldsymbol{V}^h_0$ as the Raviart-Thomas element $\mathrm{RT_{r-1}}$, and W^h_0 as the discontinuous piecewise polynomial function space of order $r-1$. The case $r=1$ corresponds to the lowest-order elements discretization, i.e., $\mathrm{P_1}$-$\mathrm{ND_1}$-$\mathrm{RT_0}$-$\mathrm{P_0}$. The methods can be written as sequences:

- $\mathbb{R}^2$: $0 \longrightarrow \mathrm{P_r} \xrightarrow{\text{curl}} \mathrm{RT_{r-1}} \xrightarrow{\text{div}} \mathrm{P_{r-1}} \longrightarrow 0$

- $\mathbb{R}^2$: $0 \longrightarrow \mathrm{P_r} \xrightarrow{\text{curl}} \mathrm{BDM_r} \xrightarrow{\text{div}} \mathrm{P_{r-1}} \longrightarrow 0$

- $\mathbb{R}^3$: $0 \longrightarrow \mathrm{P_r} \xrightarrow{\text{grad}} \mathrm{ND_r} \xrightarrow{\text{curl}} \mathrm{RT_{r-1}} \xrightarrow{\text{div}} \mathrm{P_{r-1}} \longrightarrow 0$

1.3.2 The Co-differential Operators

We now define co-differential operators and introduce the following exact sequences in the reversed ordering:

- $\mathbb{R}^2$: $0 \longleftarrow S^h \xleftarrow{\operatorname{rot}_h} \boldsymbol{V}^h \xleftarrow{\operatorname{grad}_h} W^h \longleftarrow 0$

- $\mathbb{R}^3$: $0 \longleftarrow S^h \xleftarrow{\operatorname{div}_h} \boldsymbol{U}^h \xleftarrow{\operatorname{curl}_h} \boldsymbol{V}^h \xleftarrow{\operatorname{grad}_h} W^h \longleftarrow 0$

In $\mathbb{R}^2$, the weak divergence $\operatorname{rot}_h : \boldsymbol{V}^h \to S^h$ is defined as the adjoint of curl operator in the L^2-inner product, i.e., $\operatorname{rot}_h \boldsymbol{w}_h \in S^h$, s.t.,

$$(\operatorname{rot}_h \boldsymbol{w}_h, v_h) := (\boldsymbol{w}_h, \operatorname{curl} v_h) \quad \text{for all } v_h \in S^h. \tag{1.3.1}$$

The weak grad_h operator is defined as the adjoint of $-\operatorname{div}$, i.e., $\operatorname{grad}_h w_h \in \boldsymbol{V}^h$, s.t.,

$$(\operatorname{grad}_h w_h, \boldsymbol{v}_h) := -(w_h, \operatorname{div} \boldsymbol{v}_h) \quad \text{for all } \boldsymbol{v}_h \in \boldsymbol{V}^h. \tag{1.3.2}$$

In $\mathbb{R}^3$, the weak divergence $\operatorname{div}_h : \boldsymbol{U}^h \to S^h$ is defined as the adjoint of $-\operatorname{grad}$ operator in the L^2-inner product, i.e., $\operatorname{div}_h \boldsymbol{w}_h \in S^h$, s.t.,

$$(\operatorname{div}_h \boldsymbol{w}_h, v_h) := -(\boldsymbol{w}_h, \operatorname{grad} v_h) \quad \text{for all } v_h \in S^h. \tag{1.3.3}$$

Weak curl operator curl_h and weak grad operator grad_h are defined similarly. For any $\boldsymbol{w}_h \in \boldsymbol{V}^h$, define $\operatorname{curl}_h \boldsymbol{w}^h \in \boldsymbol{U}^h$ as

$$(\operatorname{curl}_h \boldsymbol{w}_h, \boldsymbol{v}_h) := (\boldsymbol{w}_h, \operatorname{curl} \boldsymbol{v}_h) \quad \text{for all } \boldsymbol{v}_h \in \boldsymbol{U}^h. \tag{1.3.4}$$

For any $w_h \in \boldsymbol{W}^h$, define $\operatorname{grad}_h w_h \in \boldsymbol{V}^h$ as

$$(\operatorname{grad}_h w_h, \boldsymbol{v}_h) := -(w_h, \operatorname{div} \boldsymbol{v}_h) \quad \text{for all } \boldsymbol{v}_h \in \boldsymbol{V}^h. \tag{1.3.5}$$

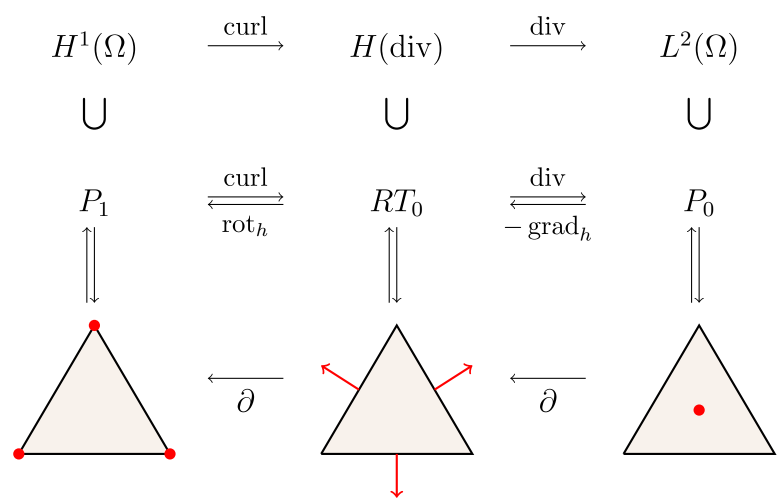

Figure 1.1: Example of appropriate discrete subspaces choice in $\mathbb{R}^2$

Similarly, we can define co-differential operators on the spaces with homogenous traces:

- $\mathbb{R}^2$: $0 \longleftarrow S_0^h \xleftarrow{\mathrm{rot}_{0,h}} \boldsymbol{V}_0^h \xleftarrow{\mathrm{grad}_{0,h}} W_0^h \longleftarrow 0$

- $\mathbb{R}^3$: $0 \longleftarrow S_0^h \xleftarrow{\mathrm{div}_{0,h}} \boldsymbol{U}_0^h \xleftarrow{\mathrm{curl}_{0,h}} \boldsymbol{V}_0^h \xleftarrow{\mathrm{grad}_{0,h}} W_0^h \longleftarrow 0$

In $\mathbb{R}^2$, the weak divergence $\mathrm{rot}_{0,h} : \boldsymbol{V}_0^h \to S_0^h$ is defined as the adjoint of curl operator in the L^2-inner product, i.e., $\mathrm{rot}_{0,h}\, \boldsymbol{w}_h \in S_0^h$, s.t.,

$$(\mathrm{rot}_{0,h}\boldsymbol{w}_h, v_h) := (\boldsymbol{w}_h, \mathrm{curl}\, v_h) \quad \text{for all } v_h \in S_0^h. \tag{1.3.6}$$

The other co-differential operators for the spaces with homogenous traces can be similarly defined.

1.3.3 The Discrete Hodge Decomposition

The Hodge decomposition plays an important role in the analysis of well-posedness and error analysis. On the continuous level, for example, the Hodge (or Helmholtz) decomposition in $\mathbb{R}^2$ is

$$\boldsymbol{L}^2 = \mathrm{curl}\, H_0(\mathrm{curl}) \oplus \mathrm{grad}\, H^1/\mathbb{R}.$$

$$
\begin{array}{ccccccc}
H^1 & \xrightarrow{\text{grad}} & H(\text{curl}) & \xrightarrow{\text{curl}} & H(\text{div}) & \xrightarrow{\text{div}} & L^2 \\
\bigcup & & \bigcup & & \bigcup & & \bigcup \\
P_1 & \underset{-\text{div}_h}{\overset{\text{grad}}{\rightleftarrows}} & ND_1 & \underset{\text{curl}_h}{\overset{\text{curl}}{\rightleftarrows}} & RT_0 & \underset{-\text{grad}_h}{\overset{\text{div}}{\rightleftarrows}} & P_0
\end{array}
$$

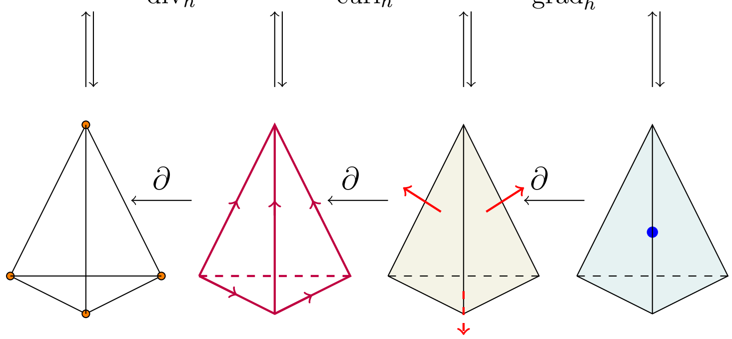

Figure 1.2: Example of appropriate discrete subspaces choice in $\mathbb{R}^3$

To prove well-posedness of discrete systems and handle the error analysis, we need analogous decomposition on the discrete level. It is easy to verify that the following sequences are exact.

- $\mathbb{R}^2$: $0 \longrightarrow S_0^h \xrightarrow{\text{curl}} \boldsymbol{V}_0^h \xrightarrow{\text{div}} W_0^h \longrightarrow 0$

  $0 \longleftarrow S_0^h \xleftarrow{\text{rot}_{0,h}} \boldsymbol{V}_0^h \xleftarrow{\text{grad}_{0,h}} W_0^h \longleftarrow 0$

- $\mathbb{R}^3$: $0 \longrightarrow S_0^h \xrightarrow{\text{grad}} \boldsymbol{U}_0^h \xrightarrow{\text{curl}} \boldsymbol{V}_0^h \xrightarrow{\text{div}} W_0^h \longrightarrow 0$

  $0 \longleftarrow S_0^h \xleftarrow{\text{div}_{0,h}} \boldsymbol{U}_0^h \xleftarrow{\text{curl}_{0,h}} \boldsymbol{V}_0^h \xleftarrow{\text{grad}_{0,h}} W_0^h \longleftarrow 0$

According to these exact sequences, we have the discrete Hodge decompositions [2]:

- $\mathbb{R}^2$: $\boldsymbol{V}_0^h = \text{curl}\, S_0^h \oplus \text{grad}_{0,h} W_0^h$
- $\mathbb{R}^3$: $\boldsymbol{U}_0^h = \text{grad}\, S_0^h \oplus \text{curl}_{0,h}\, \boldsymbol{V}_0^h$
- $\mathbb{R}^3$: $\boldsymbol{V}_0^h = \text{curl}\, \boldsymbol{U}_0^h \oplus \text{grad}_{0,h}\, W_0^h$.

These discrete version of Hodge decompositions split the subspaces into irrotational and solenoidal components, and plays an important role in the analysis.

1.4 Stochastic Finite Elements

In this section, let us introduce the notations and stochastic function spaces.

1.4.1 Notations and Function Spaces.

For the stochastic Stokes equations, we use notation Ω for the random space, and D for the physical domain. Let $D \subset \mathbb{R}^2$ be a bounded convex polygonal domain with boundary ∂D. $(\Omega, \mathcal{F}, \mathcal{P})$ denotes a complete probability space, where Ω is the set of outcomes, $\mathcal{F} \subset 2^{\Omega}$ is the $\sigma-$algebra of random events, and $\mathcal{P}$ is the probability measure. Let $\mu(\xi)$ be a random variable in $(\Omega, \mathcal{F}, \mathcal{P})$. We denote its expected value by $E[\mu] = \int_{\Omega} \mu(\omega) d\mathcal{P}(\omega) = \int_{\Gamma} \mu(y)\rho_{\xi}(y) dy$ and its variance by $Var(\mu) = E[\mu^2] - E[\mu]^2$, where $\rho_{\xi}(\cdot)$ denotes the density function of ξ.

For the stochastic functions, we introduce the tensor spaces endowed with the corresponding inner products as follows:

$$
\begin{aligned}
&L^2(\Gamma) \otimes \boldsymbol{H}_0^1(D) = \\
&\{\boldsymbol{u}(\xi, \boldsymbol{x}) : \Gamma \times D \to \mathbb{R}^2 \mid \boldsymbol{u}(\xi, \cdot) \in \boldsymbol{H}_0^1(D) \text{ a.e. on } \Gamma, \text{ and } \boldsymbol{u}(\cdot, \boldsymbol{x}) \in L^2(\Gamma) \text{ a.e. on D}\}, \\
&L^2(\Gamma) \otimes L_0^2(D) = \\
&\{q(\xi, \boldsymbol{x}) : \Gamma \times D \to \mathbb{R} \mid q(\xi, \cdot) \in L_0^2(D) \text{ a.e. on } \Gamma, \text{ and } q(\cdot, \boldsymbol{x}) \in L^2(\Gamma) \text{ a.e. on D}\}, \\
&(\boldsymbol{u}, \boldsymbol{v})_{L^2(\Gamma)\otimes \boldsymbol{H}_0^1(D)} = E[(\mathrm{rot}\, \boldsymbol{u}, \mathrm{rot}\, \boldsymbol{v}) + (\mathrm{div}\, \boldsymbol{u}, \mathrm{div}\, \boldsymbol{v})] \quad \forall \boldsymbol{u}, \boldsymbol{v} \in L^2(\Gamma) \otimes \boldsymbol{H}_0^1(D), \\
&(p, q)_{L^2(\Gamma)\otimes L_0^2(D)} = E[(p, q)], \quad \forall p, q \in L^2(\Gamma) \otimes L_0^2(D).
\end{aligned}
$$

1.4.2 The Discrete Spaces

To discretize stochastic partial differential equations, we introduce some discrete spaces to approximate $L^2(\Gamma)$, $\boldsymbol{H}_0^1(D)$, and $L_0^2(D)$. For the probability space, the generalized polynomial chaos (gPC) basis functions are chosen to span the approximation space. We denote the approximation subspace as:

$$Y^m := \text{span}\{\Psi_1, \Psi_2, \cdots, \Psi_{N_\xi}\} \subset L^2(\Gamma),$$

where $N_\xi = m+1$ is the dimension and m is the highest degree of gPC. We assume these basis functions are orthogonal and normalized, i.e., for any $i, j = 1, \cdots, m+1$, $E[\Psi_i \Psi_j] = \delta_{ij}$. For instance, if $\xi \sim U(-1,1)$, the natural choice is the Legendre orthogonal normalized polynomials

$$\Psi_k(y) = \frac{1}{2^k k!} \cdot \sqrt{\frac{2k+1}{2}} \cdot \frac{d^k}{dy^k}[(y^2-1)^k] \quad \text{on } \Gamma = (-1,1), \quad k = 0, 1, \cdots,$$

We denote the basis of $\boldsymbol{V}_0^h$ as $\{\boldsymbol{\Phi}_1, \cdots, \boldsymbol{\Phi}_{N_u}\}$, and the basis of W_0^h as $\{\chi_1, \cdots, \chi_{N_p}\}$, where N_u and N_p are the dimensions of the respective spaces.

The tensor spaces $Y^m \otimes \boldsymbol{V}_0^h \subset L^2(\Gamma) \otimes \boldsymbol{H}_0(\text{div})$ and $Y^m \otimes W_0^h \subset L^2(\Gamma) \otimes L_0^2(D)$ are the finite dimensional spaces used for the discrete functions, respectively.

Chapter 2

Multigrid Preconditioners for Mixed Finite Element Methods of Vector Laplacian

Due to the indefiniteness and poor spectral properties, the discretized linear algebraic system of the vector Laplacian by mixed finite element methods is hard to solve. A block diagonal preconditioner has been developed and shown to be an effective preconditioner by Arnold, Falk, and Winther. The purpose of this paper is to propose an alternative and efficient block diagonal preconditioner for solving this saddle point problem. A variable V-cycle multigrid method with the standard point-wise Gauss-Seidel smoother is proved to be a good preconditioner for the Schur complement A. The major benefit of our approach is that the point-wise Gauss-Seidel smoother is more algebraic and can be easily implemented as a 'black-box' smoother. The multigrid solver for the Schur complement will be further used to build preconditioners for the original saddle point systems.

In this chapter, we propose an efficient block diagonal preconditioner for solving the discretized linear system of the vector Laplacian by mixed finite element methods. This problem is considered in $\mathbb{R}^3$. While all the function spaces in this chapter will be the ones with homogenous traces, we simplify the notations as follows:

- the discrete spaces S_h, $\boldsymbol{V}_h$ and $\boldsymbol{U}_h$ are used to denote S_0^h, $\boldsymbol{V}_0^h$ and $\boldsymbol{U}_0^h$ respectively;

- the co-differential operators curl_h, grad_h and div_h are used to denote $\operatorname{curl}_{0,h}$, $\operatorname{grad}_{0,h}$ and $\operatorname{div}_{0,h}$ respectively.

2.1 The Continuous and Discrete Formulations of Vector Laplacian

2.1.1 Discrete Formulations of Vector Laplacian.

On the continuous level, the mixed formulation of the vector Laplacian in space $\boldsymbol{H}_0(\operatorname{curl})$ is: Find $\sigma \in H_0^1, \boldsymbol{u} \in \boldsymbol{H}_0(\operatorname{curl})$ such that

$$\begin{cases} -(\sigma,\tau) + (\boldsymbol{u}, \operatorname{grad}\tau) = 0 & \text{for all } \tau \in H_0^1, \\ (\operatorname{grad}\sigma, \boldsymbol{v}) + (\operatorname{curl}\boldsymbol{u}, \operatorname{curl}\boldsymbol{v}) = (\boldsymbol{f}, \boldsymbol{v}) & \text{for all } \boldsymbol{v} \in \boldsymbol{H}_0(\operatorname{curl}). \end{cases} \tag{2.1.1}$$

The problem (2.1.1) on the discrete level is: Find $\sigma_h \in S_h, \boldsymbol{u}_h \in \boldsymbol{U}_h$ such that

$$\begin{cases} -(\sigma_h,\tau_h) + (\boldsymbol{u}_h, \operatorname{grad}\tau_h) = 0 & \text{for all } \tau_h \in S_h, \\ (\operatorname{grad}\sigma_h, \boldsymbol{v}_h) + (\operatorname{curl}\boldsymbol{u}_h, \operatorname{curl}\boldsymbol{v}_h) = (\boldsymbol{f}, \boldsymbol{v}_h) & \text{for all } \boldsymbol{v}_h \in \boldsymbol{U}_h. \end{cases} \tag{2.1.2}$$

Note that the first equation of (2.1.2) can be interpreted as $\sigma_h = -\operatorname{div}_h \boldsymbol{u}_h$ and in the second equation of (2.1.2) the term $(\operatorname{grad}\sigma_h, \boldsymbol{v}_h) = -(\sigma_h, \operatorname{div}_h \boldsymbol{v}_h)$. After eliminating σ_h from the first equation, we can write the discrete vector Laplacian for edge elements as

$$-\Delta_h^c \boldsymbol{u}_h := \operatorname{curl}_h \operatorname{curl}\boldsymbol{u}_h - \operatorname{grad}\operatorname{div}_h \boldsymbol{u}_h, \tag{2.1.3}$$

which is a discretization of the identity

$$-\Delta\boldsymbol{u} = \operatorname{curl}\operatorname{curl}\boldsymbol{u} - \operatorname{grad}\operatorname{div}\boldsymbol{u}.$$

Choosing appropriate basis for the finite element spaces, we can represent the spaces S_h and $\boldsymbol{V}_h$ by $\mathbb{R}^{\dim S_h}$ and $\mathbb{R}^{\dim \boldsymbol{V}_h}$ respectively. In the following, we shall use the same notation for the vector representation of a function if no ambiguity arises. Then we have the corresponding operator and matrix formulations as: $\mathcal{L}_h^c : S_h \times \boldsymbol{U}_h \to S_h' \times \boldsymbol{U}_h'$

$$\mathcal{L}_h^c \begin{pmatrix} \sigma_h \\ \boldsymbol{u}_h \end{pmatrix} := \begin{pmatrix} -M_v & B \\ B^T & C^T M_f C \end{pmatrix} \begin{pmatrix} \sigma_h \\ \boldsymbol{u}_h \end{pmatrix} = \begin{pmatrix} 0 \\ \boldsymbol{f} \end{pmatrix}. \tag{2.1.4}$$

Here M_v and M_f are mass matrices of the vertex element and the face element, respectively, B^T corresponds to the grad operator, and C to the curl operator. We follow the convention of Stokes equations to reserve B for the (negative) divergence operator. Note that to form the corresponding matrices of weak derivative operators, the inverse of mass matrices will be involved. The Schur complement

$$A_h^c = B^T M_v^{-1} B + C^T M_f C \tag{2.1.5}$$

is the matrix representation of discrete vector Laplacian (2.1.3). The system (2.1.4) can be reduced to the Schur complement equation

$$A_h^c \boldsymbol{u}_h = \boldsymbol{f}. \tag{2.1.6}$$

Similarly, the mixed formulation of the vector Laplacian in space $\boldsymbol{H}_0(\mathrm{div})$ is: Find $\boldsymbol{\sigma} \in \boldsymbol{H}_0(\mathrm{curl}), \boldsymbol{u} \in \boldsymbol{H}_0(\mathrm{div})$ such that

$$\begin{cases} -(\boldsymbol{\sigma}, \boldsymbol{\tau}) + (\boldsymbol{u}, \mathrm{curl}\, \boldsymbol{\tau}) = 0 & \text{for all } \boldsymbol{\tau} \in \boldsymbol{H}_0(\mathrm{curl}), \\ (\mathrm{curl}\, \boldsymbol{\sigma}, \boldsymbol{v}) + (\mathrm{div}\, \boldsymbol{u}, \mathrm{div}\, \boldsymbol{v}) = (\boldsymbol{f}, \boldsymbol{v}) & \text{for all } \boldsymbol{v} \in \boldsymbol{H}_0(\mathrm{div}). \end{cases} \tag{2.1.7}$$

The corresponding discrete mixed formulation is: Find $\boldsymbol{\sigma}_h \in \boldsymbol{U}_h, \boldsymbol{u}_h \in \boldsymbol{V}_h$ such that

$$\begin{cases} -(\boldsymbol{\sigma}_h, \boldsymbol{\tau}_h) + (\boldsymbol{u}_h, \mathrm{curl}\, \boldsymbol{\tau}_h) = 0 & \text{for all } \boldsymbol{\tau}_h \in \boldsymbol{U}_h, \\ (\mathrm{curl}\, \boldsymbol{\sigma}_h, \boldsymbol{v}_h) + (\mathrm{div}\, \boldsymbol{u}_h, \mathrm{div}\, \boldsymbol{v}_h) = (\boldsymbol{f}, \boldsymbol{v}_h) & \text{for all } \boldsymbol{v}_h \in \boldsymbol{V}_h. \end{cases} \tag{2.1.8}$$

Eliminating $\boldsymbol{\sigma}_h$ from the first equation of (2.1.8), we have the discrete vector Laplacian for face elements as

$$-\Delta_h^d \boldsymbol{u}_h := \operatorname{curl} \operatorname{curl}_h \boldsymbol{u}_h - \operatorname{grad}_h \operatorname{div} \boldsymbol{u}_h, \tag{2.1.9}$$

and the operator and matrix formulations are: $\mathcal{L}_h^d : \boldsymbol{U}_h \times \boldsymbol{V}_h \to \boldsymbol{U}'_h \times \boldsymbol{V}'_h$

$$\mathcal{L}_h^d \begin{pmatrix} \boldsymbol{\sigma}_h \\ \boldsymbol{u}_h \end{pmatrix} := \begin{pmatrix} -M_e & C^T \\ C & B^T M_t B \end{pmatrix} \begin{pmatrix} \boldsymbol{\sigma}_h \\ \boldsymbol{u}_h \end{pmatrix} = \begin{pmatrix} 0 \\ \boldsymbol{f} \end{pmatrix}, \tag{2.1.10}$$

where M_t denotes the mass matrix of the discontinuous and piecewise polynomial element. The Schur complement $A_h^d = CM_e^{-1}C^T + B^T M_t B$ is the matrix representation of discrete vector Laplacian (2.1.9). Similarly, the reduced equation of (2.1.10) is

$$A_h^d \boldsymbol{u}_h = \boldsymbol{f}. \tag{2.1.11}$$

We shall develop multigrid methods for solving (2.1.6) and (2.1.11) and use them to construct efficient preconditioners for the corresponding saddle point systems (2.1.4) and (2.1.10), respectively.

2.1.2 Discrete Poincaré Inequality and Inverse Inequality

In this subsection, we define the norms associated with the discrete vector Laplacian, and prove discrete Poincaré and inverse inequalities.

Definition 2.1.1. *For $\boldsymbol{u}_h \in \boldsymbol{U}_h$, define $\|\boldsymbol{u}_h\|_{A_h^c}^2 = a_h^c(\boldsymbol{u}_h, \boldsymbol{u}_h)$, where the bilinear form $a_h^c(\cdot,\cdot)$ is defined as*

$$a_h^c(\boldsymbol{u}_h, \boldsymbol{v}_h) := (\operatorname{curl} \boldsymbol{u}_h, \operatorname{curl} \boldsymbol{v}_h) + (\operatorname{div}_h \boldsymbol{u}_h, \operatorname{div}_h \boldsymbol{v}_h).$$

Similarly, for $\boldsymbol{u}_h \in \boldsymbol{V}_h$, define $\|\boldsymbol{u}_h\|_{A_h^d}^2 = a_h^d(\boldsymbol{u}_h, \boldsymbol{u}_h)$, where the bilinear form $a_h^d(\cdot,\cdot)$ is defined as

$$a_h^d(\boldsymbol{u}_h, \boldsymbol{v}_h) := (\operatorname{curl}_h \boldsymbol{u}_h, \operatorname{curl}_h \boldsymbol{v}_h) + (\operatorname{div} \boldsymbol{u}_h, \operatorname{div} \boldsymbol{v}_h).$$

Lemma 2.1.1 (Discrete Poincaré Inequality)**.** *We have the following discrete Poincaré inequalities:*

$$\|\boldsymbol{u}_h\| \lesssim \|\boldsymbol{u}_h\|_{A_h^c} \quad \textit{for all } \boldsymbol{u}_h \in \boldsymbol{U}_h; \tag{2.1.12}$$

$$\|\boldsymbol{u}_h\| \lesssim \|\boldsymbol{u}_h\|_{A_h^d} \quad \textit{for all } \boldsymbol{u}_h \in \boldsymbol{V}_h. \tag{2.1.13}$$

Proof. Let us prove the first inequality. From the discrete Hodge decomposition, we have for $\boldsymbol{u}_h \in \boldsymbol{U}_h$, there exist $\rho \in S_h$ and $\boldsymbol{\phi} \in \boldsymbol{V}_h \cap \ker(\mathrm{curl}_h)^{\perp}$ such that

$$\boldsymbol{u}_h = \operatorname{grad} \rho + \mathrm{curl}_h \boldsymbol{\phi}. \tag{2.1.14}$$

Applying $-\operatorname{div}_h$ to (2.1.14), we have $-\operatorname{div}_h \boldsymbol{u}_h = -\operatorname{div}_h \operatorname{grad} \rho$, thus

$$\|\operatorname{grad} \rho\|^2 = (-\operatorname{div}_h \boldsymbol{u}_h, \rho) \le \|\operatorname{div}_h \boldsymbol{u}_h\| \|\rho\| \lesssim \|\operatorname{div}_h \boldsymbol{u}_h\| \|\operatorname{grad} \rho\|,$$

which leads to

$$\|\operatorname{grad} \rho\| \lesssim \|\operatorname{div}_h \boldsymbol{u}_h\|. \tag{2.1.15}$$

To control the other part, we first prove a discrete Poincaré inequality in the form

$$\|\boldsymbol{\phi}\| \lesssim \|\mathrm{curl}_h \boldsymbol{\phi}\| \quad \text{ for } \phi \in \boldsymbol{V}_h \cap \ker(\mathrm{curl}_h)^{\perp}. \tag{2.1.16}$$

By the exactness of the discrete complex, $\ker(\mathrm{curl}_h) = img(\mathrm{grad}_h)$ and thus for $\boldsymbol{\phi} \in \boldsymbol{V}_h \cap \ker(\mathrm{curl}_h)^{\perp}$, we have $\operatorname{div} \phi = 0$. Then by the exactness of the de Rham complex, there exists $\boldsymbol{v} \in \boldsymbol{U}_h \cap \ker(\mathrm{curl})^{\perp}$ such that $\boldsymbol{\phi} = \operatorname{curl} \boldsymbol{v}$. We recall another Poincaré inequality [25, 22]

$$\|\boldsymbol{v}\| \lesssim \|\operatorname{curl} \boldsymbol{v}\| \quad \text{for all } \boldsymbol{v} \in \boldsymbol{U}_h \cap \ker(\mathrm{curl})^{\perp}.$$

Then we have

$$\|\boldsymbol{\phi}\|^2 = (\boldsymbol{\phi}, \operatorname{curl} \boldsymbol{v}) = (\operatorname{curl}_h \boldsymbol{\phi}, \boldsymbol{v}) \leq \|\operatorname{curl}_h \boldsymbol{\phi}\| \|\boldsymbol{v}\| \lesssim \|\operatorname{curl}_h \boldsymbol{\phi}\| \|\operatorname{curl} \boldsymbol{v}\| = \|\operatorname{curl}_h \boldsymbol{\phi}\| \|\boldsymbol{\phi}\|.$$

Canceling one $\|\boldsymbol{\phi}\|$, we obtain the desirable inequality (2.1.16).

Applying curl to the Hodge decomposition (2.1.14) and using the inequality (2.1.16), we have $\operatorname{curl} \boldsymbol{u}_h = \operatorname{curl} \operatorname{curl}_h \boldsymbol{\phi}$, thus

$$\|\operatorname{curl}_h \boldsymbol{\phi}\|^2 = (\operatorname{curl} \boldsymbol{u}_h, \boldsymbol{\phi}) \leq \|\operatorname{curl} \boldsymbol{u}_h\| \|\boldsymbol{\phi}\| \lesssim \|\operatorname{curl} \boldsymbol{u}_h\| \|\operatorname{curl}_h \boldsymbol{\phi}\|,$$

which leads to the inequality

$$\|\operatorname{curl}_h \boldsymbol{\phi}\| \lesssim \|\operatorname{curl} \boldsymbol{u}_h\|. \tag{2.1.17}$$

Combine inequalities (2.1.15) and (2.1.17), we have proved that

$$\|\boldsymbol{u}_h\| \leq \|\operatorname{grad} \rho\| + \|\operatorname{curl}_h \boldsymbol{\phi}\| \lesssim \|\operatorname{div}_h \boldsymbol{u}_h\| + \|\operatorname{curl} \boldsymbol{u}_h\| \lesssim \|\boldsymbol{u}_h\|_{A_h^c}.$$

Analogously, applying appropriate differential operations to the discrete Hodge decomposition of $\boldsymbol{u}_h \in \boldsymbol{V}_h$ and Poincaré inequality leads to the inequality $\|\boldsymbol{u}_h\| \lesssim \|\boldsymbol{u}_h\|_{A_h^d}$. □

Remark 2.1.2. The result and the proof can be easily generalized to mixed discretization of Hodge Laplacian in discrete differential forms [2]. We keep the concrete form for the easy access of these results. □

Lemma 2.1.2 (Inverse Inequality)**.** *We have the following inverse inequalities:*

$$\|\boldsymbol{u}_h\|_{A_h^c} \lesssim h^{-1} \|\boldsymbol{u}_h\| \quad \textit{for all } \boldsymbol{u}_h \in \boldsymbol{U}_h;$$
$$\|\boldsymbol{u}_h\|_{A_h^d} \lesssim h^{-1} \|\boldsymbol{u}_h\| \quad \textit{for all } \boldsymbol{u}_h \in \boldsymbol{V}_h.$$

Proof. It suffices to prove that

$$\|\operatorname{div}_h \boldsymbol{u}_h\| \lesssim h^{-1}\|\boldsymbol{u}_h\| \quad \text{for all } \boldsymbol{u}_h \in \boldsymbol{U}_h; \tag{2.1.18}$$

$$\|\operatorname{curl}_h \boldsymbol{u}_h\| \lesssim h^{-1}\|\boldsymbol{u}_h\| \quad \text{for all } \boldsymbol{u}_h \in \boldsymbol{V}_h. \tag{2.1.19}$$

since for conforming cases, the inverse inequalities

$$\|\operatorname{grad} \sigma_h\| \lesssim h^{-1}\|\sigma_h\| \quad \text{for all } \sigma_h \in S_h;$$

$$\|\operatorname{curl} \boldsymbol{u}_h\| \lesssim h^{-1}\|\boldsymbol{u}_h\| \quad \text{for all } \boldsymbol{u}_h \in \boldsymbol{U}_h.$$

are well known.

For any $\boldsymbol{u}_h \in \boldsymbol{U}_h$, let $\sigma_h = -\operatorname{div}_h \boldsymbol{u}_h$, then we have

$$\|\operatorname{div}_h \boldsymbol{u}_h\|^2 = -(\operatorname{div}_h \boldsymbol{u}_h, \sigma_h) = (\boldsymbol{u}_h, \operatorname{grad} \sigma_h) \lesssim h^{-1}\|\boldsymbol{u}_h\|\|\sigma_h\|,$$

which implies (2.1.18). The proof of (2.1.19) is analogous. □

2.2 The Multigrid Methods for Discrete Vector Laplacian

In this section, we describe a multigrid algorithm to solve the Schur complement equations (2.1.6) and (2.1.11), and prove it is a good preconditioner.

2.2.1 Problem Setting

Let us assume that nested tetrahedral partitions of Ω are given as

$$\mathcal{T}_1 \subset \cdots \subset \mathcal{T}_J = \mathcal{T}_h,$$

and the corresponding H_0^1, $\boldsymbol{H}_0(\mathrm{curl})$ and $\boldsymbol{H}_0(\mathrm{div})$ finite element spaces are

$$
\begin{aligned}
S_1 \subset \cdots \subset S_J = S_h, \\
\boldsymbol{U}_1 \subset \cdots \subset \boldsymbol{U}_J = \boldsymbol{U}_h, \\
\boldsymbol{V}_1 \subset \cdots \subset \boldsymbol{V}_J = \boldsymbol{V}_h.
\end{aligned}
$$

For a technical reason, we assume that we use piecewise polynomials which have degree more than 2 to approximate the H_0^1 space and consequently the edge element space contains full linear polynomial. When no ambiguity can arise, we replace subscripts h by the level index k for $k = 1, 2, \ldots, J$.

The discretization (2.1.1) of the mixed formulation of vector Laplacian in space $\boldsymbol{H}_0(\mathrm{curl})$ based on $\mathcal{T}_k$, for $k = 1, 2, \ldots, J$, can be written as

$$
\begin{pmatrix} -M_{v,k} & B_k \\ B_k^T & C_k^T M_{f,k} C_k \end{pmatrix} \begin{pmatrix} \sigma_k \\ \boldsymbol{u}_k \end{pmatrix} = \begin{pmatrix} 0 \\ \boldsymbol{f}_k \end{pmatrix}. \tag{2.2.1}
$$

Eliminating σ_k from (2.2.3), we get the reduced Schur complement equation

$$
A_k^c \boldsymbol{u}_k = (B_k^T M_{v,k}^{-1} B_k + C_k^T M_{f,k} C_k) \boldsymbol{u}_k = \boldsymbol{f}_k. \tag{2.2.2}
$$

The discretization (2.1.7) of the mixed formulation of vector Laplacian in space $\boldsymbol{H}_0(\mathrm{div})$ on $\mathcal{T}_k$, for $k = 1, 2, \ldots, J$, can be written as

$$
\begin{pmatrix} -M_{e,k} & C_k^T \\ C_k & B_k^T M_{t,k} B_k \end{pmatrix} \begin{pmatrix} \boldsymbol{\sigma}_k \\ \boldsymbol{u}_k \end{pmatrix} = \begin{pmatrix} 0 \\ \boldsymbol{f}_k \end{pmatrix}, \tag{2.2.3}
$$

and the reduced Schur complement equation is

$$
A_k^d \boldsymbol{u}_k = (B_k^T M_{t,k} B_k + C_k M_{e,k}^{-1} C_k^T) \boldsymbol{u}_k = \boldsymbol{f}_k. \tag{2.2.4}
$$

We are interested in solving the Schur complement equations in the finest level, i.e., $k = J$.

Notice that A_k^c and A_k^d are defined by the discretization of the vector Laplacian on the trianglulation $\mathcal{T}_k$, but not by the Galerkin projection of A_J^c or A_J^d since the inverse of mass matrix is involved. In other words, A_k^c and A_k^d are not inherited.

When necessary, we use the notation without the superscript c and d to unify the discussion. The notation $\mathcal{V}_k$ is used to represent both $\boldsymbol{U}_k$ and $\boldsymbol{V}_k$ spaces.

2.2.2 A Variable V-cycle Multigrid Method

Before we present the multigrid algorithm to solve (2.2.2) and (2.2.4), let us introduce some operators. Let R_k denote a smoothing operator on level k, which is assumed to be symmetric and convergent. Let I_k denote the prolongation operator from level $k-1$ to level k, which is the natural inclusion since finite element spaces are nested. The transpose I_k^T then represents the restriction from level k to level $k-1$. The Galerkin projection P_k, which is from level k to level $k-1$, is defined as: for any given $\boldsymbol{u}_k \in \mathcal{V}_k$, $P_{k-1}\boldsymbol{u}_k \in \mathcal{V}_{k-1}$ satisfies

$$a_{k-1}(P_{k-1}\boldsymbol{u}_k, \boldsymbol{v}_{k-1}) = a_k(\boldsymbol{u}_k, I_k\boldsymbol{v}_{k-1}) = a_k(\boldsymbol{u}_k, \boldsymbol{v}_{k-1}) \quad \text{for all } \boldsymbol{v}_{k-1} \in \mathcal{V}_{k-1}.$$

The variable V-cycle multigrid algorithm is as following.

Algorithm 2. Multigrid Algorithm: $\boldsymbol{u}_k^{MG} = MG_k(\boldsymbol{f}_k; \boldsymbol{u}_k^0, m_k)$

Set $MG_1 = A_1^{-1}$. For $k \geq 2$, assume that MG_{k-1} has been defined and define $MG_k(\boldsymbol{f}_k)$ for $\boldsymbol{f}_k \in \mathcal{V}_k$ as follows:

- Pre-smoothing: Define $\boldsymbol{u}_k^l$ for $l = 1, 2, \cdots, m_k$ by

$$\boldsymbol{u}_k^l = \boldsymbol{u}_k^{l-1} + R_k(\boldsymbol{f}_k - A_k\boldsymbol{u}_k^{l-1}).$$

- Coarse-grid correction: Define $\boldsymbol{u}_k^{m_k+1} = \boldsymbol{u}_k^{m_k} + I_{k-1}\boldsymbol{e}_{k-1}$, where

$$\boldsymbol{e}_{k-1} = MG_{k-1}(I_{k-1}^T(\boldsymbol{f}_k - A_k\boldsymbol{u}_k^{m_k}); 0, m_{k-1}).$$

- Post-smoothing: Define $\boldsymbol{u}_k^l$ for $l = m_k + 2, \cdots, 2m_k + 1$ by

$$\boldsymbol{u}_k^l = \boldsymbol{u}_k^{l-1} + R_k(\boldsymbol{f}_k - A_k\boldsymbol{u}_k^{l-1}).$$

Define $\boldsymbol{u}_k^{MG} = \boldsymbol{u}_k^{2m_k+1}$

In this algorithm, m_k is a positive integer which may vary from level to level, and determines the number of smoothing iterations on the k-th level, see [8, 9].

2.2.3 Multigrid Analysis Framework

We employ the multigrid analysis framework developed in [8]. Denoted by λ_k the largest eigenvalue of A_k. For the multigrid algorithm to be a good preconditioner to A_k, we need to verify the following assumptions:

(A.1) "Regularity and approximation assumption": For some $0 < \alpha \leq 1$,

$$|a_k((I - P_{k-1})\boldsymbol{u}_k, \boldsymbol{u}_k)| \leq C_A \left(\frac{\|A_k\boldsymbol{u}_k\|^2}{\lambda_k}\right)^\alpha a_k(\boldsymbol{u}_k, \boldsymbol{u}_k)^{1-\alpha} \qquad \text{for all } \boldsymbol{u}_k \in \mathcal{V}_k,$$

holds with constant C_A independent of k;

(A.2) "Smoothing property":

$$\frac{\|\boldsymbol{u}_k\|^2}{\lambda_k} \leq C_R(R_k\boldsymbol{u}_k, \boldsymbol{u}_k) \qquad \text{for all } \boldsymbol{u}_k \in \mathcal{V}_k,$$

holds with constant C_R independent of k.

We begin with estimating the largest eigenvalue of A_k.

Lemma 2.2.1. *The largest eigenvalue of A_k, λ_k, satisfies $\lambda_k \eqsim h_k^{-2}$ for $k = 1, 2, \dots, J$.*

Proof. By the inverse inequality, the maximal eigenvalue of A_k^c can be bounded above by

$$\begin{aligned}\lambda_k &= \sup_{0\neq \boldsymbol{u}\in \boldsymbol{U}_k} \frac{(A_k^c \boldsymbol{u}, \boldsymbol{u})}{(\boldsymbol{u}, \boldsymbol{u})} = \sup_{0\neq \boldsymbol{u}\in \boldsymbol{U}_k} \frac{a_k^c\,(\boldsymbol{u}, \boldsymbol{u})}{(\boldsymbol{u}, \boldsymbol{u})} \\ &= \sup_{0\neq \boldsymbol{u}\in \boldsymbol{U}_k} \frac{(\operatorname{div}_k \boldsymbol{u}, \operatorname{div}_k \boldsymbol{u}) + (\operatorname{curl} \boldsymbol{u}, \operatorname{curl} \boldsymbol{u})}{(\boldsymbol{u}, \boldsymbol{u})} \lesssim h_k^{-2}.\end{aligned}$$

One the other hand, let $\tilde{\boldsymbol{u}} = \operatorname{grad} \varphi_i$, where φ_i is a basis function of Lagrangian element, then it holds

$$\begin{aligned}\lambda_k &= \sup_{0\neq \boldsymbol{u}\in \boldsymbol{U}_k} \frac{(A_k^c \boldsymbol{u}, \boldsymbol{u})}{(\boldsymbol{u}, \boldsymbol{u})} \geq \frac{(A_k^c \tilde{\boldsymbol{u}}, \tilde{\boldsymbol{u}})}{(\tilde{\boldsymbol{u}}, \tilde{\boldsymbol{u}})} = \frac{a_k^c(\tilde{\boldsymbol{u}}, \tilde{\boldsymbol{u}})}{(\tilde{\boldsymbol{u}}, \tilde{\boldsymbol{u}})} \\ &= \frac{(\operatorname{div}_k \operatorname{grad} \varphi_i, \operatorname{div}_k \operatorname{grad} \varphi_i)}{(\operatorname{grad} \varphi_i, \operatorname{grad} \varphi_i)} = \frac{\|\Delta \varphi_i\|^2}{\|\nabla \varphi_i\|^2} \eqsim h_k^{-2}.\end{aligned}$$

Thus, we have $\lambda_k \eqsim h_k^{-2}$. Similarly, we have this result for A_k^d. □

2.2.4 Smoothing Property

The symmetric Gauss-Seidel or a properly weighted Jacobi iteration both satisfy the smoothing property (A.2), a proof of which can be found in [9]. For completeness we present a short proof below.

Recall that Gauss-Seidel iteration can be understood as a successive subspace correction method apply to the basis decomposition $\mathcal{V}_k = \sum_{i=1}^{N_k} \mathcal{V}_{k,i}$ with exact local solvers [29]. For $\boldsymbol{u} \in \mathcal{V}_k$, let $\boldsymbol{u} = \sum_{i=1}^{N_k} \boldsymbol{u}_i$ be the basis decomposition. By the X-Z identity [30, 14] for the multiplicative method, we have

$$(\overline{R}_{\mathrm{GS}}^{-1} \boldsymbol{u}, \boldsymbol{u}) = \|\boldsymbol{u}\|_{A_k}^2 + \sum_{i=0}^{N} \|P_i \sum_{j>i} \boldsymbol{u}_j\|_{A_k}^2,$$

where $\overline{R}_{\rm GS}$ is a symmetrized Gauss-Seidel iteration. We then estimate the second term as

$$\sum_{i=0}^{N} \|P_i \sum_{j>i} \boldsymbol{u}_j\|_{A_k}^2 \leq \sum_{i=0}^{N} \sum_{j\in n(i)} \|\boldsymbol{u}_j\|_{A_k}^2 \lesssim \lambda_k \sum_{i=0}^{N} \|\boldsymbol{u}_j\|^2 \lesssim \lambda_k \|\boldsymbol{u}\|^2.$$

Here we use the sparsity of A_k such that the repetition in the summation is bounded above by a constant. The last step is from the stability of the basis decomposition in L^2-norm which holds for all finite element spaces under consideration.

We have thus proved that $(\overline{R}_{\rm GS}^{-1}\boldsymbol{u}, \boldsymbol{u}) \lesssim \lambda_k \|\boldsymbol{u}\|^2$ which is equivalent to the smoothing property by a simple change of variable. Proof for Jacobi iteration is similar.

2.2.5 Approximation Property

For any $2 < k \leq J$, let $\mathcal{T}_H = \mathcal{T}_{k-1}$ and $\mathcal{T}_h = \mathcal{T}_k$. Let

$$\boldsymbol{Z}_h = \{\boldsymbol{z}_h \in \boldsymbol{V}_h |\ \operatorname{div} \boldsymbol{z}_h = 0\} = \operatorname{curl} \boldsymbol{U}_h = \operatorname{curl} \operatorname{curl}_h \boldsymbol{V}_h,$$

and $Q_h^Z : L^2 \mapsto \boldsymbol{Z}_h$ be the L^2 projection to $\boldsymbol{Z}_h$. Denoted by $Q_h^W : L^2 \mapsto W_h$ the L^2 projection onto W_h. The following error estimates are obtained in [3].

Lemma 2.2.2. *Given $\boldsymbol{u}_h \in \operatorname{curl}_h \boldsymbol{V}_h$, let $\boldsymbol{u}_H$ be the unique element in $\operatorname{curl}_h \boldsymbol{V}_H$ satisfying $\operatorname{curl} \boldsymbol{u}_H = Q_H^Z \operatorname{curl} \boldsymbol{u}_h$. Then*

$$\begin{aligned} \|\boldsymbol{u}_h - \boldsymbol{u}_H\| &\lesssim H \|\operatorname{curl} \boldsymbol{u}_h\|, \\ \|\operatorname{curl}(\boldsymbol{u}_h - \boldsymbol{u}_H)\| &\lesssim H \|\operatorname{curl}_h \operatorname{curl} \boldsymbol{u}_h\|. \end{aligned}$$

In Lemma 2.2.2, by the exactness of the co-differential operators, i.e., $\ker(\operatorname{div}_H) = \operatorname{curl}_h(V_H)$, the function $\boldsymbol{u}_H$ is uniquely determined by the Maxwell equations

$$(\operatorname{curl} \boldsymbol{u}_H, \operatorname{curl} \boldsymbol{v}_H) = (\operatorname{curl} \boldsymbol{u}_h, \operatorname{curl} \boldsymbol{v}_H), \quad \text{for all } \boldsymbol{v}_H \in \boldsymbol{U}_H \tag{2.2.5}$$

$$(\boldsymbol{u}_H, \operatorname{grad} \phi_H) = 0, \quad \text{for all } \phi_H \in S_H. \tag{2.2.6}$$

The well-posedness and error estimate of (2.2.5)-(2.2.6) is well understood. The difficulty of getting estimate in Lemma 2.2.2 is the estimate using norms of the source $\operatorname{curl} \boldsymbol{u}_h$ only.

Lemma 2.2.3. *Give $\boldsymbol{v}_h \in \operatorname{grad}_h W_h$, let $\boldsymbol{v}_H$ be the unique element of $\operatorname{grad}_h W_H$ satisfying $\operatorname{div} \boldsymbol{v}_H = Q_H^W \operatorname{div} \boldsymbol{v}_h$. Then*

$$\begin{aligned} \|\boldsymbol{v}_h - \boldsymbol{v}_H\| &\lesssim H \|\operatorname{div} \boldsymbol{v}_h\|, \\ \|\operatorname{div}(\boldsymbol{v}_h - \boldsymbol{v}_H)\| &\lesssim H \|\operatorname{grad}_h \operatorname{div} \boldsymbol{v}_h\|. \end{aligned}$$

Similarly, the function $\boldsymbol{v}_H$ in Lemma 2.2.3 is uniquely determined by the mixed Poisson equation

$$\begin{aligned} (\boldsymbol{v}_H, \boldsymbol{u}_H) - (p_H, \operatorname{div} \boldsymbol{u}_H) = 0, \quad &\text{for all } \boldsymbol{u}_H \in \boldsymbol{V}_H \\ (\operatorname{div} \boldsymbol{v}_H, q_H) = (\operatorname{div} \boldsymbol{v}_h, q_H), \quad &\text{for all } q_H \in W_H. \end{aligned}$$

Approximation Property in $\boldsymbol{H}_0(\operatorname{curl})$

Let $\boldsymbol{u}_h \in \boldsymbol{U}_h$ be the solution of equation

$$a_h^c(\boldsymbol{u}_h, \boldsymbol{v}_h) = (\boldsymbol{f}_h, \boldsymbol{v}_h) \qquad \text{for all } \boldsymbol{v}_h \in \boldsymbol{U}_h, \tag{2.2.7}$$

and $\boldsymbol{u}_H \in \boldsymbol{U}_H \subset \boldsymbol{U}_h$ be the solution of equation

$$a_H^c(\boldsymbol{u}_H, \boldsymbol{v}_H) = (\boldsymbol{f}_h, \boldsymbol{v}_H) \qquad \text{for all } \boldsymbol{v}_H \in \boldsymbol{U}_H. \tag{2.2.8}$$

By the Hodge decomposition, we have

$$\boldsymbol{u}_h = \operatorname{grad}\phi_h \oplus \boldsymbol{u}_{0,h}, \quad \phi_h \in S_h,\ \boldsymbol{u}_{0,h} \in \operatorname{curl}_h \boldsymbol{V}_h, \tag{2.2.9}$$

$$\boldsymbol{u}_H = \operatorname{grad}\phi_H \oplus (\boldsymbol{u}_{0,H} + \boldsymbol{e}_H), \quad \phi_H \in S_H,\ \boldsymbol{u}_{0,H} \text{ and } \boldsymbol{e}_H \in \operatorname{curl}_h \boldsymbol{V}_H, \tag{2.2.10}$$

$$\boldsymbol{f}_h = \operatorname{grad} g_h \oplus \operatorname{curl}_h \boldsymbol{q}_h, \text{ for some } g_h \in S_h,\ \boldsymbol{q}_h \in \operatorname{curl} \boldsymbol{U}_h \subset \boldsymbol{V}_h. \tag{2.2.11}$$

Where $\boldsymbol{u}_{0,H}$ is the unique element in $\operatorname{curl}_h \boldsymbol{V}_H$ satisfying

$$\operatorname{curl} \boldsymbol{u}_{0,H} = Q_H^Z \operatorname{curl} \boldsymbol{u}_{0,h}.$$

Then by Lemma 2.2.2, we immediately get the following estimate.

Lemma 2.2.4. *Let $\boldsymbol{u}_{0,h}$ and $\boldsymbol{u}_{0,H}$ be defined as in equations* (2.2.9) *and* (2.2.10)*. It holds*

$$\|\boldsymbol{u}_{0,h} - \boldsymbol{u}_{0,H}\| \lesssim H\|\boldsymbol{u}_h\|_{A_h^c}.$$

Now we turn to the estimate of $\boldsymbol{e}_H$ being given in equation (2.2.10).

Lemma 2.2.5. *Let $\boldsymbol{e}_H \in \operatorname{curl}_h \boldsymbol{V}_H$ be defined as in equation* (2.2.10)*. It holds*

$$\|\boldsymbol{e}_H\|_{A_h^c} \lesssim H\|A_h^c \boldsymbol{u}_h\|.$$

Proof. By equations (2.2.7) and (2.2.8), we have

$$(\operatorname{curl} \boldsymbol{u}_{0,h}, \operatorname{curl} \boldsymbol{v}_h) = (\boldsymbol{q}_h, \operatorname{curl} \boldsymbol{v}_h), \quad \text{for all } \boldsymbol{v}_h \in \operatorname{curl}_h \boldsymbol{V}_h$$

$$(\operatorname{curl}(\boldsymbol{u}_{0,H} + \boldsymbol{e}_H), \operatorname{curl} \boldsymbol{v}_H) = (\operatorname{grad} g_h, \boldsymbol{v}_H) + (\boldsymbol{q}_h, \operatorname{curl} \boldsymbol{v}_H), \quad \text{for all } \boldsymbol{v}_H \in \operatorname{curl}_h \boldsymbol{V}_H,$$

where g_h and $\boldsymbol{q}_h$ are defined in equation (2.2.11). Then

$$(\operatorname{curl} \boldsymbol{e}_H, \operatorname{curl} \boldsymbol{v}_H) = (\operatorname{grad} g_h, \boldsymbol{v}_H) \qquad \text{for all } \boldsymbol{v}_H \in \operatorname{curl}_h \boldsymbol{V}_H. \tag{2.2.12}$$

Note that, for $g_h \in S_h \subset H_0^1(\Omega)$, there exists an $\boldsymbol{e} \in \boldsymbol{H}_0(\mathrm{curl})$ such that

$$(\operatorname{grad} g_h, e) = 0 \quad \text{and} \quad \|\boldsymbol{e} - \boldsymbol{e}_H\| \lesssim H \|\operatorname{curl} \boldsymbol{e}_H\|.$$

Then,

$$(\operatorname{curl} \boldsymbol{e}_H, \operatorname{curl} \boldsymbol{e}_H) \;=\; (\operatorname{grad} g_h, \boldsymbol{e}_H) = (\operatorname{grad} g_h, \boldsymbol{e}_H - \boldsymbol{e}) \lesssim H \|\operatorname{grad} g_h\| \|\operatorname{curl} \boldsymbol{e}_H\|.$$

It holds

$$\|\operatorname{curl} \boldsymbol{e}_H\| \lesssim H \|\operatorname{grad} g_h\| \le H \|\boldsymbol{f}_h\| = H \|A_h^c \boldsymbol{u}_h\|.$$

Now we turn to the estimate of $\|\operatorname{div}_h \boldsymbol{e}_H\|$. Not that we also can find $\boldsymbol{e}_h \in \operatorname{curl}_h \boldsymbol{V}_h$ satisfying that

$$(\operatorname{grad} g_h, \boldsymbol{e}_h) = 0, \qquad \text{and } \|\boldsymbol{e}_h - \boldsymbol{e}_H\| \le h \|\operatorname{curl} \boldsymbol{e}_H\|.$$

Then by inverse inequality, it holds

$$\|\operatorname{div}_h \boldsymbol{e}_H\| = \|\operatorname{div}_h (\boldsymbol{e}_H - \boldsymbol{e}_h)\| \lesssim h^{-1} \|\boldsymbol{e}_h - \boldsymbol{e}_H\| \lesssim \frac{H}{h} \|\operatorname{curl} \boldsymbol{e}_H\| \lesssim H \|A_h^c \boldsymbol{u}_h\|.$$

The desired results follow. □

We now explore the relation between ϕ_h, ϕ_H, and g_h defined in equations (2.2.9)-(2.2.11).

Lemma 2.2.6. *Let $\phi_h \in S_h$ and $\phi_H \in S_H$ be defined as in equations* (2.2.9) *and* (2.2.10). *It holds*

$$\|\operatorname{grad} \phi_h - \operatorname{grad} \phi_H\| \lesssim H \|\boldsymbol{u}_h\|_{A_h^c}.$$

Proof. For equation (2.2.7), test with $\boldsymbol{v}_h \in \operatorname{grad} S_h$ to get

$$(\operatorname{div}_h \operatorname{grad} \phi_h, \operatorname{div}_h \boldsymbol{v}_h) = (\operatorname{grad} g_h, \boldsymbol{v}_h) = -(g_h, \operatorname{div}_h \boldsymbol{v}_h),$$

which implies $-\operatorname{div}_h \operatorname{grad} \phi_h = -\operatorname{div}_h \boldsymbol{u}_h = g_h$, i.e.,

$$-\Delta_h \phi_h = g_h. \tag{2.2.13}$$

From equation (2.2.13), we can see that ϕ_h is the Galerkin projection of ϕ to S_h, where $\phi \in H_0^1(\Omega)$ satisfies the Poisson equation:

$$-\Delta \phi = g_h.$$

Therefore by the standard error estimate of finite element methods, we have

$$\|\nabla \phi - \nabla \phi_h\| \lesssim H \|g_h\|.$$

Let P_H^S denote the H^1-projection to the space S_H. For equation (2.2.8), choose $\boldsymbol{v}_H = \operatorname{grad} \psi_H \in \operatorname{grad} S_H$, we have

$$(\operatorname{div}_H \operatorname{grad} \phi_H, \operatorname{div}_H \boldsymbol{v}_H) = (\operatorname{grad} g_h, \operatorname{grad} \psi_H) = (\operatorname{grad} P_H^S g_h, \operatorname{grad} \psi_H),$$

which implies $-\operatorname{div}_H \operatorname{grad} \phi_H = P_H^S g_h$, i.e.,

$$-\Delta_H \phi_H = P_H^S g_h. \tag{2.2.14}$$

From equation (2.2.14), we can see that ϕ_H is the Galerkin projection of $\tilde{\phi}$ to S_H, where $\tilde{\phi} \in H_0^1(\Omega)$ satisfies the Poisson equation:

$$-\Delta \tilde{\phi} = P_H^S g_h.$$

The H^1-projection P_H^S is not stable in L^2-norm. However, applied to functions in S_h, we can recover one as follows

$$\|(I - P_H^S) g_h\| \lesssim H \|\operatorname{grad}(I - P_H^S) g_h\| \lesssim H \|\operatorname{grad} g_h\| \lesssim H/h \|g_h\| \lesssim \|g_h\|.$$

In the last step, we use the fact that the ratio of the mesh size between consecutive levels is bounded, i.e., $H/h \le C$.

We then have

$$\|\operatorname{grad}(\tilde{\phi} - \phi_H)\| \lesssim H\|P_H^S g_h\| \le H\|g_h\| + H\|(I - P_H^S)g_h\| \lesssim H\|g_h\|.$$

And

$$\begin{aligned}\|\operatorname{grad}(\phi_h - \phi_H)\| &\le \|\operatorname{grad}(\phi_h - \phi)\| + \|\operatorname{grad}(\phi_H - \tilde{\phi})\| + \|\operatorname{grad}(\phi - \tilde{\phi})\| \\ &\lesssim H\|g_h\| + \|g_h - P_H^S g_h\|_{-1}.\end{aligned}$$

By the error estimate of negative norms and the inverse inequality, we have

$$\|g_h - P_H^S g_h\|_{-1} \lesssim H^2\|g_h\|_1 \lesssim H\|g_h\|.$$

Here we use H^{-1} norm estimate, which requires that the piecewise polynomials in S_H have degree greater than or equal to 2. Noticing that $g_h = \operatorname{div}_h \boldsymbol{u}_h$, we thus get

$$\|\operatorname{grad}(\phi_h - \phi_H)\| \lesssim H\|\operatorname{div}_h \boldsymbol{u}_h\|. \tag{2.2.15}$$

which implies the desired result. □

As a summary the the above results, we have the following theorem.

Theorem 2.2.1. *Condition (A.1) holds with $\alpha = \frac{1}{2}$, i.e. for any $\boldsymbol{u}_k \in \boldsymbol{U}_k$, there hold*

$$a_k^c((I - P_{k-1})\boldsymbol{u}_k, \boldsymbol{u}_k) \lesssim \left(\frac{\|A_k^c \boldsymbol{u}_k\|^2}{\lambda_k}\right)^{\frac{1}{2}} a_k^c(\boldsymbol{u}_k, \boldsymbol{u}_k)^{\frac{1}{2}}. \tag{2.2.16}$$

Proof. We use h to denote k and H to denote $k-1$. Let $\boldsymbol{f}_h = A_h^c \boldsymbol{u}_h$ and $\boldsymbol{u}_H = P_H \boldsymbol{u}_h$, then we have

$$
\begin{aligned}
a_h^c(\boldsymbol{u}_h, \boldsymbol{v}_h) &= (\boldsymbol{f}_h, \boldsymbol{v}_h) \qquad \text{for all } \boldsymbol{v}_h \in \boldsymbol{U}_h, \\
a_H^c(\boldsymbol{u}_H, \boldsymbol{v}_H) &= a_h^c(\boldsymbol{u}_h, \boldsymbol{v}_H) = (\boldsymbol{f}_h, \boldsymbol{v}_H) \qquad \text{for all } \boldsymbol{v}_H \in \boldsymbol{U}_H.
\end{aligned}
$$

$\boldsymbol{u}_h$, $\boldsymbol{u}_H$ and $\boldsymbol{f}_h$ can be decomposed as in equations (2.2.9)-(2.2.11). Let $I_1 = \boldsymbol{u}_{0,h} - \boldsymbol{u}_{0,H}$, $I_2 = \operatorname{grad}\phi_h - \operatorname{grad}\phi_H$, by Lemmas 2.2.4, 2.2.5 and 2.2.6, it holds

$$
\begin{aligned}
a_h^c((I - P_H)\boldsymbol{u}_h, \boldsymbol{u}_h) &= a_h^c(I_1, \boldsymbol{u}_h) + a_h^c(I_2, \boldsymbol{u}_h) + a_h^c(\boldsymbol{e}_H, \boldsymbol{u}_h) \\
&\leq \|I_1\|\|A_h^c\boldsymbol{u}_h\| + \|I_2\|\|A_h^c\boldsymbol{u}_h\| + \|\boldsymbol{e}_H\|_{A_h^c}\|\boldsymbol{u}_h\|_{A_h^c} \\
&\lesssim H\|\boldsymbol{u}_h\|_{A_h^c}\|A_h^c\boldsymbol{u}_h\|.
\end{aligned}
$$

□

Approximation Property in $\boldsymbol{H}_0(\mathrm{div})$

Let $\boldsymbol{u}_h \in \boldsymbol{V}_h$ be the solution of equation

$$
a_h^d(\boldsymbol{u}_h, \boldsymbol{v}_h) = (\boldsymbol{f}_h, \boldsymbol{v}_h) \qquad \text{for all } \boldsymbol{v}_h \in \boldsymbol{V}_h, \tag{2.2.17}
$$

and $\boldsymbol{u}_H \in \boldsymbol{V}_H \subset \boldsymbol{V}_h$ be the solution of equation

$$
a_H^d(\boldsymbol{u}_H, \boldsymbol{v}_H) = (\boldsymbol{f}_h, \boldsymbol{v}_H) \qquad \text{for all } \boldsymbol{v}_H \in \boldsymbol{V}_H. \tag{2.2.18}
$$

We can easily see that $\boldsymbol{f}_h = A_h^d\boldsymbol{u}_h$. By the Hodge decomposition, we have

$$
\boldsymbol{u}_h = \operatorname{curl}\boldsymbol{\phi}_h \oplus \boldsymbol{u}_{0,h} \quad \boldsymbol{\phi}_h \in \operatorname{curl}_h\boldsymbol{V}_h,\ \boldsymbol{u}_{0,h} \in \operatorname{grad}_h W_h, \tag{2.2.19}
$$

$$
\boldsymbol{u}_H = \operatorname{curl}\boldsymbol{\phi}_H \oplus (\boldsymbol{u}_{0,H} + \boldsymbol{e}_H) \quad \boldsymbol{\phi}_H \in \operatorname{curl}_h\boldsymbol{V}_H,\ \boldsymbol{u}_{0,H} \text{ and } \boldsymbol{e}_H \in \operatorname{grad}_h W_H, \tag{2.2.20}
$$

$$
\boldsymbol{f}_h = \operatorname{curl}\boldsymbol{g}_h \oplus \operatorname{grad}_h q_h \quad \text{for some } \boldsymbol{g}_h \in \operatorname{curl}_h\boldsymbol{V}_h,\ q_h \in W_h, \tag{2.2.21}
$$

where $\boldsymbol{u}_{0,H} \in \operatorname{grad}_h W_H$ is the unique element satisfying

$$\operatorname{div} \boldsymbol{u}_{0,H} = Q_H^W \operatorname{div} \boldsymbol{u}_{0,h}.$$

By Lemma 2.2.3, we immediately have the following result.

Lemma 2.2.7. *Let $\boldsymbol{u}_{0,h} \in \operatorname{grad}_h W_h$ and $\boldsymbol{u}_{0,H} \in \operatorname{grad}_h W_H$ be defined as in equations* (2.2.19) *and* (2.2.20). *It holds*

$$\|\boldsymbol{u}_{0,h} - \boldsymbol{u}_{0,H}\| \lesssim H \| \operatorname{div} \boldsymbol{u}_{0,h}\|.$$

Now we turn to the estimate of $\boldsymbol{e}_H \in \operatorname{grad}_h W_H$ defined in equation (2.2.20).

Lemma 2.2.8. *Assume that $\boldsymbol{e}_H \in \operatorname{grad}_h W_H$ be defined as in equation* (2.2.20). *Then it holds*

$$\|\boldsymbol{e}_H\|_{A_h^d} \lesssim \|A_h^d \boldsymbol{u}_h\|.$$

Proof. The equations (2.2.17) and (2.2.18) imply

$$\begin{aligned}
(\operatorname{div} \boldsymbol{u}_{0,h}, \operatorname{div} \boldsymbol{v}_h) &= -(q_h, \operatorname{div} \boldsymbol{v}_h) \qquad \text{for all } \boldsymbol{v}_h \in \operatorname*{grad}_h W_h, \\
(\operatorname{div} (u_{0,H} + \boldsymbol{e}_H), \operatorname{div} \boldsymbol{v}_H) &= -(q_h, \operatorname{div} \boldsymbol{v}_H) + (\operatorname{curl} \boldsymbol{g}_h, \boldsymbol{v}_H) \quad \text{for all } \boldsymbol{v}_H \in \operatorname*{grad}_H W_H,
\end{aligned}$$

where $\boldsymbol{u}_{0,h}$, $\boldsymbol{u}_{0,H}$, $\boldsymbol{e}_H$, q_h and $\boldsymbol{g}_h$ are defined as in equations (2.2.19)-(2.2.21). Namely $q_h = -\operatorname{div} \boldsymbol{u}_{0,h}$ and

$$(\operatorname{div} \boldsymbol{e}_H, \operatorname{div} \boldsymbol{v}_H) = (\operatorname{curl} \boldsymbol{g}_h, \boldsymbol{v}_H) \quad \text{for all } \ \boldsymbol{v}_H \in \operatorname{grad}_h W_H.$$

Note the fact that for $\boldsymbol{e}_H \in \boldsymbol{V}_H$, there exist $\boldsymbol{e} \in H_0(\operatorname{div})$ and $p \in H_0^1(\Omega)$, such that

$$\begin{cases} \boldsymbol{e} &= \operatorname{grad} p \\ \operatorname{div} \boldsymbol{e} &= \operatorname{div} \boldsymbol{e}_H \end{cases}, \qquad \text{and} \qquad \|\boldsymbol{e} - \boldsymbol{e}_H\| \lesssim H \| \operatorname{div} \boldsymbol{e}_H\|.$$

Then

$$(\operatorname{curl} \boldsymbol{g}_h, e) = (\operatorname{div} \operatorname{curl} \boldsymbol{g}_h, p) = 0.$$

and

$$\begin{aligned}
(\operatorname{div} \boldsymbol{e}_H, \operatorname{div} \boldsymbol{e}_H) &= (\operatorname{curl} \boldsymbol{g}_h, \boldsymbol{e}_H) = (\operatorname{curl} \boldsymbol{g}_h, \boldsymbol{e}_H - \boldsymbol{e}) \\
&\leq \|\operatorname{curl} \boldsymbol{g}_h\| \|\boldsymbol{e}_H - \boldsymbol{e}\| \lesssim H \|\operatorname{curl} \boldsymbol{g}_h\| \|\operatorname{div} \boldsymbol{e}_H\| \\
&\lesssim \|A_h^d \boldsymbol{u}_h\| \|\operatorname{div} \boldsymbol{e}_H\|.
\end{aligned}$$

Which implies

$$\|\operatorname{div} \boldsymbol{e}_H\| \lesssim H \|A_h^d \boldsymbol{u}_h\|.$$

Now we turn to the estimate of $\|\operatorname{curl}_h \boldsymbol{e}_H\|$. Note that we can also find $\boldsymbol{e}_h \in \operatorname{grad}_h W_h$ and $p_h \in W_h$ satisfying

$$\begin{cases} \boldsymbol{e}_h &= \operatorname{grad}_h p_h \\ \operatorname{div} \boldsymbol{e}_h &= \operatorname{div} \boldsymbol{e}_H \end{cases}, \qquad \text{and} \qquad \|\boldsymbol{e}_h - \boldsymbol{e}_H\| \lesssim H \|\operatorname{div} \boldsymbol{e}_H\|.$$

Then by inverse inequality it holds

$$\|\operatorname{curl}_h \boldsymbol{e}_H\| = \|\operatorname{curl}_h (e_H - e_h)\| \lesssim h^{-1} \|\boldsymbol{e}_H - \boldsymbol{e}_h\| \lesssim \|\operatorname{div} \boldsymbol{e}_H\|.$$

The desired result follows. $\square$

We now explore the relation between $\boldsymbol{\phi}_h$, $\boldsymbol{\phi}_H$, and $\boldsymbol{g}_h$ defined in equations (2.2.19)-(2.2.21). Firstly, we define

$$M = \operatorname{grad} H_0^1(\Omega) \qquad \text{and} \qquad M_h = \operatorname{grad} S_h,$$

and

$$M^\perp = \left\{ \boldsymbol{u} \in \boldsymbol{H}_0(\operatorname{curl}) | \, (\boldsymbol{u}, \operatorname{grad} s) = 0, \quad \text{for all } s \in H_0^1(\Omega) \right\} \quad \text{and} \quad M_h^\perp = \operatorname{curl}_h \boldsymbol{V}_h.$$

Then we have the following lemma.

Lemma 2.2.9. *Assume that $\boldsymbol{\psi}_h \in M_h^{\perp}$, let $\boldsymbol{\zeta}_h \in M_h^{\perp}$ be the solution of equation*

$$(\operatorname{curl} \boldsymbol{\zeta}_h, \operatorname{curl} \boldsymbol{\tau}_h) = (\boldsymbol{\psi}_h, \boldsymbol{\tau}_h) \qquad \text{for all } \boldsymbol{\tau}_h \in M_h^{\perp},$$

and $\boldsymbol{\zeta} \in M^{\perp}$ be the solution of equation

$$\begin{cases} (\operatorname{curl} \boldsymbol{\zeta}, \operatorname{curl} \boldsymbol{\tau}) &= (Q^{M^{\perp}} \boldsymbol{\psi}_h, \boldsymbol{\tau}) \quad \text{for all } \boldsymbol{\tau} \in M^{\perp} \\ \operatorname{div} \boldsymbol{\zeta} &= 0 \end{cases}$$

where $Q^{M^{\perp}} : \boldsymbol{H}_0(\operatorname{curl}) \mapsto M^{\perp}$ is the L^2 projection operator. Then, it holds

$$\| \operatorname{curl}(\boldsymbol{\zeta} - \boldsymbol{\zeta}_h) \| \lesssim h \| \boldsymbol{\psi}_h \|.$$

Proof. By the definition of $\boldsymbol{\zeta}$ and $\boldsymbol{\zeta}_h$, we have

$$(\operatorname{curl}(\boldsymbol{\zeta} - \boldsymbol{\zeta}_h), \operatorname{curl} \boldsymbol{\tau}_h) = (\boldsymbol{\psi}_h - Q_h^{M^{\perp}} \boldsymbol{\psi}_h, \boldsymbol{\tau}_h) \qquad \text{for all } \boldsymbol{\tau}_h \in \boldsymbol{U}_h.$$

Thus

$$\begin{aligned} \| \operatorname{curl}(\boldsymbol{\zeta} - \boldsymbol{\zeta}_h) \|^2 &= (\operatorname{curl}(\boldsymbol{\zeta} - \boldsymbol{\zeta}_h), \operatorname{curl}(\boldsymbol{\zeta} - \Pi_h^U \boldsymbol{\zeta})) + (\operatorname{curl}(\boldsymbol{\zeta} - \boldsymbol{\zeta}_h), \operatorname{curl}(\Pi_h^U \boldsymbol{\zeta} - \boldsymbol{\zeta}_h)) \\ &= (\operatorname{curl}(\boldsymbol{\zeta} - \boldsymbol{\zeta}_h), \operatorname{curl}(\boldsymbol{\zeta} - \Pi_h^U \boldsymbol{\zeta})) + (\boldsymbol{\psi}_h - Q_h^{M^{\perp}} \boldsymbol{\psi}_h, (\Pi_h^U \boldsymbol{\zeta} - \boldsymbol{\zeta}_h)) \\ &\lesssim h \| \operatorname{curl}(\boldsymbol{\zeta} - \boldsymbol{\zeta}_h) \| \| \operatorname{curl} \boldsymbol{\zeta} \|_1 + \left| (\boldsymbol{\psi}_h - Q_h^{M^{\perp}} \boldsymbol{\psi}_h, (\Pi_h^U \boldsymbol{\zeta} - \boldsymbol{\zeta}_h)) \right| \\ &\lesssim h \| \operatorname{curl}(\boldsymbol{\zeta} - \boldsymbol{\zeta}_h) \| \| \boldsymbol{\psi}_h \| + \left| (\boldsymbol{\psi}_h - Q_h^{M^{\perp}} \boldsymbol{\psi}_h, (\Pi_h^U \boldsymbol{\zeta} - \boldsymbol{\zeta}_h)) \right|. \end{aligned}$$

We can decompose $\Pi_h^U \boldsymbol{\zeta} - \boldsymbol{\zeta}_h$ as

$$\Pi_h^U \boldsymbol{\zeta} - \boldsymbol{\zeta}_h = \boldsymbol{w} + \operatorname{grad} p, \qquad \boldsymbol{w} \in M^{\perp},\ p \in H_0^1(\Omega),$$

and we can also write $\Pi_h^U \boldsymbol{\zeta} - \boldsymbol{\zeta}_h$ as

$$\Pi_h^U \boldsymbol{\zeta} - \boldsymbol{\zeta}_h = \Pi_h^U \boldsymbol{w} + \operatorname{grad} p_h, \qquad \boldsymbol{w} \in M^{\perp},\ p_h \in S_h.$$

Thus

$$
\begin{aligned}
(\boldsymbol{\psi}_h - Q_h^{M^\perp}\boldsymbol{\psi}_h, (\Pi_h^U \boldsymbol{\zeta} - \boldsymbol{\zeta}_h)) &= (\boldsymbol{\psi}_h - Q_h^{M^\perp}\boldsymbol{\psi}_h, \Pi_h^U \boldsymbol{w}) = (\boldsymbol{\psi}_h - Q_h^{M^\perp}\boldsymbol{\psi}_h, \Pi_h^U \boldsymbol{w} - \boldsymbol{w}) \\
&\lesssim h\|\boldsymbol{\psi}_h - Q_h^{M^\perp}\boldsymbol{\psi}_h\|\|\boldsymbol{w}\|_1 \lesssim h\|\boldsymbol{\psi}_h\|\|\operatorname{curl}\boldsymbol{w}\| \\
&= h\|\boldsymbol{\psi}_h\|\|\operatorname{curl}(\Pi_h^U \boldsymbol{\zeta} - \boldsymbol{\zeta}_h)\| = h\|\boldsymbol{\psi}_h\|\|\Pi_h^V \operatorname{curl}(\boldsymbol{\zeta} - \boldsymbol{\zeta}_h)\| \\
&\lesssim h\|\boldsymbol{\psi}_h\|\|\operatorname{curl}(\boldsymbol{\zeta} - \boldsymbol{\zeta}_h)\|.
\end{aligned}
$$

The desired result follows. □

Lemma 2.2.10. *Let $\boldsymbol{\phi}_h \in \boldsymbol{U}_h$ and $\boldsymbol{\phi}_H \in \boldsymbol{U}_H$ be defined as in equations* (2.2.19) *and* (2.2.20). *It holds*

$$\|\operatorname{curl}\boldsymbol{\phi}_h - \operatorname{curl}\boldsymbol{\phi}_H\| \lesssim H\|\boldsymbol{u}_h\|_{A_h^d}.$$

Proof. Let $\boldsymbol{v}_h = \operatorname{curl}\boldsymbol{w}_h$, $\boldsymbol{w}_h \in \boldsymbol{U}_h$, equation (2.2.17) implies

$$
\begin{aligned}
(\operatorname{curl}_h \boldsymbol{u}_h, \operatorname{curl}_h \operatorname{curl}\boldsymbol{w}_h) &= (\operatorname{curl}_h \operatorname{curl}\phi_h, \operatorname{curl}_h \operatorname{curl}\boldsymbol{w}_h) = (\operatorname{curl}\phi_h, \operatorname{curl}\operatorname{curl}_h \operatorname{curl}\boldsymbol{w}_h) \\
&= (\boldsymbol{f}_h, \operatorname{curl}\boldsymbol{w}_h) = (\operatorname{curl}\boldsymbol{g}_h, \operatorname{curl} w_h) = (\boldsymbol{g}_h, \operatorname{curl}_h \operatorname{curl}\boldsymbol{w}_h)
\end{aligned}
$$

Let $\tau_h = \operatorname{curl}_h \operatorname{curl}\boldsymbol{w}_h \in \operatorname{curl}_h \boldsymbol{V}_h \subset \boldsymbol{U}_h$, we get

$$(\operatorname{curl}\phi_h, \operatorname{curl}\tau_h) = (\boldsymbol{g}_h, \tau_h) \qquad \text{for all } \tau_h \in \operatorname{curl}_h \operatorname{curl}\boldsymbol{U}_h = \operatorname{curl}_h \boldsymbol{V}_h.$$

Which implies $\operatorname{curl}_h \operatorname{curl}\boldsymbol{\phi}_h = \operatorname{curl}_h \boldsymbol{u}_h = \boldsymbol{g}_h$. We can see that $\boldsymbol{\phi}_h$ is the Galerkin projection of $\boldsymbol{\phi}$ to $\operatorname{curl}_h \boldsymbol{V}_h \subset \boldsymbol{U}_h$, where $\boldsymbol{\phi} \in M^\perp$ satisfying the Maxwell equation:

$$\operatorname{curl}\operatorname{curl}\boldsymbol{\phi} = Q^{M^\perp}\boldsymbol{g}_h, \qquad \operatorname{div}\boldsymbol{\phi} = 0.$$

Therefore by Lemma 2.2.9, we have

$$\|\operatorname{curl}(\boldsymbol{\phi}-\boldsymbol{\phi}_h)\| \lesssim h\|\boldsymbol{g}_h\|.$$

Similarly, equation (2.2.18) implies

$$(\operatorname{curl}\phi_H, \operatorname{curl}\tau_H) = (\boldsymbol{g}_H, \tau_H) \qquad \text{for all } \tau_H \in \operatorname{curl}_h \operatorname{curl} \boldsymbol{U}_H = \operatorname{curl}_h \boldsymbol{V}_H.$$

where $\boldsymbol{g}_H = P_H^U g_h$ and $P_H^U : \operatorname{curl}_h \boldsymbol{V}_h \mapsto \operatorname{curl}_h \boldsymbol{V}_H$ is a projection in $(\operatorname{curl}(\cdot), \operatorname{curl}(\cdot))$. Which implies $\operatorname{curl}_h \operatorname{curl} \boldsymbol{\phi}_H = P_H^U \boldsymbol{g}_h$. We can see that $\boldsymbol{\phi}_H$ is the Galerkin projection of $\tilde{\boldsymbol{\phi}}$ to $\operatorname{curl}_h \boldsymbol{V}_H$, where $\tilde{\boldsymbol{\phi}} \in H_0(\operatorname{curl})$ satisfies the Maxwell equation:

$$\operatorname{curl}\operatorname{curl}\tilde{\boldsymbol{\phi}} = Q^{M^\perp} P_H^U \boldsymbol{g}_h, \qquad \operatorname{div}\tilde{\boldsymbol{\phi}} = 0.$$

The $H(\operatorname{curl})$-projection P_H^U is not stable in L^2-norm. However, applied to functions in $\boldsymbol{U}_h$, we can recover one as follows

$$\|(I-P_H^U)\boldsymbol{g}_h\| \lesssim H\|\operatorname{curl}(I-P_H^U)\boldsymbol{g}_h\| \lesssim H\|\operatorname{curl}\boldsymbol{g}_h\| \lesssim H/h\|\boldsymbol{g}_h\| \lesssim \|\boldsymbol{g}_h\|.$$

In the last step, we use the fact that the ratio of the mesh size between consecutive levels is bounded, i.e., $H/h \le C$. We then have

$$\|\operatorname{curl}(\tilde{\boldsymbol{\phi}}-\boldsymbol{\phi}_H)\| \lesssim H\|P_H^U\boldsymbol{g}_h\| \le H\|\boldsymbol{g}_h\| + H\|(I-P_H^U)\boldsymbol{g}_h\| \lesssim H\|\boldsymbol{g}_h\|.$$

Now we turn to the estimate of $\|\operatorname{curl}(\boldsymbol{\phi}-\tilde{\boldsymbol{\phi}})\|$. We have $\boldsymbol{\phi}$ and $\tilde{\boldsymbol{\phi}}$ in $M^\perp$, satisfying

$$\begin{cases} (\operatorname{curl}\boldsymbol{\phi}, \operatorname{curl}\boldsymbol{\psi}) &=& (Q^{M^\perp}\boldsymbol{g}_h, \boldsymbol{\psi}) \quad \text{for all } \boldsymbol{\psi} \in M^\perp \\ (\boldsymbol{\phi}, \boldsymbol{\psi}) &=& 0 \end{cases}$$

and

$$\begin{cases} (\operatorname{curl}\tilde{\boldsymbol{\phi}}, \operatorname{curl}\boldsymbol{\psi}) &=& (Q^{M^\perp}\boldsymbol{g}_H, \boldsymbol{\psi}) \quad \text{for all } \boldsymbol{\psi} \in M^\perp \\ (\tilde{\boldsymbol{\phi}}, \boldsymbol{\psi}) &=& 0 \end{cases}$$

Thus, for all $\boldsymbol{\psi} \in M^{\perp}$

$$(\operatorname{curl}(\boldsymbol{\phi} - \tilde{\boldsymbol{\phi}}), \operatorname{curl} \boldsymbol{\psi}) = (\boldsymbol{g}_h - \boldsymbol{g}_H, \boldsymbol{\psi}) = (\tilde{\boldsymbol{g}}_h - \tilde{\boldsymbol{g}}_H, \boldsymbol{\psi}),$$

where $\tilde{\boldsymbol{g}}_h$ and $\tilde{\boldsymbol{g}}_H$ are in $M^{\perp}$ and satisfying $\operatorname{curl} \tilde{\boldsymbol{g}}_h = \operatorname{curl} \boldsymbol{g}_h$ and $\operatorname{curl} \tilde{\boldsymbol{g}}_H = \operatorname{curl} \boldsymbol{g}_H$, respectively. Let $\boldsymbol{\zeta} \in M^{\perp}$ satisfying

$$\begin{cases} (\operatorname{curl} \boldsymbol{\zeta}, \operatorname{curl} \boldsymbol{\tau}) &= (\boldsymbol{\psi}, \boldsymbol{\tau}) \quad \text{for all } \boldsymbol{\tau} \in M^{\perp} \\ \operatorname{div} \boldsymbol{\zeta} &= 0 \end{cases}$$

Then,

$$\begin{aligned} (\tilde{\boldsymbol{g}}_h - \tilde{\boldsymbol{g}}_H, \boldsymbol{\psi}) &= (\operatorname{curl} \boldsymbol{\zeta}, \operatorname{curl}(\tilde{\boldsymbol{g}}_h - \tilde{\boldsymbol{g}}_H)) = (\operatorname{curl} \boldsymbol{\zeta}, \operatorname{curl}(\boldsymbol{g}_h - \boldsymbol{g}_H)) \\ &= (\operatorname{curl}(\boldsymbol{\zeta} - P_H^U \boldsymbol{\zeta}), \operatorname{curl}(\boldsymbol{g}_h - \boldsymbol{g}_H)) \\ &\leq \| \operatorname{curl}(\boldsymbol{\zeta} - P_H^U \boldsymbol{\zeta}) \| \| \operatorname{curl}(\boldsymbol{g}_h - \boldsymbol{g}_H) \| \\ &\lesssim H \| \operatorname{curl} \boldsymbol{\zeta} \|_2 \| \boldsymbol{g}_h \| \lesssim H \| \operatorname{curl} \boldsymbol{\psi} \| \| \boldsymbol{g}_h \|. \end{aligned}$$

which implies

$$\| \operatorname{curl}(\boldsymbol{\phi} - \tilde{\boldsymbol{\phi}}) \| \lesssim H \| \boldsymbol{g}_h \|.$$

Then

$$\| \operatorname{curl}(\boldsymbol{\phi}_h - \boldsymbol{\phi}_H) \| \leq \| \operatorname{curl}(\boldsymbol{\phi}_h - \boldsymbol{\phi}) \| + \| \operatorname{curl}(\boldsymbol{\phi}_H - \tilde{\boldsymbol{\phi}}) \| + \| \operatorname{curl}(\boldsymbol{\phi} - \tilde{\boldsymbol{\phi}}) \| \lesssim H \| \boldsymbol{g}_h \|.$$

□

As a summary the the above results, we have the following theorem.

Theorem 2.2.2. *Condition (A.1) holds with $\alpha = \frac{1}{2}$, i.e. for any $\boldsymbol{u}_k \in \boldsymbol{V}_k$, there hold*

$$a_k^d((I - P_{k-1}) \boldsymbol{u}_k, \boldsymbol{u}_k) \lesssim \left(\frac{\| A_k^d \boldsymbol{u}_k \|^2}{\lambda_k} \right)^{\frac{1}{2}} a_k^d(\boldsymbol{u}_k, \boldsymbol{u}_k)^{\frac{1}{2}}. \tag{2.2.22}$$

Proof. We use h to denote k and H to denote $k-1$. Let $\boldsymbol{f}_h = A_h^d \boldsymbol{u}_h$ and $\boldsymbol{u}_H = P_H \boldsymbol{u}_h$, then we have

$$\begin{aligned} a_h^d(\boldsymbol{u}_h, \boldsymbol{v}_h) &= (\boldsymbol{f}_h, \boldsymbol{v}_h) \qquad \text{for all } \boldsymbol{v}_h \in \boldsymbol{V}_h, \\ a_H^d(\boldsymbol{u}_H, \boldsymbol{v}_H) &= a_h^d(\boldsymbol{u}_h, \boldsymbol{v}_H) = (\boldsymbol{f}_h, \boldsymbol{v}_H) \qquad \text{for all } \boldsymbol{v}_H \in \boldsymbol{V}_H. \end{aligned}$$

$\boldsymbol{u}_h$, $\boldsymbol{u}_H$ and $\boldsymbol{f}_h$ can be decomposed as in equations (2.2.9)-(2.2.11). Let $I_1 = \boldsymbol{u}_{0,h} - \boldsymbol{u}_{0,H}$, $I_2 = \operatorname{curl} \boldsymbol{\phi}_h - \operatorname{curl} \boldsymbol{\phi}_H$, by Lemmas 2.2.7, 2.2.8 and 2.2.10, it holds

$$\begin{aligned} a_h^d((I-P_H)\boldsymbol{u}_h, \boldsymbol{u}_h) &= a_h^d(I_1, \boldsymbol{u}_h) + a_h^d(I_2, \boldsymbol{u}_h) + a_h^d(\boldsymbol{e}_H, \boldsymbol{u}_h) \\ &\le \|I_1\| \|A_h^d \boldsymbol{u}_h\| + \|I_2\| \|A_h^d \boldsymbol{u}_h\| + \|\boldsymbol{e}_H\|_{A_h^d} \|\boldsymbol{u}_h\|_{A_h^d} \\ &\lesssim H \|\boldsymbol{u}_h\|_{A_h^d} \|A_h^d \boldsymbol{u}_h\|. \end{aligned}$$

□

2.2.6 Results

According to the multigrid framework in [8], we conclude that the variable V-cycle multigrid algorithm is a good preconditioner for the Schur complement equations (2.1.6) and (2.1.11). We summarize the result in the following theorem.

Theorem 2.2.3. *Let V_k denote the operator of one V-ycle of MG_k in Algorithm 2 with homogenous data, i.e., $\boldsymbol{f}_k = 0$. Assume the smoothing steps m_k satisfy*

$$\beta_0 m_k \le m_{k-1} \le \beta_1 m_k.$$

Here we assume that β_0 and β_1 are constants which are greater than one and independent of k. Then the condition number of $V_J A_J$ is $\mathcal{O}(1)$.

Remark 2.2.4. *As noticed in [9], W-cycle or two V-cycles may not be a valid preconditioner as the corresponding operator may not be positive definite. In other words, the proposed multigrid* *method for the Schur complement cannot be used as an iterative method but one V-cycle can be used as an effective preconditioner.*

2.3 Uniform Preconditioner

In this section, we will show that the multigrid solver for the Schur complement equations can be used to build efficient preconditioners for the mixed formulations of vector Laplacian (2.1.4) and (2.1.10). We also apply the multigrid preconditioner of the vector Laplacian to the Maxwell equation discretized as a saddle point system. We prove that the preconditioned systems have condition numbers independent of mesh parameter h.

2.3.1 Block Diagonal Preconditioner

It is easy to see that the inverses of the symmetric positive definite matrices M_v, M_e, A_h^c and A_h^d exist, which implies the existence of the operators $(\mathcal{L}_h^c)^{-1}$, $(\mathcal{L}_h^d)^{-1}$, and the block diagonal preconditioners defined as following.

Definition 2.3.1. *We define the operator $\mathcal{P}_h^c : S_h' \times \boldsymbol{U}_h' \to S_h \times \boldsymbol{U}_h$ with the matrix representation*

$$\mathcal{P}_h^c = \begin{pmatrix} M_v^{-1} & 0 \\ 0 & (A_h^c)^{-1} \end{pmatrix}, \tag{2.3.1}$$

and the operator $\mathcal{P}_h^d : \boldsymbol{U}_h' \times \boldsymbol{V}_h' \to \boldsymbol{U}_h \times \boldsymbol{V}_h$ with the matrix representation

$$\mathcal{P}_h^d = \begin{pmatrix} M_e^{-1} & 0 \\ 0 & (A_h^d)^{-1} \end{pmatrix}. \tag{2.3.2}$$

In the sequel, to unify the notation, we use M for the mass matrix and A the vector Laplacian. The inverse of the mass matrix can be thought of as the matrix representation of the Riesz representation induced by the L^2-inner product and the inverse of A is the Riesz representation of the A-inner product. The preconditioners $\mathcal{P}_h^c$ and $\mathcal{P}_h^d$ are Riesz representation of $L^2 \times A$-inner product. Let $\langle \cdot, \cdot \rangle$ be the duality pair. We clarify the norm notations using M and A as follows:

- $\| \cdot \|_M$: $\quad \|\sigma_h\|_M^2 = \langle M\sigma_h, \sigma_h \rangle$;
- $\| \cdot \|_A$: $\quad \|u_h\|_A^2 = \langle A_h u_h, u_h \rangle$;
- $\| \cdot \|_{M^{-1}}$: $\|g_h\|_{M^{-1}}^2 = \langle M^{-1} g_h, g_h \rangle$;
- $\| \cdot \|_{A^{-1}}$: $\|f_h\|_{A^{-1}}^2 = \langle A_h^{-1} f_h, f_h \rangle$.

Follow the framework in [24], it suffices to prove the boundedness of operators $\mathcal{L}_h^c$ and $\mathcal{L}_h^d$ and their inverse in the appropriate norms. The following lemma gives a bound of the Schur complement $BA^{-1}B^T$ similar to the corresponding result of the Stokes equation.

Lemma 2.3.1. *We have the inequality*

$$\langle B(A_h^c)^{-1} B^T \phi_h, \phi_h \rangle \leq \langle M_v \phi_h, \phi_h \rangle \quad \textit{for all } \phi_h \in S_h, \tag{2.3.3}$$

Proof. Let $\boldsymbol{v}_h = (A_h^c)^{-1} B^T \phi_h$. Then

$$\langle B(A_h^c)^{-1} B^T \phi_h, \phi_h \rangle = \langle (A_h^c)^{-1} B^T \phi_h, B^T \phi_h \rangle = \langle A_h^c \boldsymbol{v}_h, \boldsymbol{v}_h \rangle = \|\boldsymbol{v}_h\|_A^2.$$

Now we identify $\boldsymbol{v}_h \in \boldsymbol{V}_h'$ by the Riesz map in the A-inner product, and then we have

$$\begin{aligned} \|\boldsymbol{v}_h\|_A &= \sup_{\boldsymbol{u}_h \in \boldsymbol{V}_h} \frac{(\boldsymbol{v}_h, \boldsymbol{u}_h)_A}{\|\boldsymbol{u}_h\|_A} = \sup_{\boldsymbol{u}_h \in \boldsymbol{V}_h} \frac{\langle B^T \phi_h, \boldsymbol{u}_h \rangle}{\|\boldsymbol{u}_h\|_A} = \sup_{\boldsymbol{u}_h \in \boldsymbol{V}_h} \frac{\langle \phi_h, B\boldsymbol{u}_h \rangle}{\|\boldsymbol{u}_h\|_A} \\ &\leq \sup_{\boldsymbol{u}_h \in \boldsymbol{V}_h} \frac{\|\phi_h\|_M \|B\boldsymbol{u}_h\|_{M^{-1}}}{\|\boldsymbol{u}_h\|_A} \leq \|\phi_h\|_M. \end{aligned}$$

In the last step, we have used the identity (2.1.5) which implies $\|B\boldsymbol{u}_h\|_{M^{-1}} \leq \|\boldsymbol{u}_h\|_A$. The desirable result (2.3.3) then follows easily. $\square$

We present a stability result of the mixed formulation of vector Laplacian which is different with that established in [2].

Theorem 2.3.2. *The operators $\mathcal{L}_h^c, \mathcal{L}_h^d$ and there inverse are both bounded operators:*

$$\|\mathcal{L}_h^c\|_{\mathrm{L}(S_h\times\boldsymbol{U}_h, S_h'\times\boldsymbol{U}_h')}, \|\mathcal{L}_h^d\|_{\mathrm{L}(\boldsymbol{U}_h\times\boldsymbol{V}_h,\boldsymbol{U}_h'\times\boldsymbol{V}_h')},$$

are bounded and independent of h from $(\|\cdot\|_{M^{-1}}, \|\cdot\|_{A^{-1}}) \to (\|\cdot\|_M, \|\cdot\|_A)$, and

$$\|(\mathcal{L}_h^c)^{-1}\|_{\mathrm{L}(S_h'\times\boldsymbol{U}_h', S_h\times\boldsymbol{U}_h)}, \|(\mathcal{L}_h^d)^{-1}\|_{\mathrm{L}(\boldsymbol{U}_h'\times\boldsymbol{V}_h',\boldsymbol{U}_h\times\boldsymbol{V}_h)}$$

are bounded and independent of h from $(\|\cdot\|_M, \|\cdot\|_A) \to (\|\cdot\|_{M^{-1}}, \|\cdot\|_{A^{-1}})$.

Proof. We prove the $\boldsymbol{H}_0(\mathrm{curl})$ case below. The proof of the $\boldsymbol{H}_0(\mathrm{div})$ case is similar.

Let $(\sigma_h, \boldsymbol{u}_h) \in S_h \times \boldsymbol{U}_h$ and $(g_h, \boldsymbol{f}_h) \in S_h' \times \boldsymbol{U}_h'$ be given by the relation with

$$\mathcal{L}_h^c \begin{pmatrix} \sigma_h \\ \boldsymbol{u}_h \end{pmatrix} = \begin{pmatrix} -M_v & B \\ B^T & C^T M_f C \end{pmatrix} \begin{pmatrix} \sigma_h \\ \boldsymbol{u}_h \end{pmatrix} = \begin{pmatrix} g_h \\ \boldsymbol{f}_h \end{pmatrix}. \tag{2.3.4}$$

To prove $\|\mathcal{L}_h^c\|_{\mathrm{L}(S_h\times\boldsymbol{U}_h, S_h'\times\boldsymbol{U}_h')} \lesssim 1$, it is sufficient to prove

$$\|g_h\|_{M^{-1}} + \|\boldsymbol{f}_h\|_{A^{-1}} \lesssim \|\sigma_h\|_M + \|\boldsymbol{u}_h\|_A. \tag{2.3.5}$$

From (2.3.4), we have $g_h = -M_v\sigma_h + B\boldsymbol{u}_h$ and $\boldsymbol{f}_h = A_h^c\boldsymbol{u}_h - B^T M_v^{-1} g_h$. The norm of g_h is easy to bound as follows

$$\|g_h\|_{M^{-1}}^2 \leq 2\|M_v\sigma_h\|_{M^{-1}}^2 + 2\|B\boldsymbol{u}_h\|_{M^{-1}}^2 \leq 2\|\sigma_h\|_M^2 + 2\|\boldsymbol{u}_h\|_A^2.$$

To bound the norm of $\boldsymbol{f}_h$, we first have

$$\|\boldsymbol{f}_h\|_{A^{-1}}^2 \leq 2\|B^T M_v^{-1} g_h\|_{A^{-1}}^2 + 2\|A_h^c \boldsymbol{u}_h\|_{A^{-1}}^2 \leq 2\|B^T M_v^{-1} g_h\|_{A^{-1}}^2 + 2\|\boldsymbol{u}_h\|_A^2.$$

Let $\phi_h = M_v^{-1} g_h$, by Lemma 2.3.1, we have

$$\|B^T M_v^{-1} g_h\|_{A^{-1}}^2 = \|B^T \phi_h\|_{A^{-1}}^2 = \langle B(A_h^c)^{-1} B^T \phi_h, \phi_h\rangle \leq \|\phi_h\|_M^2 = \|g_h\|_{M^{-1}}^2.$$

Thus we get

$$\|\boldsymbol{f}_h\|_{A^{-1}}^2 \leq 2\|g_h\|_{M^{-1}}^2 + 2\|\boldsymbol{u}_h\|_A^2 \leq 4\|\sigma_h\|_M^2 + 6\|\boldsymbol{u}_h\|_A^2.$$

Then the desired inequality (2.3.5) follows from the bound of $\|g_h\|_{M^{-1}}$ and $\|\boldsymbol{f}_h\|_{A^{-1}}$.

To prove $\|(\mathcal{L}_h^c)^{-1}\|_{\mathrm{L}(S_h' \times \boldsymbol{U}_h', S_h \times \boldsymbol{U}_h)} \lesssim 1$, we need to prove

$$\|\sigma_h\|_M + \|\boldsymbol{u}_h\|_A \lesssim \|g_h\|_{M^{-1}} + \|\boldsymbol{f}_h\|_{A^{-1}}. \tag{2.3.6}$$

From (2.3.4), we have $\boldsymbol{u}_h = (A_h^c)^{-1}(f_h + B^T M_v^{-1} g_h)$. Then

$$\begin{aligned} \|\boldsymbol{u}_h\|_A^2 &= \|\boldsymbol{f}_h + B^T M_v^{-1} g_h\|_{A^{-1}}^2 \\ &\leq 2\|\boldsymbol{f}_h\|_{A^{-1}}^2 + 2\|B^T M_v^{-1} g_h\|_{A^{-1}}^2 \leq 2\|\boldsymbol{f}_h\|_{A^{-1}}^2 + 2\|g_h\|_{M^{-1}}^2. \end{aligned}$$

We also have $\sigma_h = M_v^{-1}(B\boldsymbol{u}_h - g_h)$ and thus

$$\|\sigma_h\|_M^2 = \|B\boldsymbol{u}_h - g_h\|_{M^{-1}}^2 \leq 2\|B\boldsymbol{u}_h\|_{M^{-1}}^2 + 2\|g_h\|_{M^{-1}}^2 \leq 2\|\boldsymbol{u}_h\|_A^2 + 2\|g_h\|_{M^{-1}}^2.$$

Combining with the bound for $\|\boldsymbol{u}_h\|_A$, we obtain the desirable stability (2.3.6).

□

From Theorem 2.3.2, we can conclude that the proposed preconditioners are uniformly bounded with respect to h.

Theorem 2.3.3. *The $\mathcal{P}_h^c$ and $\mathcal{P}_h^d$ are uniform preconditioners for $\mathcal{L}_h^c$ and $\mathcal{L}_h^d$, respectively, i.e., the* *corresponding operator norms*

$$\|\mathcal{P}_h^c\mathcal{L}_h^c\|_{\mathrm{L}(S_h\times\boldsymbol{U}_h,S_h\times\boldsymbol{U}_h)}, \|(\mathcal{L}_h^c\mathcal{P}_h^c)^{-1}\|_{\mathrm{L}(S_h\times\boldsymbol{U}_h,S_h\times\boldsymbol{U}_h)},$$
$$\|\mathcal{P}_h^d\mathcal{L}_h^d\|_{\mathrm{L}(\boldsymbol{U}_h\times\boldsymbol{V}_h,\boldsymbol{U}_h\times\boldsymbol{V}_h)}, \|(\mathcal{P}_h^d\mathcal{L}_h^d)^{-1}\|_{\mathrm{L}(\boldsymbol{U}_h\times\boldsymbol{V}_h,\boldsymbol{U}_h\times\boldsymbol{V}_h)}$$

are bounded and independent with parameter h.

2.3.2 Mass Lumping

The inverse of the mass matrices M_v^{-1} and M_e^{-1} are in general dense. To be practical, the exact Schur complement can be replaced by an approximation

$$\tilde{A}_h^c = B^T\tilde{M}_v^{-1}B + C^TM_fC, \tag{2.3.7}$$
$$\tilde{A}_h^d = C\tilde{M}_e^{-1}C^T + B^TM_tB, \tag{2.3.8}$$

with $\tilde{M}_v$ and $\tilde{M}_e$ easy-to-invert matrices, e.g., diagonal or mass lumping of M_v and M_e, respectively. In this way, we actually change the L^2-inner product of spaces S_h and $\boldsymbol{U}_h$ into a discrete L^2 inner product. We then define the adjoint operators with respect to the discrete L^2-inner product. For example, we define $\widetilde{\mathrm{div}}_h\boldsymbol{w}_h \in S_h$, s.t.,

$$\langle\widetilde{\mathrm{div}}_h\boldsymbol{w}_h, v_h\rangle_h := -(\boldsymbol{w}_h, \mathrm{grad}\, v_h) \quad \text{for all } v_h \in S_h, \tag{2.3.9}$$

where $\langle\cdot,\cdot\rangle_h$ is the discrete L^2-inner product defined by $\tilde{M}_v$.

The operator and matrix formulations of the vector Laplacian $\widetilde{\mathcal{L}_h^c} : S_h\times\boldsymbol{U}_h \to S_h'\times\boldsymbol{U}_h'$

$$\widetilde{\mathcal{L}_h^c}\begin{pmatrix}\sigma_h\\ \boldsymbol{u}_h\end{pmatrix} := \begin{pmatrix}-\tilde{M}_v & B\\ B^T & C^TM_fC\end{pmatrix}\begin{pmatrix}\sigma_h\\ \boldsymbol{u}_h\end{pmatrix} = \begin{pmatrix}0\\ \boldsymbol{f}\end{pmatrix}. \tag{2.3.10}$$

And $\widetilde{\mathcal{L}_h^d} : \boldsymbol{U}_h \times \boldsymbol{V}_h \to \boldsymbol{U}'_h \times \boldsymbol{V}'_h$

$$\widetilde{\mathcal{L}_h^d} \begin{pmatrix} \boldsymbol{\sigma}_h \\ \boldsymbol{u}_h \end{pmatrix} := \begin{pmatrix} -\tilde{M}_e & C^T \\ C & B^T M_t B \end{pmatrix} \begin{pmatrix} \boldsymbol{\sigma}_h \\ \boldsymbol{u}_h \end{pmatrix} = \begin{pmatrix} 0 \\ \boldsymbol{f} \end{pmatrix}. \tag{2.3.11}$$

The associated diagonal preconditioners are

$$\widetilde{\mathcal{P}_h^c} = \begin{pmatrix} \tilde{M}_v^{-1} & 0 \\ 0 & (\tilde{A}_h^c)^{-1} \end{pmatrix} \tag{2.3.12}$$

and

$$\widetilde{\mathcal{P}_h^d} = \begin{pmatrix} \tilde{M}_e^{-1} & 0 \\ 0 & (\tilde{A}_h^d)^{-1} \end{pmatrix}. \tag{2.3.13}$$

It is not hard to see that the modification of the L^2-inner product will not bring any essential difficulty to the proof of the previous results. We can easily reproduce all the results that we have proved in the previous sections with the help of the following proposition whose proof can be found in [66].

Proposition 2.3.4. *Assume that the discrete L^2 norm is equivalent to the L^2 norm. Then the norm $\|\cdot\|_{\widetilde{A}_h^c}$ is equivalent to $\|\cdot\|_{A_h^c}$, and $\|\cdot\|_{\widetilde{A}_h^d}$ is equivalent to $\|\cdot\|_{A_h^d}$ i.e.,*

$$\|\boldsymbol{u}\|_{\widetilde{A}_h^c} \lesssim \|\boldsymbol{u}\|_{A_h^c} \lesssim \|\boldsymbol{u}\|_{\widetilde{A}_h^c} \quad \textit{for all } \boldsymbol{u} \in \boldsymbol{U}_h; \tag{2.3.14}$$

$$\|\boldsymbol{u}\|_{\widetilde{A}_h^d} \lesssim \|\boldsymbol{u}\|_{A_h^d} \lesssim \|\boldsymbol{u}\|_{\widetilde{A}_h^d} \quad \textit{for all } \boldsymbol{u} \in \boldsymbol{V}_h. \tag{2.3.15}$$

2.3.3 Triangular Preconditioner

When a diagonal mass matrix is used, we can make use of the block decomposition

$$\begin{pmatrix} -\tilde{M}_v & B \\ B^T & C^T M_f C \end{pmatrix} \begin{pmatrix} I & \tilde{M}_v^{-1} B \\ 0 & I \end{pmatrix} = \begin{pmatrix} -\tilde{M}_v & 0 \\ B^T & \tilde{A}_h^c \end{pmatrix} \tag{2.3.16}$$

to obtain a triangular preconditioner.

Definition 2.3.5. *We define the operator* $\mathcal{G}_h^c : S_h' \times \boldsymbol{U}_h' \to S_h \times \boldsymbol{U}_h$

$$\mathcal{G}_h^c = \begin{pmatrix} I & \tilde{M}_v^{-1}B \\ 0 & I \end{pmatrix} \begin{pmatrix} -\tilde{M}_v & 0 \\ B^T & \tilde{A}_h^c \end{pmatrix}^{-1}, \tag{2.3.17}$$

and the operator $\mathcal{G}_h^d : \boldsymbol{U}_h' \times \boldsymbol{V}_h' \to \boldsymbol{U}_h \times \boldsymbol{V}_h$

$$\mathcal{G}_h^d = \begin{pmatrix} I & \tilde{M}_e^{-1}C^T \\ 0 & I \end{pmatrix} \begin{pmatrix} -\tilde{M}_e & 0 \\ C^T & \tilde{A}_h^d \end{pmatrix}^{-1}. \tag{2.3.18}$$

From the definition, it is trivial to verify that $\mathcal{G}_h^c = \widetilde{\mathcal{L}_h^c}^{-1}$ and $\mathcal{G}_h^d = \widetilde{\mathcal{L}_h^c}^{-1}$ and thus conclude that the proposed triangular preconditioners are uniform.

Theorem 2.3.6. *Assume $\tilde{M}$ is spectrally equivalent to M. Then the $\mathcal{G}_h^c$ and $\mathcal{G}_h^d$ are uniform preconditioners for $\mathcal{L}_h^c$ and $\mathcal{L}_h^d$, respectively, i.e., the corresponding operator norms*

$$\begin{aligned} &\|\mathcal{G}_h^c\mathcal{L}_h^c\|_{\mathrm{L}(S_h\times\boldsymbol{U}_h, S_h\times\boldsymbol{U}_h)}, \|(\mathcal{L}_h^c\mathcal{G}_h^c)^{-1}\|_{\mathrm{L}(S_h\times\boldsymbol{U}_h, S_h\times\boldsymbol{U}_h)}, \\ &\|\mathcal{G}_h^d\mathcal{L}_h^d\|_{\mathrm{L}(\boldsymbol{U}_h\times\boldsymbol{V}_h, \boldsymbol{U}_h\times\boldsymbol{V}_h)}, \|(\mathcal{G}_h^d\mathcal{L}_h^d)^{-1}\|_{\mathrm{L}(\boldsymbol{U}_h\times\boldsymbol{V}_h, \boldsymbol{U}_h\times\boldsymbol{V}_h)} \end{aligned}$$

are bounded and independent with parameter h.

In both diagonal and triangular preconditioners, to be practical, we do not compute A^{-1} or $\tilde{A}^{-1}$. Instead we apply one and only one V-cycle multigrid for $\tilde{A}^{-1}$.

2.3.4 Maxwell Equations with Divergence-Free Constraint

We consider a prototype of Maxwell equations with divergence-free constraint

$$\operatorname{curl}\operatorname{curl}\boldsymbol{u} = \boldsymbol{f},\ \operatorname{div}\boldsymbol{u} = 0,\ \text{ in } \Omega, \qquad \boldsymbol{u}\times\boldsymbol{n} = 0 \text{ on } \partial\Omega.$$

The solution $\boldsymbol{u}$ is approximated using edge element space $\boldsymbol{U}_h$. The divergence-free constraint can then be understood in the weak sense, i.e., $\operatorname{div}_h \boldsymbol{u} = 0$. By introducing a Lagrangian multiplier $p \in S_h$, the matrix form is

$$\begin{pmatrix} C^T M_f C & B^T \\ B & O \end{pmatrix} \begin{pmatrix} \boldsymbol{u} \\ p \end{pmatrix} = \begin{pmatrix} \boldsymbol{f} \\ g \end{pmatrix}. \tag{2.3.19}$$

We can apply the augmented Lagrangian method [19], by adding $B^T M_v^{-1} B$ to the first equation, to get an equivalent matrix equation

$$\begin{pmatrix} A & B^T \\ B & O \end{pmatrix} \begin{pmatrix} \boldsymbol{u} \\ p \end{pmatrix} = \begin{pmatrix} \boldsymbol{f} + B^T M_v^{-1} g \\ g \end{pmatrix}. \tag{2.3.20}$$

Now the $(1,1)$ block $A = C^T M_f C + B^T M_v^{-1} B$ in (2.3.20) is a discrete vector Laplacian and the whole system (2.3.20) is in Stokes type.

We can thus use the following diagonal preconditioner.

Theorem 2.3.7. *The following block-diagonal matrix*

$$\begin{pmatrix} A^{-1} & 0 \\ 0 & M_v^{-1} \end{pmatrix} \tag{2.3.21}$$

is a uniform preconditioner for the regularized Maxwell operator $\begin{pmatrix} A & B^T \\ B & O \end{pmatrix}$.

Proof. It suffices to prove that the Schur complement $S = BA^{-1}B^T$ is spectral equivalent to M_v. The inequality $(Sp, p) \leq (M_v p, p)$ for all $p \in S_h$ has been proved in Lemma 2.3.1. To prove the inequality in the other way, it suffices to prove the inf-sup condition: there exists a constant β independent of h such that

$$\inf_{p_h \in S_h} \sup_{v_h \in U_h} \frac{(Bv_h, p_h)}{\|v_h\|_A \|q_h\|} = \beta > 0. \tag{2.3.22}$$

Given $p_h \in S_h$, we solve the Poisson equation $\Delta\phi = p_h$ with homogenous Dirichlet boundary condition and let $\boldsymbol{v} = \operatorname{grad}\phi$. Then $\boldsymbol{v} \in \boldsymbol{H}_0(\mathrm{curl})$ and $\operatorname{div}\boldsymbol{v} = p_h$ holds in L^2. We define $\boldsymbol{v}_h = Q_h\boldsymbol{v}$ where $Q_h : \boldsymbol{H}_0(\mathrm{curl}) \to U_h$ is the L^2 projection. Then $(\operatorname{div}_h \boldsymbol{v}_h, q_h) = (\boldsymbol{v}_h, \operatorname{grad} q_h) = (\boldsymbol{v}, \operatorname{grad} q_h) = -(\operatorname{div}\boldsymbol{v}, q_h) = (p_h, q_h)$, i.e., $\operatorname{div}_h \boldsymbol{v}_h = p_h$. To control the norm of $\operatorname{curl}\boldsymbol{v}_h$, we denote $\boldsymbol{v}_0$ as the piecewise constant projection of $\boldsymbol{v}$. Then

$$\|\operatorname{curl}\boldsymbol{v}_h\| = \|\operatorname{curl}(\boldsymbol{v}_h - \boldsymbol{v}_0)\| \lesssim h^{-1}\|\boldsymbol{v}_h - \boldsymbol{v}_0\| \leq \|\boldsymbol{v}\|_1 \lesssim \|p_h\|.$$

In the last step, we have used the H^2-regularity result.

In summary, given $p_h \in S_h$, we have found a $\boldsymbol{v}_h \in U_h$ such that $(B\boldsymbol{v}_h, p_h) = \|p_h\|^2$ while $\|\boldsymbol{v}_h\|_A^2 = \|\operatorname{div}_h \boldsymbol{v}_h\|^2 + \|\operatorname{curl}\boldsymbol{v}_h\|^2 \lesssim \|p_h\|^2$. Therefore the inf-sup condition (2.3.22) has been proved which implies the inequality $(Sp, p) \geq \beta^2(M_v p, p)$. $\square$

To design an efficient triangular preconditioner for (2.3.20), we explore the commutator

$$AG = \tilde{G}A_p, \tag{2.3.23}$$

where $G = M_e^{-1}B^T$ is the matrix representation of the gradient operator $S_h \to U_h$, $\hat{G} = B^T M_v^{-1}$ is another scaled gradient operator, and $A_p = BG$ represents the discrete Laplacian operator $S_h \to S_h$. The identity (2.3.23) is a discrete version of the following identity

$$\boldsymbol{\Delta}\operatorname{grad} = \operatorname{grad}\Delta, \tag{2.3.24}$$

where the first $\boldsymbol{\Delta}$ is the vector Laplacian operator and the second Δ is the scalar Laplacian, and can be verified by noticing that $CG = \operatorname{curl}\operatorname{grad} = 0$.

With (2.3.23), we have the following block factorization

$$\begin{pmatrix} A & B^T \\ B & O \end{pmatrix}\begin{pmatrix} I & G \\ O & -M_v^{-1}A_p \end{pmatrix} = \begin{pmatrix} A & O \\ B & A_p \end{pmatrix}. \tag{2.3.25}$$

When S_h is the linear (P_1) element, M_v^{-1} can be approximated accurately by using the mass lump-

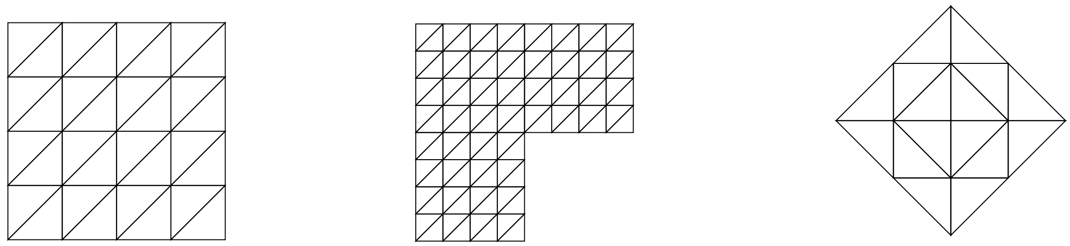

A mesh for the unit square | A mesh for a L-shape domain | A mesh for a crack domain

Figure 2.1: Meshes for Example 5.1

Table 2.1: Iteration steps and CPU time of the diagonal and the triangular preconditioners for the vector Laplace equation in $\boldsymbol{H}_0(\mathrm{curl})$ space: the square domain $(0,1)^2$.

h	Dof	Iteration (D)	Time	Iteration (T)	Time
1/32	4,225	28	0.20 s	13	0.18s
1/64	16,641	28	0.68 s	14	0.34s
1/128	66,049	27	1.90 s	14	1.30s
1/256	263,169	27	8.80 s	14	6.80s

Table 2.2: Iteration steps and CPU time of the diagonal and the triangular preconditioners for the lowest order discretization of the vector Laplace equation in $\boldsymbol{H}_0(\mathrm{curl})$ space: the L-shape domain $(-1,1)^2\backslash\{[0,1]\times[-1,0]\}$.

h	Dof	Iteration (D)	Time	Iteration (T)	Time
1/32	3,201	33	0.24 s	15	0.19s
1/64	12,545	35	0.63 s	16	0.40s
1/128	49,665	39	2.50 s	16	1.90s
1/256	197,633	41	7.20 s	16	5.50s

Table 2.3: Iteration steps and CPU time of the diagonal and the triangular preconditioners for the lowest order discretization of the vector Laplace equation in $\boldsymbol{H}_0(\mathrm{curl})$ space: the crack domain $\{|x|+|y|<1\}\backslash\{0\le x\le 1, y=0\}$.

h	Dof	Iteration (D)	Time	Iteration (T)	Time
1/16	2,145	34	0.13 s	15	0.08 s
1/32	8,385	38	0.54 s	15	0.30 s
1/64	33,153	41	1.60 s	16	1.00 s
1/128	131,841	44	6.70 s	16	3.60 s

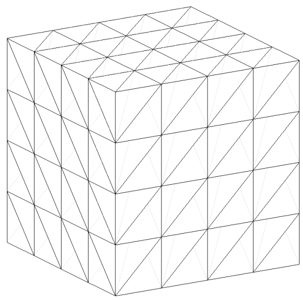

A mesh for the unit cube

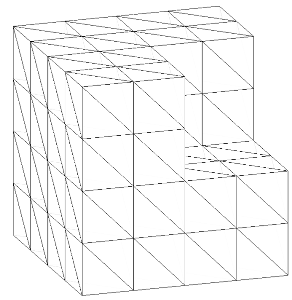

A mesh for a L-shaped domain

Figure 2.2: Meshes for Example 5.2

Table 2.4: Iteration steps and CPU time of the diagonal and triangular preconditioners for the lowest order discretization of the vector Laplace equation in $\boldsymbol{H}_0(\mathrm{curl})$ space in three dimensions: the unit cube domain.

h	Dof	Iteration (D)	Time	Iteration (T)	Time
1/4	729	21	0.25 s	12	0.15 s
1/8	4,913	29	0.48 s	16	0.28 s
1/16	35,937	33	3.90 s	18	4.0 s
1/32	274,625	33	40 s	19	27 s

ing of the P_1 element. Therefore we can easily solve (2.3.19) by inverting two Laplacian operators: one is a vector Laplacian of the edge element and another is a scalar Laplacian for the P_1 element. In general M_v^{-1} will be replaced by a sparse approximation $\tilde{M}_v^{-1}$ and (2.3.25) can be used to construct effective block-triangular preconditioners:

$$\begin{pmatrix} I & G \\ O & -\tilde{M}_v^{-1} A_p \end{pmatrix} \begin{pmatrix} \tilde{A} & O \\ B & A_p \end{pmatrix}^{-1}. \tag{2.3.26}$$

Again in practice, the $\tilde{A}^{-1}$ and A_p^{-1} will be replaced by one multigrid V-cycle.

2.4 Numerical Examples

In this section, we will show the efficiency and the robustness of the proposed diagonal and triangular preconditioners. We perform the numerical experiments using the iFEM package [13].

Table 2.5: Iteration steps and CPU time of the diagonal and triangular preconditioners for the lowest order discretization of the vector Laplace equation in $\boldsymbol{H}_0(\mathrm{curl})$ space in three dimensions: L-shape domain $(-1,1)^3\backslash\{(-1,0)\times(0,1)\times(0,1)\}$.

h	Dof	Iteration (D)	Time	Iteration (T)	Time
1/2	665	20	0.03 s	12	0.06 s
1/4	4,401	34	0.54 s	16	0.37 s
1/8	31,841	42	5.50 s	20	3.60 s
1/16	241,857	48	48 s	23	33 s

Table 2.6: Iteration steps and CPU time of the diagonal and triangular preconditioners for the lowest order discretization of Maxwell equations in the saddle point form in three dimensions: the unit cube domain.

h	Dof	Iteration (D)	Time	Iteration (T)	Time
1/4	729	21	0.40 s	12	0.80 s
1/8	4,913	27	1.3 s	16	1.3 s
1/16	35,937	31	4.30 s	18	4.8 s
1/32	274,625	31	40 s	19	39 s

Example 2.4.1 (Two Dimensional Vector Laplacian using Edge Elements)**.** We first consider the mixed system (2.1.4) arising from the lowest order discretization of the vector Laplace equation in $\boldsymbol{H}_0(\mathrm{curl})$ space.

We consider three domains in two dimensions: the unit square $(0,1)^2$, the L-shape domain $(-1,1)^2\backslash\{[0,1]\times[-1,$ and the crack domain $\{|x|+|y|<1\}\backslash\{0\le x\le 1, y=0\}$.

We use the diagonal preconditioner (2.3.12) in the MINRES method and the triangular preconditioner (2.3.17) in GMRES (with the restart step 20) to solve (2.1.4). In these preconditioners, one and only one variable V-cycle is used for approximating $\tilde{A}^{-1}$. In the variable V-cycle, we chose $m_J = 2$ and $m_k = \lceil 1.5^{J-k} m_J \rceil$ for $k = J, \ldots, 1$. We stop the Krylov space iteration when the relative residual is less than or equal to 10^{-8}. Iteration steps and CPU time are summarized in Table 2.1, 2.2, and 2.3.

Example 2.4.2 (Three Dimensional Vector Laplacian using Edge Elements)**.** We then consider the three dimensional case. Still consider the lowest order discretization of the vector Laplace equation in $\boldsymbol{H}_0(\mathrm{curl})$ space. We use almost the same setting except $m_J = 3$ for which the performance is more robust.

Table 2.7: Iteration steps and CPU time of the diagonal and triangular preconditioners for the lowest order discretization of Maxwell equations in the saddle point form in three dimensions: L-shape domain $(-1,1)^3 \backslash \{(-1,0) \times (0,1) \times (0,1)\}$.

h	Dof	Iteration (D)	Time	Iteration (T)	Time
1/2	665	20	0.47 s	10	0.68 s
1/4	4,401	28	0.58 s	14	1.10 s
1/8	31,841	34	5.70 s	17	4.00 s
1/16	241,857	37	40 s	19	38 s

We consider two domains. One is the unit cube $(0,1)^3$ for which the full regularity assumption holds and another is a L-shape domain $(-1,1)^3 \backslash \{(-1,0) \times (0,1) \times (0,1)\}$ which violates the full regularity assumption. Iteration steps and CPU time are summarized in Table 2.4 and 2.5.

Based on these tables, we present some discussion on our preconditioners.

1. Both diagonal and triangular preconditioners perform very well. The triangular one is more robust and efficient.

2. The diagonal preconditioner is more sensitive to the elliptic regularity result as the iteration steps are slowly increased, which is more evident in the three dimensional case; see the third column of Table 2.4 and 2.5. For general domains, the $\boldsymbol{H}_0(\text{curl}) \cap \boldsymbol{H}(\text{div})$ is a strict subspace of $\boldsymbol{H}^1$ and thus the approximation property may fail. On the other hand, the numerical effectiveness even in the partial regularity cases is probably due to the fact that the full regularity of elliptic equation always holds in the interior of the domain. Additional smoothing for near boundary region might compensate the loss of full regularity.

3. Only the lowest order element is tested while our theory assumes the finite element space should contain full linear polynomial to ensure the approximation property. This violation may also contribute to the slow increase of the iteration steps. We do not test the second type of edge element due to the complication of the prolongation operators. The lowest order edge element is the most popular edge element. For high order edge elements, we prefer to use the V-cycle for the lowest order element plus additional Gauss-Seidel smoothers in the finest level to construct preconditioners.

Example 2.4.3 (Three dimensional Maxwell equations with divergent-free constraint)**.** We consider the lowest order discretization of Maxwell equations in the saddle point form (2.3.19) and solve the regularized formulation (2.3.20). We test the block-diagonal preconditioner (2.3.21) and triangular preconditioner (2.3.26). We use the same setting as in Example 5.2 and report the iteration steps and corresponding CPU time in Table 2.6 and 2.7.

From these results, we conclude our block-diagonal and block-triangular preconditioners works pretty well for the Maxwell equations discretized in the saddle point form. The iteration steps may increase but very slowly. Although the block-triangular preconditioner requires less iteration steps, the computational time is almost the same. This is due to the fact, now for the $(2, 2)$ block, the block-triangular preconditioners requires a V-cycle for the scalar Laplacian while in the block-diagonal preconditioner it is only a diagonal approximation of the mass matrix.

Chapter 3

Robust Error Estimate and Uniform Preconditioners of TMAC Discretization of Darcy-Stokes Equations

In this chapter, we propose a discretization method for the Darcy-Stokes equations. The discretization is shown to be uniform with respect to the perturbation parameter. A preconditioner for the discrete system is also proposed and shown to be efficient. We follow the notations from the previous chapter.

3.1 TMAC Discretization

3.1.1 Weak Formulation of Darcy-Stokes Equations

Let $\boldsymbol{V}$ and W denote the velocity space and the pressure space, respectively. A weak formulation of the Darcy-Stokes equations (0.2.1): find $(\boldsymbol{u}, p) \in \boldsymbol{V} \times W$ satisfying

$$\begin{cases} a^\epsilon(\boldsymbol{u}, \boldsymbol{v}) + b(\boldsymbol{v}, p) = \langle \boldsymbol{f}, \boldsymbol{v} \rangle & \text{for all } \ \boldsymbol{v} \in \boldsymbol{V}, \\ \qquad\qquad b(\boldsymbol{u}, q) = 0 & \text{for all } \ q \in W, \end{cases} \tag{3.1.1}$$

where the bilinear forms $a^\epsilon(\cdot, \cdot)$ and $b(\cdot, \cdot)$ are defined as

$$\begin{aligned} a^\epsilon(\boldsymbol{u}, \boldsymbol{v}) &:= (\boldsymbol{u}, \boldsymbol{v}) + \epsilon^2 \left[(\operatorname{rot} \boldsymbol{u}, \operatorname{rot} \boldsymbol{v}) + (\operatorname{div} \boldsymbol{u}, \operatorname{div} \boldsymbol{v}) \right] \qquad && \text{for all } \ \boldsymbol{u}, \boldsymbol{v} \in \boldsymbol{H}_0^1, \\ b(\boldsymbol{v}, q) &:= -(\operatorname{div} \boldsymbol{v}, q) && \text{for all } \ \boldsymbol{v} \in \boldsymbol{H}_0^1, \ q \in L_0^2. \end{aligned}$$

Let the operator $A^\epsilon : \boldsymbol{V} \to \boldsymbol{V}'$ introduced by the bilinear form $a^\epsilon(\cdot, \cdot)$ and $B : \boldsymbol{V} \to W'$ introduced by $b(\cdot, \cdot)$. We can write the operator form of (3.1.1)

$$\begin{pmatrix} A^\epsilon & B^T \\ B & O \end{pmatrix} \begin{pmatrix} \boldsymbol{u} \\ p \end{pmatrix} = \begin{pmatrix} \boldsymbol{f} \\ 0 \end{pmatrix}. \tag{3.1.2}$$

It is well known that (3.1.1) is well posed if and only if the following so-called Brezzi conditions [12] hold for an appropriate norms $\| \cdot \|_V$ for V and $\| \cdot \|_W$ for W:

1. Continuity of bilinear forms $a^\epsilon(\cdot, \cdot)$ and $b(\cdot, \cdot)$: there exist constants $c_a, c_b > 0$ such that

$$a^\epsilon(\boldsymbol{u}, \boldsymbol{v}) \le c_a \|\boldsymbol{u}\|_V \|\boldsymbol{v}\|_V, \quad b(\boldsymbol{v}, q) \le c_b \|\boldsymbol{v}\|_V \|q\|_W, \quad \text{for all } \boldsymbol{u}, \boldsymbol{v} \in \boldsymbol{V}, q \in W.$$

2. Coercivity of $a^\epsilon(\cdot, \cdot)$ in the kernel space. There exists a constant $\alpha > 0$ such that

$$a^\epsilon(\boldsymbol{u}, \boldsymbol{u}) \ge \alpha \|\boldsymbol{u}\|_V^2 \quad \text{for all } \boldsymbol{u} \in \ker(B),$$

where $\ker(B) = \{\boldsymbol{v} \in \boldsymbol{V} : b(\boldsymbol{v}, q) = 0 \text{ for all } q \in W\}$.

3. Inf-sup condition of $b(\cdot,\cdot)$. There exists a constant $\beta > 0$ such that

$$\inf_{p\in W, p\neq 0} \sup_{\boldsymbol{v}\in \boldsymbol{V}, \tau\neq 0} \frac{b(\boldsymbol{v}, p)}{\|\boldsymbol{v}\|_{\boldsymbol{V}}\|p\|_W} \geq \beta.$$

Furthermore to get a scheme robust to ϵ, all constants involved in these conditions should be ϵ-independent.

We then discuss one possible choice of spaces and verify all these conditions. A natural space for the pressure is $W = L_0^2$. Based on $a^\epsilon(\cdot,\cdot)$, we can use $\boldsymbol{H}^1$ with a scaled $\boldsymbol{H}^1$ norm induced by $a^\epsilon(\cdot,\cdot)$. But to impose the uniform continuity of bilinear form $b(\cdot,\cdot)$, we need to include $H(\mathrm{div})$ norm into the space $\boldsymbol{V}$. In summary we chose $\boldsymbol{V} = \boldsymbol{H}_0^1, W = L_0^2$ with norms:

$$\|\boldsymbol{v}\|_V := \left(\|\boldsymbol{v}\|_{A^\epsilon}^2 + \|\operatorname{div}\boldsymbol{v}\|^2\right)^{1/2}, \quad \|q\|_W = \|q\|.$$

The continuity and the coercivity of $a^\epsilon(\cdot,\cdot)$ in the null space of div is obvious. The inf-sup condition is derived from that of Stokes equation, i.e., for any $p \in L_0^2$, we can find a $\boldsymbol{v} \in \boldsymbol{H}_0^1$ such that $\operatorname{div} v = p$ and $\|\nabla \boldsymbol{v}\| \lesssim \|p\|$. Then by the Poincaré inequality, we can also control the L^2-norm of $\|\boldsymbol{v}\| \lesssim \|\nabla\boldsymbol{v}\| \lesssim \|p\|$.

3.1.2 TMAC Discretization

We shall chose $H_0(\mathrm{div})$ conforming finite element spaces for velocity and discontinuous polynomial space for pressure. Suppose that the mesh $\mathcal{T}_h$ is a shape regular mesh. Suppose that $S_h \subset H(\mathrm{curl})$, $\boldsymbol{V}_h \subset \boldsymbol{H}_0(\mathrm{div})$ and $W_h \subset L_0^2$ are appropriate finite element spaces so that the following sequence is exact

$$0 \to S_h \cap H_0(\mathrm{curl}) \xrightarrow{\mathrm{curl}} \boldsymbol{V}_h \xrightarrow{\mathrm{div}} W_h \to 0. \tag{3.1.3}$$

Since $\operatorname{div}\boldsymbol{V}_h \subset W_h$, $\operatorname{div} u_h = 0$ implies u_h is divergence free point-wisely.

We shall discretize the vector Laplacian operator based on the following identity:

$$-\boldsymbol{\Delta} = -\operatorname{grad}\operatorname{div} + \operatorname{curl}\operatorname{rot}.$$

Since we use $H(\operatorname{div})$ conforming element for the velocity, div operator is a natural discretization. To discretize the vector Laplacian for a $H(\operatorname{div})$ element, we introduce the weak rot_h operator as the dual of curl operator .

Definition 3.1.1. *The linear operator* $\operatorname{rot}_h : \boldsymbol{V}_h \to S_h$ *is defined as follows: for a given* $\boldsymbol{u} \in \boldsymbol{V}_h$, $\operatorname{rot}_h \boldsymbol{u} \in S_h$ *such that*

$$(\operatorname{rot}_h \boldsymbol{u}, \tau) = (\boldsymbol{u}, \operatorname{curl}\tau) \qquad \textit{for all } \tau \in S_h. \tag{3.1.4}$$

The operators rot_h is well defined, since the system involved is a non-singular finite dimensional square system. The auxiliary variable $\omega_h = \operatorname{rot}_h \boldsymbol{u}$ can be thought of as an approximation of the vorticity ω.

With the help of operator rot_h, we define the discrete bilinear form $a_h^\epsilon(\cdot,\cdot)$ on the discrete space $\boldsymbol{V}_h$ as

$$a_h^\epsilon(\boldsymbol{u},\boldsymbol{v}) := (\boldsymbol{u},\boldsymbol{v}) + \epsilon^2\left[(\operatorname{rot}_h\boldsymbol{u}, \operatorname{rot}_h\boldsymbol{v}) + (\operatorname{div}\boldsymbol{u}, \operatorname{div}\boldsymbol{v})\right] \qquad \text{for } \boldsymbol{u},\boldsymbol{v} \in \boldsymbol{V}_h. \tag{3.1.5}$$

The TMAC discretization of (3.1.1) is: find $(\boldsymbol{u}_h, p_h) \in \boldsymbol{V}_h \times W_h$ such that:

$$\begin{cases} a_h^\epsilon(\boldsymbol{u}_h,\boldsymbol{v}_h) + b(\boldsymbol{v}_h, p_h) = (\boldsymbol{f}, \boldsymbol{v}_h) & \text{for all } \boldsymbol{v}_h \in \boldsymbol{V}_h, \\ b(\boldsymbol{u}_h, q_h) = 0 & \text{for all } q_h \in W_h. \end{cases} \tag{3.1.6}$$

For $\boldsymbol{u} \in \boldsymbol{V}_h$, define

$$\|\boldsymbol{u}\|_{1,h}^2 = (\operatorname{rot}_h\boldsymbol{u}, \operatorname{rot}_h\boldsymbol{v}) + (\operatorname{div}\boldsymbol{u}, \operatorname{div}\boldsymbol{v}), \quad \|\boldsymbol{u}\|_{A^\epsilon}^2 = a_h^\epsilon(\boldsymbol{u},\boldsymbol{u}).$$
$$\|\boldsymbol{u}\|_{V_h}^2 = \|\boldsymbol{u}\|^2 + \epsilon^2\|\boldsymbol{u}\|_{1,h}^2 + \|\operatorname{div}\boldsymbol{u}\|^2 = \|\boldsymbol{u}\|_{A^\epsilon}^2 + \|\operatorname{div}\boldsymbol{u}\|^2.$$

In [66] we have proved the following discrete Poincaré inequality.

Lemma 3.1.1 (Discrete Poincaré Inequality [66])**.** *We have the following discrete Poincaré inequality with respect to* $\|\cdot\|_{1,h}$*:*

$$\|\boldsymbol{u}_h\| \lesssim \|\boldsymbol{u}_h\|_{1,h} \quad \textit{for all } \boldsymbol{u}_h \in \boldsymbol{V}_h. \tag{3.1.7}$$

According to Lemma 3.1.1, we can obtain the continuity and coercivity of the bilinear form $a_h^{\epsilon}(\cdot,\cdot)$ restricted to the null space

1. Continuity: $a_h^{\epsilon}(\boldsymbol{u},\boldsymbol{v}) \lesssim \|\boldsymbol{u}\|_{V_h}\|\boldsymbol{v}\|_{V_h}$;
2. Coercivity in the null space of B: $a_h^{\epsilon}(\boldsymbol{u},\boldsymbol{u}) = \|\boldsymbol{u}\|_{V_h}^2$ for all $\boldsymbol{u} \in \boldsymbol{V}_h \cap \ker(B)$.

Lemma 3.1.2. *For any* $q_h \in W_h$*, there exists* $\boldsymbol{v}_h \in \boldsymbol{V}_h$ *such that*

$$\operatorname{div} \boldsymbol{v}_h = q_h, \ \textit{and} \ \|\boldsymbol{v}_h\|_{V_h} \lesssim \|q_h\|.$$

Proof. First of all the following inf-sup condition

$$\operatorname{div} \boldsymbol{v}_h = q_h, \ \text{and} \ \|\boldsymbol{v}_h\|_{1,h} \lesssim \|q_h\|.$$

is established in [66]. By the discrete Poincaré inequality, we can control the $\|\boldsymbol{v}_h\| \lesssim \|\boldsymbol{v}_h\|_{1,h}$ and thus the inf-sup condition in $\|\boldsymbol{v}\|_{V_h}$ norm follows. □

By Lemma 3.1.2 and continuity and coercivity of $a_h^{\epsilon}(\cdot,\cdot)$, we have the wellposedness of the weak formulation.

Theorem 3.1.2. *There exists a unique solution* $(\boldsymbol{u}_h, p_h) \in \boldsymbol{V}_h \times W_h$ *to the weak formulation of the Darcy-Stokes equations* (3.1.6)*, and*

$$\|\boldsymbol{u}_h\|_{V_h} + \|p_h\| \lesssim \|\boldsymbol{f}\|_{V_h'},$$

where $\|\boldsymbol{f}\|_{V_h'} = \sup\limits_{\boldsymbol{v}_h \in \boldsymbol{V}_h} \dfrac{(\boldsymbol{f},\boldsymbol{v}_h)}{\|\boldsymbol{v}_h\|_{V_h}} \leq \|\boldsymbol{f}\|.$

3.2 Error Analysis

In this section, we prove that for the RT_0-P_0 approximation, the convergence order depends on the symmetry of the mesh, and both velocity and pressure can achieve optimal first-order convergence on mildly structured meshes. For the BDM_1-P_0 approximation, first-order convergence is always achieved. The convergence rates are uniform with respect to the parameter ϵ.

We will employ the canonical interpolation operators for $H(\mathrm{curl})$ and $H(\mathrm{div})$ elements and use subscript $(\cdot)_I$ to denote such interpolation. It is well known that the canonical interpolations is commuted with the corresponding differential operators [22].

3.2.1 Basic Error Bound

Denoted by $Q_h : L^2 \to S_h$ the L^2 projection.

Theorem 3.2.1. *Assume that the solution of the Darcy-Stokes equations satisfies $\boldsymbol{u} \in \boldsymbol{H}_0^1$ and $\mathrm{rot}\,\boldsymbol{u} \in H(\mathrm{curl})$. Let $\boldsymbol{u}_h$ and p_h be the solution of the TMAC discretization* (3.1.6)*. Then, we have the following error estimate*

$$\|\boldsymbol{u}_h - \boldsymbol{u}_I\|_{A_h^\epsilon} + \|p_h - p_I\| \lesssim \epsilon\|\mathrm{rot}\boldsymbol{u} - \mathrm{rot}_h\boldsymbol{u}_I\| + \epsilon^2\|\,\mathrm{curl}(I - Q_h)\mathrm{rot}\boldsymbol{u}\| + \|\boldsymbol{u} - \boldsymbol{u}_I\|.$$

Proof. Use $\boldsymbol{f} = \epsilon^2(\mathrm{curl}\,\mathrm{curl} - \mathrm{grad}\,\mathrm{div})\boldsymbol{u} + \boldsymbol{u} + \nabla p$ and $\mathrm{div}\,\boldsymbol{u} = \mathrm{div}\,\boldsymbol{u}_h = \mathrm{div}\,\boldsymbol{u}_I = 0$, for $\boldsymbol{v}_h \in \ker(\mathrm{div})$, we obtain the error equation

$$\begin{aligned}
&a_h^\epsilon(\boldsymbol{u}_h - \boldsymbol{u}_I, \boldsymbol{v}_h)\\
&= (\boldsymbol{f}, \boldsymbol{u}_h - \boldsymbol{u}_I) - \epsilon^2(\mathrm{rot}_h\boldsymbol{u}_I, \boldsymbol{v}_h) - (\boldsymbol{u}_I, \boldsymbol{v}_h)\\
&= \epsilon^2(\mathrm{curl}\,\mathrm{rot}\boldsymbol{u}, \boldsymbol{v}_h) - \epsilon^2(\mathrm{rot}_h\boldsymbol{u}_I, \mathrm{rot}_h\boldsymbol{v}_h) + (\boldsymbol{u} - \boldsymbol{u}_I, \boldsymbol{v}_h)\\
&= \epsilon^2(\mathrm{rot}\boldsymbol{u} - \mathrm{rot}_h\boldsymbol{u}_I, \mathrm{rot}_h\boldsymbol{v}_h) + \epsilon^2(\mathrm{curl}(I - Q_h)\mathrm{rot}\boldsymbol{u}, \boldsymbol{v}_h) + (\boldsymbol{u} - \boldsymbol{u}_I, \boldsymbol{v}_h).
\end{aligned}$$

Here in the third step, we use

$$(\operatorname{rot}\boldsymbol{u}, \operatorname{rot}_h\boldsymbol{v}_h) = (Q_h \operatorname{rot}\boldsymbol{u}, \operatorname{rot}_h\boldsymbol{v}_h) = (\operatorname{curl} Q_h \operatorname{rot}\boldsymbol{u}, \boldsymbol{v}_h)$$

Substitute $\boldsymbol{v}_h = \boldsymbol{u}_h - \boldsymbol{u}_I$ and apply Cauchy-Schwarz inequality to get the desired error estimate of $\|\boldsymbol{u}_h - \boldsymbol{u}_I\|_{A_h^\epsilon}$.

To prove the error estimate of the pressure, by the inf-sup condition presented in Lemma 3.1.2, we can choose $\boldsymbol{v}_h \in \boldsymbol{V}_h$ such that

$$\operatorname{div}\boldsymbol{v}_h = p_I - p_h, \text{ and } \|\boldsymbol{v}_h\|_{A_h^\epsilon} \lesssim \|p_I - p_h\|.$$

With such $\boldsymbol{v}_h$, we have

$$\begin{aligned} b(p_I - p_h, \boldsymbol{v}_h) &= b(p_I, \boldsymbol{v}_h) + a_h^\epsilon(\boldsymbol{u}_h, \boldsymbol{v}_h) - (\boldsymbol{f}, \boldsymbol{v}_h) \\ &= \left[a_h^\epsilon(\boldsymbol{u}_h, \boldsymbol{v}_h) - \epsilon^2(\operatorname{curl}\operatorname{rot}\boldsymbol{u}, \boldsymbol{v}_h) - (\boldsymbol{u}, \boldsymbol{v}_h)\right] + b(p_I - p, \boldsymbol{v}_h) \\ &= \epsilon^2(\operatorname{rot}_h\boldsymbol{u}_h - \operatorname{rot}\boldsymbol{u}, \operatorname{rot}_h\boldsymbol{v}_h) + \epsilon^2(\operatorname{curl}(Q_h - I)\operatorname{rot}\boldsymbol{u}, \boldsymbol{v}_h) + (\boldsymbol{u}_h - \boldsymbol{u}, \boldsymbol{v}_h). \end{aligned}$$

Here we use the fact that p_I is the L^2 projection of p to W_h space and thus

$$b(p_I - p, \boldsymbol{v}_h) = (p_I - p, \operatorname{div}\boldsymbol{v}_h) = 0.$$

Apply Cauchy-Schwarz inequality and notice that $\operatorname{div}\boldsymbol{v}_h = p_I - p_h$ and $\|\boldsymbol{v}_h\|_{A_h^\epsilon} \lesssim \|p_I - p_h\|$, we get

$$\begin{aligned} \|p_I - p_h\| &\le \epsilon\|\operatorname{rot}\boldsymbol{u} - \operatorname{rot}_h\boldsymbol{u}_h\| + \epsilon^2\|\operatorname{curl}(I - Q_h)\operatorname{rot}\boldsymbol{u}\| + \|\boldsymbol{u} - \boldsymbol{u}_h\| \\ &\lesssim \|\boldsymbol{u}_I - \boldsymbol{u}_h\|_{A_h^\epsilon} + \epsilon\|\operatorname{rot}\boldsymbol{u} - \operatorname{rot}_h\boldsymbol{u}_I\| + \|\boldsymbol{u} - \boldsymbol{u}_I\| + \epsilon^2\|\operatorname{curl}(I - Q_h)\operatorname{rot}\boldsymbol{u}\|. \end{aligned}$$

□

Remark 3.2.2. Notice that $\operatorname{div}\boldsymbol{u}_h = 0$ and $\operatorname{div}\boldsymbol{u}_I = \operatorname{div}\Pi_{V_h}\boldsymbol{u} = \Pi_{W_h}\operatorname{div}\boldsymbol{u} = 0$. Then

$$\|\boldsymbol{u}_h - \boldsymbol{u}_I\|_{V_h} = \|\boldsymbol{u}_h - \boldsymbol{u}_I\|_{A_h^\epsilon}.$$

The interpolant $\boldsymbol{u}_I$ can be changed to any divergence free interpolant of $\boldsymbol{u}$. But when interpolant p_I is replaced by an easy computable one p_{II}(e.g. the nodal interpolation at the center of elements), an additional term $\|p - p_{II}\|$ should be included in the estimate of $\|p_h - p_{II}\|$. $\square$

We then study the three terms in the error estimate obtained in Theorem 3.2.1. First of all, the following approximation properties of the L^2 projection are well known.

Lemma 3.2.1. *For any quasi-uniform mesh with mesh size h, the L^2 projection $Q_h : L^2 \to \mathrm{P_r}$ satisfies*

$$\|\phi - Q_h\phi\| + h|\phi - Q_h\phi|_1 \lesssim h^s|\phi|_s \quad \textit{for all } \phi \in H^s,$$

where $1 \leq s \leq r$, and $\mathrm{P_r}$ denotes the polynomial up to degree r for an positive integer r.

The interpolation error in L^2-norm is also well known. If the polynoimal space P^r is contained in $\boldsymbol{V}_h$, then for $\boldsymbol{u} \in H^r$:

$$\|\boldsymbol{u} - \boldsymbol{u}_I\| \lesssim h^r\|\boldsymbol{u}\|_r. \tag{3.2.1}$$

The subtle term is the interpolation error: $\|\mathrm{rot}\boldsymbol{u} - \mathrm{rot}_h\boldsymbol{u}_I\|$. The convergence rate of this term depends on the symmetry of the triangulation for RT_0-P_0 scheme, while the first-order convergence can be guaranteed for BDM_1-P_0 scheme on general quasi-uniform grids. We show the details in the following two subsections.

3.2.2 Error Analysis of BDM_1-P_0.

In this subsection, we present the error estimates for the discrete formulation (3.1.6) with the BDM_1-P_0 element.

Lemma 3.2.2 (Lemma 13 in Chen, Wang and Zhong [66])**.** *Assume that $\boldsymbol{u} \in \boldsymbol{H}^2 \cap \boldsymbol{H}_0^1$, and $\mathrm{div}\,\boldsymbol{u} = 0$. Let $\boldsymbol{u}_I$ be the canonical interpolation of $\boldsymbol{u}$ on to BDM_1. Then, we have the error estimate*

$$\|\,\mathrm{rot}\,\boldsymbol{u} - \mathrm{rot}_h\boldsymbol{u}_I\| \lesssim h\|\boldsymbol{u}\|_2.$$

So we get the error estimates for the BDM_1-P_0.

Theorem 3.2.3. *Assume that the solution of the Darcy-Stokes equations satisfies* $\boldsymbol{u} \in \boldsymbol{H}^2 \cap \boldsymbol{H}_0^1$ *and* $\operatorname{rot} \boldsymbol{u} \in H^2$*. Let* $\boldsymbol{u}_h$ *and* p_h *be the solution of the* BDM_1-P_0 *approximation using formulation* (3.1.6)*. Then, we have the following error estimate*

$$\|\boldsymbol{u}_h - \boldsymbol{u}_I\|_{V_h} + \|p_h - p_I\| \lesssim (\epsilon h + h^2)\|\boldsymbol{u}\|_2 + \epsilon^2 h \|\operatorname{rot} \boldsymbol{u}\|_2.$$

As $\epsilon \to 0$, we obtain the second order convergence of L^2-norm of the BDM_1-P_0 approximation of Darcy system and when $\epsilon \to 1$, we obtain the first order convergence of a H^1-type norm for Stokes equations.

Note that the computation of rot_h operator requires inverting the mass matrix of S_h space. For BDM_1-P_0 pair, the S_h space is the quadratic Lagrange element for which an accurate mass lumping is not available. We follow [85] to add a cubic bubble into P_2 and can thus obtain a accurate mass lumping. The resulting scheme will be denoted by $\mathrm{BDM}_1^{\mathrm{b}}$-$\mathrm{P}_0$ element. Details of the mass lumping and the error estimate can be found in [66].

3.2.3 Error Analysis of RT_0-P_0.

The estimate of RT_0 is more complicated. Let us recall the definition for the irregular triangulation following Bank and Xu [7], and two approximation properties.

Definition 3.2.4. *A triangulation* $\mathcal{T}_h$ *is* $\mathcal{O}(h^{2\sigma})$ *irregular if the following holds:*
(a) Let $\mathcal{E} = \mathcal{E}_1 \oplus \mathcal{E}_2$ *denote the set of interior edges in the triangulation mesh. For any* $e \in \mathcal{E}_1$*, two triangles* τ_e *and* τ_e' *containing* e *form an* $\mathcal{O}(h^2)$ *approximate parallelogram, and* $\sum_{e\in\mathcal{E}_2} |\tau_e| + |\tau_e'| = \mathcal{O}(h^{2\sigma})$.

(b) Let $\mathcal{P} = \mathcal{P}_1 \oplus \mathcal{P}_2$ denote the set of boundary vertices. The elements associated with each $x \in \mathcal{P}_1$ form an $\mathcal{O}(h^2)$ approximate parallelogram, and $|\mathcal{P}_2| = \kappa$, where κ is independent of h.

Lemma 3.2.3 (Lemma 8 in Chen, Wang, and Zhong [66])**.** *Assume that $\boldsymbol{u} \in \boldsymbol{W}^{2,\infty} \cap \boldsymbol{H}_0^1$, $\operatorname{div} \boldsymbol{u} = 0$, and the triangulation is $\mathcal{O}(h^{2\sigma})$ irregular. We have the error estimate:*

$$\|\operatorname{rot} \boldsymbol{u} - \operatorname{rot}_h \boldsymbol{u}_I\| \lesssim h^{\min(1,\sigma)} |\log h|^{1/2} \|\boldsymbol{u}\|_{2,\infty}.$$

Theorem 3.2.5. *Assume that the solution of the Darcy-Stokes equations satisfies $\boldsymbol{u} \in \boldsymbol{W}^{2,\infty} \cap \boldsymbol{H}_0^1$ and $\operatorname{rot} \boldsymbol{u} \in \boldsymbol{H}^2$. Assume the triangulation mesh is $\mathcal{O}(h^{2\sigma})$ irregular. Let $\boldsymbol{u}_h$ and p_h be the solution of the RT_0-P_0 approximation using formulation (3.1.6). Then, we have the error estimate*

$$\|\boldsymbol{u}_h - \boldsymbol{u}_I\|_{V_h} + \|p_h - p_I\| \lesssim \epsilon h^{\min(1,\sigma)} |\log h|^{1/2} \|\boldsymbol{u}\|_{2,\infty} + \epsilon^2 h \|\operatorname{rot} \boldsymbol{u}\|_2 + h\|\boldsymbol{u}\|_1.$$

As $\epsilon \to 0$, we obtain the first order convergence of L^2-norm since RT_0 contains only piecewise constant polynomial not full linear polynomial. When $\epsilon \to 1$, we obtain near first order convergence of a H^1-type norm if the mesh is symmetry in the sense that $\sigma \gg 1$.

3.3 A uniform preconditioner

We shall use the framework developed in [80]. Roughly speaking if an operator $\mathcal{L}$ from an Hilbert space X to its dual X^* is continuous and stable in the inner product $(\cdot,\cdot)_X$, then the Riesz representation induced by this inner product will be a good preconditioner of $\mathcal{L}$.

Therefore stability in Section 2 leads to a preconditioner in the form

$$\begin{pmatrix} (I_u - \epsilon^2 \Delta - \operatorname{grad} \operatorname{div})^{-1} & O \\ O & I_p^{-1} \end{pmatrix}. \tag{3.3.1}$$

As $\epsilon \to 0$, a fast solver for inverting $I_u - \operatorname{grad} \operatorname{div}$ is needed which requires a special smoother taking care of the large null space of div operator. We could expect the multigrid methods for

$H(\mathrm{div})$ problems developed in [3, 20] will work using preconditioner (3.3.1).

Here we shall follow [79] to establish a stability in a different norm. We first introduce the intersection and the sum of two Hilbert spaces. For Hilbert spaces X and Y, which are both contained in some larger Hilbert space, the intersection $X \cap Y$ and the sum $X + Y$ are both Hilbert spaces with norms given by

$$\|x\|_{X\cap Y}^2 = \|x\|_X^2 + \|x\|_Y^2$$

and

$$\|z\|_{X+Y}^2 = \inf_{x\in X, y\in Y, z=x+y} \left(\|x\|_X^2 + \|y\|_Y^2\right).$$

Furthermore, when $X \cap Y$ are dense in both spaces X and Y,

$$(X \cap Y)^* = X^* + Y^* \quad (X+Y)^* = X^* \cap Y^*. \tag{3.3.2}$$

For detailed proof of (3.3.2), we refer to [82].

Let us write the system (0.2.1) in the operator form

$$\mathcal{A}^\epsilon \begin{pmatrix} \boldsymbol{u} \\ p \end{pmatrix} = \begin{pmatrix} \boldsymbol{f} \\ 0 \end{pmatrix} \tag{3.3.3}$$

where

$$\mathcal{A}^\epsilon = \begin{pmatrix} I - \epsilon^2 \Delta & \mathrm{grad} \\ -\mathrm{div} & 0 \end{pmatrix}. \tag{3.3.4}$$

We define the spaces $X_\epsilon = \boldsymbol{V} \times W$ and $X_\epsilon^* = \boldsymbol{V}^* \times W^*$ by

$$X_\epsilon = (\boldsymbol{L}^2 \cap \epsilon \boldsymbol{H}_0^1) \times ((H^1 \cap L_0^2) + \epsilon^{-1} L_0^2)$$

and

$$X_\epsilon^* = (\boldsymbol{L}^2 + \epsilon^{-1} \boldsymbol{H}^{-1}) \times (H_0^{-1} \cap \epsilon L_0^2),$$

where $H_0^{-1} := (H^1 \cap L_0^2)^*$. The norm for velocity space $\boldsymbol{L}^2 \cap \epsilon \boldsymbol{H}_0^1$ is

$$\|\boldsymbol{v}\|^2_{\boldsymbol{L}^2 \cap \epsilon \boldsymbol{H}_0^1} = \|\boldsymbol{v}\|^2 + \epsilon^2 \|\nabla \boldsymbol{v}\|^2 = a^\epsilon(\boldsymbol{v}, \boldsymbol{v}),$$

and the norm for pressure space is

$$\|p\|^2_{H^1 + \epsilon^{-1} L_0^2} = \inf_{p_1 \in H^1 \cap L_0^2} \|p_1\|_1^2 + \epsilon^{-2} \|p - p_1\|^2.$$

Note that spaces chosen here are equivalent to the choices in Section 2 as linear spaces but with different norms.

By the definition of these norms, we can easily the continuity and the coercivity of bilinear form $a^\epsilon(\cdot, \cdot)$. We then verify the continuity of $b(\cdot, \cdot)$ in this norm.

Lemma 3.3.1. *The bilinear form* $b(\cdot, \cdot)$ *is continuous, i.e.,*

$$b(\boldsymbol{v}, p) \lesssim \|\boldsymbol{v}\|_{\boldsymbol{L}^2 \cap \epsilon \boldsymbol{H}_0^1} \|p\|_{H^1 + \epsilon^{-1} L_0^2}.$$

Proof. For any $q \in H^1 \cap L_0^2$,

$$\begin{aligned}
b(\boldsymbol{v}, p) &= -(\operatorname{div} \boldsymbol{v}, p - q) - (\operatorname{div} \boldsymbol{v}, q) \\
&\le \epsilon \|\operatorname{div} \boldsymbol{v}\| \epsilon^{-1} \|p - q\| + \|\boldsymbol{v}\| \|\operatorname{grad} q\| \\
&\lesssim (\|\boldsymbol{v}\| + \epsilon \|\operatorname{div} \boldsymbol{v}\|)(\epsilon^{-1} \|p - q\| + \|q\|_1) \\
&\lesssim \|\boldsymbol{v}\|_{\boldsymbol{L}^2 \cap \epsilon \boldsymbol{H}_0^1} \|p\|_{H^1 + \epsilon^{-1} L_0^2}.
\end{aligned}$$

□

The inf-sup condition in these non-standard norm can be derived from the existence of a right inverse of div operator

$$S \in \mathcal{L}(L_0^2, \boldsymbol{H}_0^1) \cap \mathcal{L}(H_0^{-1}, \boldsymbol{L}^2) \quad \text{and } \operatorname{div} S f = f.$$

The operator S is known as Bogovskii operator and can be found in many places, e.g. [17, 18]. We include the simple proof in [81] for the completeness.

Lemma 3.3.2. *The bilinear form $b(\cdot,\cdot)$ satisfies the inf-sup condition:*

$$\inf_{q\in W}\sup_{\boldsymbol{v}\in\boldsymbol{V}}\frac{b(\boldsymbol{v},q)}{\|\boldsymbol{v}\|_{\boldsymbol{L}^2\cap\epsilon\boldsymbol{H}_0^1}\|q\|_{H^1+\epsilon^{-1}L_0^2}}\geq\beta,$$

where the positive constant β is independent of the parameter ϵ.

Proof. For any $q\in L_0^2(\Omega)$, we have

$$\|q\|_{H^1+\epsilon^{-1}L_0^2}=\sup_{g\in H_0^{-1}\cap\epsilon L_0^2}\frac{\langle g,q\rangle}{\|g\|_{H_0^{-1}\cap\epsilon L_0^2}}\lesssim\sup_{g\in H_0^{-1}\cap\epsilon L_0^2}\frac{\langle \operatorname{div} Sg,q\rangle}{\|Sg\|_{\boldsymbol{L}^2\cap\epsilon\boldsymbol{H}_0^1}}\lesssim\sup_{\boldsymbol{v}\in\boldsymbol{V}}\frac{b(\boldsymbol{v},q)}{\|\boldsymbol{v}\|_{\boldsymbol{L}^2\cap\epsilon\boldsymbol{H}_0^1}}.$$

□

The well-posedness of the operator $\mathcal{A}^\epsilon$ from $X_\epsilon\to X_\epsilon^*$ leads to the block diagonal preconditioner

$$\mathcal{B}^\epsilon=\begin{pmatrix}(I-\epsilon^2\Delta)^{-1} & 0\\ 0 & (-\Delta_N)^{-1}+\epsilon^2 I\end{pmatrix},\tag{3.3.5}$$

where $-\Delta_N$ is the operator of Laplacian equation with pure Neumann boundary condition. The preconditioned operator $\mathcal{B}^\epsilon\mathcal{A}^\epsilon$ is uniformly bounded and consequently the inverse of $\mathcal{B}^\epsilon\mathcal{A}^\epsilon$ can be computed efficiently by Krylov space method.

We then move to the TMAC discretization. The discrete system (3.1.6) can be written as

$$\mathcal{A}_h^\epsilon\begin{pmatrix}\boldsymbol{u}_h\\ p_h\end{pmatrix}=\begin{pmatrix}\boldsymbol{f}_h\\ 0\end{pmatrix}\tag{3.3.6}$$

where

$$\mathcal{A}_h^\epsilon=\begin{pmatrix}M_u-\epsilon^2\Delta_h & \operatorname{grad}_h\\ -\operatorname{div} & 0\end{pmatrix},\tag{3.3.7}$$

with the discrete vector Laplacian $-\Delta_h = \operatorname{curl} \operatorname{rot}_h - \operatorname{grad}_h \operatorname{div}$. The corresponding block diagonal and positive definite operator is given by

$$\mathcal{B}_h^\epsilon = \begin{pmatrix} (M_u - \epsilon^2 \Delta_h)^{-1} & 0 \\ 0 & (-\Delta_{N,h})^{-1} + \epsilon^2 M_p^{-1} \end{pmatrix}, \tag{3.3.8}$$

where $-\Delta_{N,h} = -\operatorname{div} \operatorname{grad}_h$ and M_u, M_p are mass matrices for velocity and pressure, respectively.

Notice that our pressure space is not a subspace of H^1 and thus we cannot follow [81] by constructing a Fortin operator stable in both L^2 and H^1-norm. Instead we follow the approach in [82].

Let P_h denote the orthogonal projection $V_h' \to \operatorname{grad}_h(W_h)$ in the A_h^{-1} inner product. Let us introduce a lemma in [82] which presents a characterization of this operator.

Lemma 3.3.3. *Let $I : V_h \to V_h'$ be the Riesz isomorphism induced by the inner product $(\cdot,\cdot)_{1,h}$, i.e., $\langle I\boldsymbol{u}, \boldsymbol{v}\rangle = (\operatorname{rot}_h \boldsymbol{u}, \operatorname{rot}_h \boldsymbol{v}) + (\operatorname{div} \boldsymbol{u}, \operatorname{div} \boldsymbol{v})$. For $\boldsymbol{f} \in V_h'$, let $(\boldsymbol{u}_h, p_h) \in (V_h, W_h)$ be the unique solution of*

$$I\boldsymbol{u}_h + \operatorname{grad}_h p_h = \boldsymbol{f}, \tag{3.3.9}$$

$$-\operatorname{div} \boldsymbol{u}_h = 0. \tag{3.3.10}$$

Define the solution operator as $R : V_h' \to W_h$ by $\boldsymbol{f} \to p_h$. Then $P_h = \operatorname{grad}_h R$.

Introduce the vorticity $w_h = \operatorname{rot}_h u_h$ and stream function ϕ_h so that $\boldsymbol{u}_h = \operatorname{curl} \phi_h$. Then equations (3.3.9)-(3.3.10) is equivalent to the mixed formulation of biharmonic equation

$$\Delta w_h = \operatorname{rot} \boldsymbol{f}, \quad w_h = \Delta \phi_h.$$

Note that if $\boldsymbol{f} \in L^2$, then $\operatorname{curl} w_h = \boldsymbol{f}$ holds in L^2 and

$$b(\boldsymbol{v}_h, p_h) = (\boldsymbol{f}, \boldsymbol{v}_h) - (\operatorname{curl} w_h, \boldsymbol{v}_h), \quad \text{for all } \boldsymbol{v}_h \in V_h.$$

It suffices to verify the L^2 stability of the H^{-1} type projection P_h.

Lemma 3.3.4. *Assume the H^2-regularity holds for Stokes equation. For* BDM_1-P_0 *element, we have*

$$\|P_h \boldsymbol{f}_h\| \lesssim \|\boldsymbol{f}_h\|. \tag{3.3.11}$$

Proof. By definition, we have $P_h \boldsymbol{f}_h = \operatorname{grad}_h p_h = \operatorname{grad}_h R\boldsymbol{f}_h$ where R is defined as in Lemma 3.3.3.

Use the same data $\boldsymbol{f}_h$, we solve Stokes equations to get $\boldsymbol{u} \in H^2$ and let $w = \operatorname{rot} \boldsymbol{u}$. Then $\operatorname{curl} w = \boldsymbol{f}_h$ holds in L^2 and by the H^2-regularity assumption $\|w\|_1 = \|\boldsymbol{u}\| \lesssim \|\boldsymbol{f}_h\|$.

We start from the identity

$$\|P_h \boldsymbol{f}_h\| = \|\operatorname{grad}_h p_h\| = \sup_{\boldsymbol{v}_h \in \boldsymbol{V}_h} \frac{b(\boldsymbol{v}_h, p_h)}{\|\boldsymbol{v}_h\|} = \sup_{\boldsymbol{v}_h \in \boldsymbol{V}_h} \frac{(\operatorname{curl} w - \operatorname{curl} w_h, \boldsymbol{v}_h)}{\|\boldsymbol{v}_h\|},$$

and get $\|P_h \boldsymbol{f}_h\| \lesssim \|\operatorname{curl} w - \operatorname{curl} w_h\|$. We then estimate the error $\|\operatorname{curl} w - \operatorname{curl} w_h\|$ as follows. Let w_I be a quasi-interpolation of w satisfying

$$\|w - w_I\| + h\|\operatorname{curl}(w - w_I)\| \lesssim h\|w\|_1$$

Then

$$\begin{aligned}
\|\operatorname{curl} w - \operatorname{curl} w_h\| &\lesssim \|\operatorname{curl} w - \operatorname{curl} w_I\| + h^{-1}\|w_I - w_h\| \\
&\lesssim \|w\|_1 + h^{-1}\left(\|w - w_I\| + \|w - w_h\|\right) \\
&\lesssim \|\boldsymbol{f}_h\|.
\end{aligned}$$

In the third step, we use the error estimate obtained in [1] for biharmonic equation

$$\|w - w_h\| \lesssim h\|\boldsymbol{f}_h\|,$$

which only true when H^2-regularity result holds and the degree of the polynomial space for w_h is greater than or equal to 2 which is equivalent to using BDM_1 for velocity. □

According to Lemma 3.3.4, we can apply Theorem 4.2 in [82] to conclude that $(-\Delta_{N,h})^{-1}+\epsilon^2 M_p^{-1}$ is equivalent to the Schur complement of system $\mathcal{A}_h^\epsilon$.

Theorem 3.3.1. *Assume the H^2-regularity holds for Stokes equation. Let $\tilde{S}_h = (-\Delta_{N,h})^{-1} + \epsilon^2 M_p^{-1}$ and $S_h = -\operatorname{div}(M_u - \epsilon^2\Delta)^{-1}\operatorname{grad}_h$. There exist positive constant c_d, independent of h and ϵ, such for all $p_h \in W_h$ the following holds:*

$$c_d(\tilde{S}_h p_h, p_h) \le (S_h p_h, p_h) \le 2(\tilde{S}_h p_h, p_h).$$

Consequently, $\mathcal{B}_h^\epsilon$ is a uniform preconditioner of $\mathcal{A}_h^\epsilon$.

It is easy to verify that $\mathcal{B}_h^\epsilon$ is a uniform preconditioner of $\mathcal{A}_h^\epsilon$ by following the framework of [79], and similar proof can be found in [15].

3.4 Numerical Experiments

In the numerical tests with the square domain $[-1,1]\times[-1,1]$, the Dirichlet boundary condition for $\boldsymbol{u}$ are chosen, and the analytical solutions are

$$\boldsymbol{u}(x,y) = \operatorname{curl}\sin^2(\pi x)\sin^2(\pi y), \quad p(x,y) = \sin(\pi x).$$

Thus the righthand side $\boldsymbol{f} = \boldsymbol{u} - \epsilon^2\Delta\boldsymbol{u} - \operatorname{grad} p$.

We present numerical tests for both the RT_0-P_0 discretization and the $\mathrm{BDM}_1^{\mathrm{b}}$-$\mathrm{P}_0$ discretization. In order to avoid taking the inverse of the mass matrix in the discrete system, we consider the lumped schemes only. For both schemes, we consider two different types of grids: a crisscross grid (also referred to as a bisection grid), a three-directional structured grid (all triangles are formed by edges parallel to three directions only). We refer to Figure 3.1 for an illustration. We use a uniform bisect strategy for refining the bisection grid. That is the triangle is bisected twice by connecting the midpoint of the longest edge to its opposite vertex. In the so-called red refinement the triangle is divided into four congruent sub-triangles by connecting the midpoint of each edge. We use a uniform red refinement for refining the three-directional grids such that the resulting grids remains three-directional.

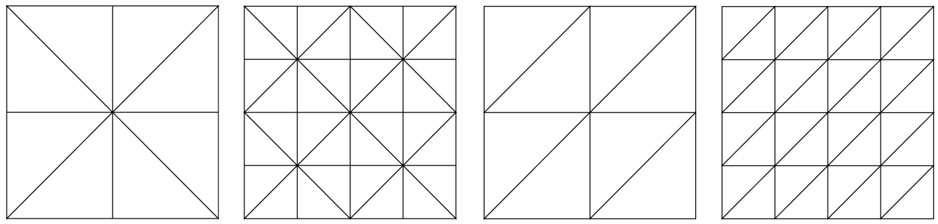

Figure 3.1: Bisection grids and three-directional structured grids of a square domain.

We implemented the schemes by using the MATLAB© software package iFEM [13].

3.4.1 Uniform convergence

In this subsection, we present that the discrete systems are uniformly convergent. By using BDM1b-P_0 or RT_0-P_0, the convergence rates is uniform with respect to the perturbation parameter ϵ by red refinement meshes.

ϵ \ h	2^{-2}	2^{-3}	2^{-4}	2^{-5}	2^{-6}	Rate
1	0.5633	0.1515	0.0383	0.0096	0.0024	1.9739
2^{-2}	0.5625	0.1515	0.0383	0.0096	0.0024	1.9735
2^{-4}	0.5593	0.1516	0.0383	0.0096	0.0024	1.9719
2^{-8}	0.5583	0.1538	0.0386	0.0096	0.0024	1.9732
0	0.5583	0.1539	0.0387	0.0096	0.0024	1.9730

Table 3.1: $\|\boldsymbol{u} - \boldsymbol{u}_h\|$ obtained by BDM1b-P_0 element by red refinement

ϵ \ h	2^{-2}	2^{-3}	2^{-4}	2^{-5}	2^{-6}	Rate
1	8.2503	3.2262	0.9753	0.2614	0.0724	1.7289
2^{-2}	2.0820	0.8101	0.2441	0.0653	0.0173	1.7457
2^{-4}	0.5921	0.2151	0.0623	0.0164	0.0043	1.7955
2^{-8}	0.3004	0.0701	0.0118	0.0019	0.0003	2.4775
0	0.2988	0.0688	0.0110	0.0015	0.0002	2.6739

Table 3.2: $\|\boldsymbol{u}_h - \boldsymbol{u}_I\|_{V_h}$ obtained by BDM1b-P_0 element by red refinement

ϵ \ h	2^{-2}	2^{-3}	2^{-4}	2^{-5}	2^{-6}	Rate
1	0.9424	0.2944	0.1024	0.0421	0.0188	1.4104
2^{-2}	0.2676	0.1319	0.0656	0.0328	0.0164	1.0071
2^{-4}	0.2603	0.1307	0.0654	0.0327	0.0164	0.9982
2^{-8}	0.2602	0.1307	0.0654	0.0327	0.0164	0.9980
0	0.2602	0.1307	0.0654	0.0327	0.0164	0.9980

Table 3.3: $\|p - p_h\|$ obtained by BDM1b-P_0 element by red refinement

ϵ \ h	2^{-2}	2^{-3}	2^{-4}	2^{-5}	2^{-6}	Rate
1	2.1312	1.1086	0.5609	0.2813	0.1407	0.9820
2^{-2}	2.0815	1.1028	0.5601	0.2812	0.1407	0.9745
2^{-4}	2.0244	1.0947	0.5591	0.2810	0.1407	0.9655
2^{-8}	2.0221	1.0942	0.5590	0.2810	0.1407	0.9651
0	2.0221	1.0942	0.5590	0.2810	0.1407	0.9651

Table 3.4: $\|\boldsymbol{u} - \boldsymbol{u}_h\|$ obtained by RT_0-P_0 element by red refinement

ϵ \ h	2^{-2}	2^{-3}	2^{-4}	2^{-5}	2^{-6}	Rate
1	4.6551	1.2145	0.3038	0.0766	0.0315	1.8403
2^{-2}	1.1194	0.2965	0.0741	0.0185	0.0056	1.9295
2^{-4}	0.4932	0.1415	0.0360	0.0090	0.0022	1.9531
2^{-8}	0.4731	0.1410	0.0368	0.0093	0.0023	1.9253
0	0.4730	0.1410	0.0368	0.0093	0.0023	1.9247

Table 3.5: $\|\boldsymbol{u}_h - \boldsymbol{u}_I\|_{V_h}$ obtained by RT_0-P_0 element by red refinement

h / ϵ	2^{-2}	2^{-3}	2^{-4}	2^{-5}	2^{-6}	Rate
1	3.7024	1.0016	0.2614	0.0717	0.0229	1.8480
2^{-2}	0.3856	0.1510	0.0682	0.0331	0.0164	1.1300
2^{-4}	0.2705	0.1321	0.0656	0.0327	0.0164	1.0106
2^{-8}	0.2672	0.1316	0.0655	0.0327	0.0164	1.0065
0	0.2672	0.1316	0.0655	0.0327	0.0164	1.0065

Table 3.6: $\|p - p_h\|$ obtained by RT_0-P_0 element by red refinement

3.4.2 Robustness to meshes

In this subsection, we present the convergence rates of BDM1b-P_0 element and RT_0-P_0 element by bisection refinement meshes. We can see that the convergence rate of BDM1b-P_0 element is robust to the meshes, while $\|\boldsymbol{u}_h - \boldsymbol{u}_I\|_{V_h}$ obtained by RT_0-P_0 element by bisection refinement diverges for some values of ϵ.

h / ϵ	2^{-2}	2^{-3}	2^{-4}	2^{-5}	2^{-6}	Rate
1	0.5633	0.1442	0.0366	0.0092	0.0023	1.9850
2^{-2}	0.5625	0.1441	0.0366	0.0092	0.0023	1.9845
2^{-8}	0.5593	0.1436	0.0366	0.0092	0.0023	1.9824
2^{-8}	0.5583	0.1443	0.0366	0.0092	0.0023	1.9826
0	0.5583	0.1444	0.0367	0.0092	0.0023	1.9826

Table 3.7: $\|\boldsymbol{u} - \boldsymbol{u}_h\|$ obtained by BDM1b-P_0 element by bisection refinement

h / ϵ	2^{-2}	2^{-3}	2^{-4}	2^{-5}	2^{-6}	Rate
1	8.2503	2.8396	1.2806	0.6139	0.3040	1.1734
2^{-2}	2.0820	0.7137	0.3206	0.1535	0.0759	1.1772
2^{-4}	0.5921	0.1928	0.0818	0.0386	0.0190	1.2250
2^{-8}	0.3004	0.0739	0.0172	0.0046	0.0015	1.9273
0	0.2988	0.0730	0.0164	0.0039	0.0009	2.0838

Table 3.8: $\|\boldsymbol{u}_h - \boldsymbol{u}_I\|_{V_h}$ obtained by BDM1b-P_0 element by bisection refinement

ϵ \ h	2^{-2}	2^{-3}	2^{-4}	2^{-5}	2^{-6}	Rate
1	0.9424	0.2993	0.1035	0.0426	0.0189	1.4085
2^{-2}	0.2676	0.1319	0.0656	0.0328	0.0164	1.0070
2^{-4}	0.2603	0.1307	0.0654	0.0327	0.0164	0.9982
2^{-8}	0.2602	0.1307	0.0654	0.0327	0.0164	0.9980
0	0.2602	0.1307	0.0654	0.0327	0.0164	0.9980

Table 3.9: $\|p - p_h\|$ obtained by BDM1b-P_0 element by bisection refinement

ϵ \ h	2^{-2}	2^{-3}	2^{-4}	2^{-5}	2^{-6}	Rate
1	2.1312	1.0628	0.5263	0.2626	0.1312	1.0060
2^{-2}	2.0815	1.0544	0.5255	0.2625	0.1312	0.9982
2^{-4}	2.0244	1.0398	0.5240	0.2623	0.1312	0.9883
2^{-8}	2.0221	1.0373	0.5235	0.2622	0.1311	0.9878
0	2.0221	1.0373	0.5235	0.2622	0.1311	0.9878

Table 3.10: $\|\boldsymbol{u} - \boldsymbol{u}_h\|$ obtained by RT_0-P_0 element by bisection refinement

ϵ \ h	2^{-2}	2^{-3}	2^{-4}	2^{-5}	2^{-6}	Rate
1	4.6551	10.1485	9.8943	9.8522	9.8532	-0.2121
2^{-2}	1.1194	2.5551	2.4806	2.4650	2.4638	-0.2224
2^{-4}	0.4932	0.7273	0.6489	0.6240	0.6179	-0.0429
2^{-8}	0.4731	0.3776	0.2031	0.1086	0.0640	0.7569
0	0.4730	0.3756	0.1995	0.1016	0.0511	0.8305

Table 3.11: $\|\boldsymbol{u}_h - \boldsymbol{u}_I\|_{V_h}$ obtained by RT_0-P_0 element by bisection refinement

ϵ \ h	2^{-2}	2^{-3}	2^{-4}	2^{-5}	2^{-6}	Rate
1	3.7024	1.7085	0.9651	0.6409	0.4453	0.7526
2^{-2}	0.3856	0.1721	0.0896	0.0519	0.0323	0.8885
2^{-4}	0.2705	0.1315	0.0656	0.0328	0.0165	1.0078
2^{-8}	0.2672	0.1309	0.0654	0.0327	0.0164	1.0059
0	0.2672	0.1309	0.0654	0.0327	0.0164	1.0059

Table 3.12: $\|p - p_h\|$ obtained by RT_0-P_0 element by bisection refinement

3.4.3 Uniform Preconditioner

In this subsection, we can see that the preconditioned discrete systems can be solved by Minres with uniformly bounded steps.

ϵ \ h	2^{-2}	2^{-3}	2^{-4}	2^{-5}	2^{-6}
1	21	13	11	9	9
2^{-2}	21	25	27	29	17
2^{-4}	21	23	25	29	31
2^{-8}	23	23	23	23	21
0	23	23	23	23	23

Table 3.13: Minres iteration steps to 10^{-6} obtained by BDM_1-P_0 element with red refinement

ϵ \ h	2^{-2}	2^{-3}	2^{-4}	2^{-5}	2^{-6}
1	21	13	11	9	7
2^{-2}	21	21	21	23	15
2^{-4}	21	19	19	21	17
2^{-8}	23	17	17	15	15
0	23	17	17	15	15

Table 3.14: Minres iteration steps to 10^{-6} obtained by BDM_1-P_0 element with bisection refinement

ϵ \ h	2^{-2}	2^{-3}	2^{-4}	2^{-5}	2^{-6}
1	19	11	11	9	7
2^{-2}	19	21	25	27	17
2^{-4}	19	21	23	25	29
2^{-8}	23	23	23	21	19
0	23	23	23	23	23

Table 3.15: Minres iteration steps to 10^{-6} obtained by RT_0-P_0 element with red refinement

ϵ \ h	2^{-2}	2^{-3}	2^{-4}	2^{-5}	2^{-6}
1	19	19	11	9	9
2^{-2}	19	19	21	21	15
2^{-4}	19	17	19	21	17
2^{-8}	23	13	13	13	13
0	23	11	11	9	9

Table 3.16: Minres iteration steps to 10^{-6} obtained by RT_0-P_0 element with bisection refinement

Chapter 4

Block Triangular Preconditioner for the Stochatic Stokes Equations

We study efficient iterative solvers for the stochastic Galerkin discretization of the Stokes equations with random viscosity. The stochastic saddle-point linear systems are obtained by using H(div) finite element discretization in physical space and generalized polynomial chaos expansion in random space. We prove the existence and uniqueness of the solutions to the continuous problem and its corresponding stochastic Galerkin discretization. Optimal error estimates are also derived. We construct block-diagonal/triangular preconditioners for use with the generalized minimum residual method and the bi-conjugate gradient stabilized method. An optimal multigrid solver is applied to efficiently solve the diagonal blocks that correspond to deterministic discrete Stokes systems. We also design a multigrid method with either the block Jacobi method or block Gauss-Seidel method as the smoother for solving the stochastic saddle-point systems. It is shown that the multigrid method using the block Gauss-Seidel smoother is more efficient and robust than that using the block Jacobi smoother. To demonstrate the efficiency and robustness of the proposed block preconditioners and multigrid method with respect to all discretization parameters and random viscosity variance, various numerical examples also are provided.

We use notation Ω for the random space, and D for the physical domain. Let $D \subset \mathbb{R}^2$ be a bounded convex polygonal domain with boundary ∂D. $(\Omega, \mathcal{F}, \mathcal{P})$ denotes a complete probability space, where Ω is the set of outcomes, $\mathcal{F} \subset 2^{\Omega}$ is the $\sigma-$algebra of random events, and $\mathcal{P}$ is the probability measure.

4.1 Stokes Equations with Random Viscosity

We consider the following steady-state Stokes equations with random coefficient:

$$\begin{cases} -\nu(\omega)\Delta \boldsymbol{u}(\omega, x) + \operatorname{grad} p(\omega, x) = & \boldsymbol{f}(x) \qquad \text{in } \Omega \times D, \\ -\operatorname{div} \boldsymbol{u}(\omega, x) = & 0 \qquad \text{in } \Omega \times D, \\ \boldsymbol{u}(\omega, x) = & \boldsymbol{g}_D(x) \quad \text{on } \Omega \times \partial D, \end{cases} \tag{4.1.1}$$

where $\boldsymbol{u}$ is the velocity field, p is the pressure, ν is random viscosity, and $\boldsymbol{f}$ is an external force field. For simplicity, we assume that $\boldsymbol{f}$ and $\boldsymbol{g}_D$ are deterministic functions. We also assume that ν is bounded and uniformly coercive, i.e.,

$$\exists \nu_{min}, \nu_{max} \in (0, +\infty) : \mathcal{P}(\omega \in \Omega : \nu(\omega) \in [\nu_{min}, \nu_{max}]) = 1. \tag{4.1.2}$$

In this paper, we consider a special case where the viscosity is given in the form $\nu(\omega) = \nu(\xi(\omega))$, and ξ is assumed to be a random variable, having probability density function $\rho_{\xi} : \Gamma \to \mathbb{R}^{+}$ with bounded $\Gamma := \xi(\Omega)$. We also assume that the Dirichlet boundary condition $\boldsymbol{g}_D(x) = 0$. By the Doob-Dynkin lemma [69], the random fields $\boldsymbol{u}$ and p can also be expressed as functions of ξ, i.e., $\boldsymbol{u} = \boldsymbol{u}(\xi, x)$ and $p = p(\xi, x)$. Then, the stochastic Stokes equations (4.1.1) can be written in the following deterministic parameterized form:

$$\begin{cases} -\nu(\xi)\Delta \boldsymbol{u}(\xi, x) + \operatorname{grad} p(\xi, x) = & \boldsymbol{f}(x) \qquad \text{in } \Gamma \times D, \\ -\operatorname{div} \boldsymbol{u}(\xi, x) = & 0 \qquad \text{in } \Gamma \times D, \\ \boldsymbol{u}(\xi, x) = & \boldsymbol{0} \qquad \text{on } \Gamma \times \partial D. \end{cases} \tag{4.1.3}$$

4.1.1 The Velocity-Pressure Formulation.

For any $\boldsymbol{u} \in \boldsymbol{H}_0^1(D)$, the following identity for the vector Laplacian holds in $\boldsymbol{H}^{-1}(D)$ topology:

$$-\Delta \boldsymbol{u} = \operatorname{curl} \operatorname{rot} \boldsymbol{u} - \operatorname{grad} \operatorname{div} \boldsymbol{u}.$$

A variational formulation of the stochastic Stokes equations (4.1.3) is: find $\boldsymbol{u} \in L^2(\Gamma) \otimes \boldsymbol{H}_0^1(D)$ and $p \in L^2(\Gamma) \otimes L_0^2(D)$ such that

$$\begin{cases} A(\boldsymbol{u}, \boldsymbol{v}) + B(\boldsymbol{v}, p) = E[(\boldsymbol{f}, \boldsymbol{v})] & \text{for all } \ \boldsymbol{v} \in L^2(\Gamma) \otimes \boldsymbol{H}_0^1(D), \\ B(\boldsymbol{u}, q) = 0 & \text{for all } \ q \in L^2(\Gamma) \otimes L_0^2(D), \end{cases} \tag{4.1.4}$$

where the bilinear forms $A(\cdot,\cdot)$ and $B(\cdot,\cdot)$ are defined as: for $\boldsymbol{u}, \boldsymbol{v} \in L^2(\Gamma) \otimes \boldsymbol{H}_0^1(D)$,

$$A(\boldsymbol{u}, \boldsymbol{v}) := E[\nu(\xi)(\operatorname{rot} \boldsymbol{u}, \operatorname{rot} \boldsymbol{v}) + \nu(\xi)(\operatorname{div} \boldsymbol{u}, \operatorname{div} \boldsymbol{v})];$$

and for $\boldsymbol{v} \in L^2(\Gamma) \otimes \boldsymbol{H}_0^1(D),\ q \in L^2(\Gamma) \otimes L_0^2(D)$,

$$B(\boldsymbol{v}, q) := -E[(\operatorname{div} \boldsymbol{v}, q)].$$

4.1.2 The Wellposedness.

According to the definition of the bilinear forms $A(\boldsymbol{u}, \boldsymbol{v})$ and $B(\boldsymbol{v}, q)$ and the boundedness and coercivity of the random variable $\nu(\xi)$, it is straightforward to verify both the continuity and coercivity of A, i.e., for all $\boldsymbol{u}, \boldsymbol{v} \in L^2(\Gamma) \otimes \boldsymbol{H}_0^1(D)$

$$|A(\boldsymbol{u}, \boldsymbol{v})| \leq \nu_{max} \|\boldsymbol{u}\|_{L^2(\Gamma)\otimes \boldsymbol{H}_0^1(D)} \|\boldsymbol{v}\|_{L^2(\Gamma)\otimes \boldsymbol{H}_0^1(D)},$$
$$|A(\boldsymbol{u}, \boldsymbol{u})| \geq \nu_{min} \|\boldsymbol{u}\|^2_{L^2(\Gamma)\otimes \boldsymbol{H}_0^1(D)},$$

and the continuity of B, i.e., for all $\boldsymbol{u} \in L^2(\Gamma) \otimes \boldsymbol{H}_0^1(D)$ and $q \in L^2(\Gamma) \otimes L_0^2(D)$

$$|B(\boldsymbol{u}, q)| \leq \|\boldsymbol{u}\|_{L^2(\Gamma)\otimes \boldsymbol{H}_0^1(D)} \|q\|_{L^2(\Gamma)\otimes L_0^2(D)}.$$

Hence, to prove the well-posedness of (4.1.4), it is sufficient to prove the inf-sup condition for the bilinear form $B(\cdot,\cdot)$. Thus, we prove the following lemma, which is equivalent to the inf-sup condition.

Lemma 4.1.1. *For any $q(\xi, \boldsymbol{x}) \in L^2(\Gamma) \otimes L_0^2(D)$, there exists a $\boldsymbol{v}(\xi, \boldsymbol{x}) \in L^2(\Gamma) \otimes \boldsymbol{H}_0^1(D)$ such that*

$$\operatorname{div} \boldsymbol{v} = q, \quad \textit{and} \quad \|\boldsymbol{v}\|_{L^2(\Gamma)\otimes \boldsymbol{H}_0^1(D)} \lesssim \|q\|_{L^2(\Gamma)\otimes L_0^2(D)}.$$

Proof. For any $q(\xi, \boldsymbol{x}) \in L^2(\Gamma) \otimes L_0^2(D)$, we can expand $q(\xi, \boldsymbol{x})$ in the form:

$$q(\xi, \boldsymbol{x}) = \sum_{i=1}^{\infty} q^i(\boldsymbol{x}) \Psi_i(\xi),$$

where $q^i(\boldsymbol{x}) = E[q(\xi, \boldsymbol{x})\Psi_i(\xi)] \in L_0^2(D)$. Then, the tensor norm can be written as the summation of the L^2 norm of each coefficient, i.e., $\|q\|^2_{L^2(\Gamma)\otimes L_0^2(D)} = \sum_{i=1}^{\infty} \|q^i(\boldsymbol{x})\|^2$.

It is already known that for each $q^i(\boldsymbol{x}) \in L_0^2(D)$, there exists a corresponding $\boldsymbol{v}^i(\boldsymbol{x}) \in \boldsymbol{H}_0^1(D)$, such that

$$\operatorname{div} \boldsymbol{v}^i(\boldsymbol{x}) = q^i(\boldsymbol{x}) \quad \text{and} \quad \|\boldsymbol{v}^i(\boldsymbol{x})\|_1 \leq c\|q^i(\boldsymbol{x})\|,$$

where $c > 0$ (see [70]). With $\boldsymbol{v}^i(\boldsymbol{x})$ as the coefficients, we can define the function $\boldsymbol{v}(\xi, \boldsymbol{x}) := \sum_{i=1}^{\infty} \boldsymbol{v}^i(\boldsymbol{x})\Psi_i(\xi)$.

$$\begin{aligned}\|\boldsymbol{v}(\xi, \boldsymbol{x})\|_{L^2(\Gamma)\otimes \boldsymbol{H}_0^1(D)} &= \sum_{i=1}^{\infty} (\|\operatorname{rot} \boldsymbol{v}^i(\boldsymbol{x})\|^2 + \|\operatorname{div} \boldsymbol{v}^i(\boldsymbol{x})\|^2) \leq 2c \sum_{i=1}^{\infty} \|q^i(\boldsymbol{x})\|^2 \\ &\leq 2c\|q(\xi, \boldsymbol{x})\|_{L^2(\Gamma)\otimes L_0^2(D)} < \infty.\end{aligned}$$

Then, $\boldsymbol{v}(\xi, \boldsymbol{x}) \in L^2(\Gamma) \otimes \boldsymbol{H}_0^1(D)$ and satisfies

$$\operatorname{div} \boldsymbol{v} = q, \ \text{ and } \ \|\boldsymbol{v}\|_{L^2(\Gamma)\otimes \boldsymbol{H}_0^1(D)} \lesssim \|q\|_{L^2(\Gamma)\otimes L_0^2(D)}.$$

Then, we prove that $\boldsymbol{v}(\xi, \boldsymbol{x})$ is a well-defined function, which satisfies the conditions. $\square$

In summary, we acquire the following result for the well-posedness of the variational formulation (4.1.4)

Theorem 4.1.1. *There exists a unique solution $\boldsymbol{u} \in L^2(\Gamma) \otimes \boldsymbol{H}_0^1(D)$ and $p \in L^2(\Gamma) \otimes L_0^2(D)$ to the variational formulation* (4.1.4)*, and*

$$\|\boldsymbol{u}\|_{L^2(\Gamma)\otimes \boldsymbol{H}_0^1(D)} + \|p\|_{L^2(\Gamma)\otimes L_0^2(D)} \lesssim \|\boldsymbol{f}\|_{L^2(\Gamma)\otimes \boldsymbol{H}_0^{-1}(D)},$$

where $\|\boldsymbol{f}\|_{L^2(\Gamma)\otimes \boldsymbol{H}_0^{-1}(D)} = \sup_{\boldsymbol{v}\in L^2(\Gamma)\otimes \boldsymbol{H}_0^1(D)} \dfrac{E[(\boldsymbol{f}, \boldsymbol{v})]}{\|\boldsymbol{v}\|_{L^2(\Gamma)\otimes \boldsymbol{H}_0^1(D)}}$.

4.2 The Discrete Problem

4.2.1 The Discrete Problem.

In the tensor space $L^2(\Gamma) \otimes \boldsymbol{V}_0^h$, we define the following inner product and the associated norm:

Definition 4.2.1. *For any $\boldsymbol{u}, \boldsymbol{v} \in L^2(\Gamma) \otimes \boldsymbol{V}_0^h$, the inner product*

$$(\boldsymbol{u}, \boldsymbol{v})_{L^2(\Gamma)\otimes \boldsymbol{V}_0^h} := E[(\mathrm{rot}_h \boldsymbol{u}, \mathrm{rot}_h \boldsymbol{v}) + (\operatorname{div} \boldsymbol{u}, \operatorname{div} \boldsymbol{v})]$$

defines an associated norm

$$\|\boldsymbol{u}\|^2_{L^2(\Gamma)\otimes \boldsymbol{V}_0^h} := (\boldsymbol{u}, \boldsymbol{u})_{L^2(\Gamma)\otimes \boldsymbol{V}_0^h}.$$

By following [66], we can easily verify the well-posedness of the discrete operator rot_h and the inner product $(\cdot, \cdot)_{L^2(\Gamma)\otimes \boldsymbol{V}_0^h}$. Based on these, we obtain a discrete variational formulation of (4.1.4):

find $\boldsymbol{u}_{m,h} \in Y^m \otimes \boldsymbol{V}_0^h$ and $p_{m,h} \in Y^m \otimes W_0^h$, such that

$$\begin{cases} A_h(\boldsymbol{u}_{m,h}, \boldsymbol{v}_{m,h}) + B(\boldsymbol{v}_{m,h}, p_{m,h}) = E[(\boldsymbol{f}, \boldsymbol{v}_{m,h})] & \text{for all } \boldsymbol{v}_{m,h} \in Y^m \otimes \boldsymbol{V}_0^h, \\ B(\boldsymbol{u}_{m,h}, q_{m,h}) = 0 & \text{for all } q_{m,h} \in Y^m \otimes W_0^h, \end{cases} \tag{4.2.1}$$

where the discrete bilinear form A_h is defined as: for $\boldsymbol{u}_{m,h}, \boldsymbol{v}_{m,h} \in Y^m \otimes \boldsymbol{V}_0^h$

$$A_h(\boldsymbol{u}_{m,h}, \boldsymbol{v}_{m,h}) := E[\nu(\xi)(\mathrm{rot}_h \boldsymbol{u}_{m,h}, \mathrm{rot}_h \boldsymbol{v}_{m,h}) + \nu(\xi)(\mathrm{div}\, \boldsymbol{u}_{m,h}, \mathrm{div}\, \boldsymbol{v}_{m,h})].$$

4.2.2 The Matrix Form

The bilinear forms A_h and B can be represented by the tensor product of the spacial matrices:

$$K = \left(\int_D \mathrm{rot}_h \boldsymbol{\Phi}_i(\boldsymbol{x}) \mathrm{rot}_h \boldsymbol{\Phi}_j(\boldsymbol{x}) + \mathrm{div}\, \boldsymbol{\Phi}_i(\boldsymbol{x})\, \mathrm{div}\, \boldsymbol{\Phi}_i(\boldsymbol{x}) d\boldsymbol{x} \right)_{i,\ j=1,\cdots,N_u},$$
$$W = \left(\int_D \mathrm{div}\, \boldsymbol{\Phi}_i(\boldsymbol{x}) \chi_j(\boldsymbol{x}) d\boldsymbol{x} \right)_{i=1,\cdots,N_e,\ j=1,\ldots,N_p},$$

and the stochastic matrices:

$$G_0 = \left(\int_\Gamma \Psi_i(y)\Psi_j(y)\rho_\xi(y) dy \right)_{i,\ j=1,\cdots,N_\xi},$$
$$G_1 = \left(\int_\Gamma \nu(y)\Psi_i(y)\Psi_j(y)\rho_\xi(y) dy \right)_{i,\ j=1,\cdots,N_\xi}.$$

With the expansion

$$\boldsymbol{u}_{m,h} = \sum_{j=1}^{N_\xi} \sum_{i=1}^{N_u} U_{(j-1)N_u+i} \boldsymbol{\Phi}_i(\boldsymbol{x}) \Psi_j(\xi), \quad p_{m,h} = \sum_{j=1}^{N_\xi} \sum_{i=1}^{N_p} P_{(j-1)N_p+i} \chi_i(\boldsymbol{x}) \Psi_j(\xi),$$

we obtain the matrix form of the discrete formulation (4.2.1) :

$$L \begin{pmatrix} \vec{U} \\ \vec{P} \end{pmatrix} := \begin{pmatrix} G_1 \otimes K & G_0 \otimes W' \\ G_0 \otimes W & 0 \end{pmatrix} \begin{pmatrix} \vec{U} \\ \vec{P} \end{pmatrix} = \begin{pmatrix} \vec{F} \\ \vec{0} \end{pmatrix}, \tag{4.2.2}$$

where $F_{(j-1)N_u+i} = E[(\boldsymbol{f}, \Phi_i(x)\Psi_j(\xi))]$, $\vec{F} = (F_i)_{i=1,\dots,N_u \times N_\xi}$, $\vec{U} = (U_i)_{i=1,\dots,N_u \times N_\xi}$, $\vec{P} = (P_i)_{i=1,\dots,N_p \times N_\xi}$.

4.2.3 Well-posedness of the Discrete Problem.

At the discrete level, we consider the velocity $\boldsymbol{u} \in Y^m \otimes \boldsymbol{V}_0^h \subset L^2(\Gamma) \otimes \boldsymbol{H}_0(\mathrm{div})$, which is not in $L^2(\Gamma) \otimes \boldsymbol{H}_0^1(D)$. We prove the well-posedness of the discrete variational formulation (4.2.1) based on a weaker norm on the subspace $L^2(\Gamma) \otimes \boldsymbol{V}_0^h$.

Theorem 4.2.2. *There exists a unique solution $\boldsymbol{u}_{m,h} \in Y^m \otimes \boldsymbol{V}_0^h$ and $p_{m,h} \in Y^m \otimes W_0^h$ to the variational formulation* (4.2.1)*, and*

$$\|\boldsymbol{u}_{m,h}\|_{L^2(\Gamma)\otimes \boldsymbol{V}_0^h} + \|p_{m,h}\|_{L^2(\Gamma)\otimes L_0^2(D)} \lesssim \|\boldsymbol{f}\|_{L^2(\Gamma)\otimes \boldsymbol{V}_0^{h\prime}},$$

where $\|\boldsymbol{f}\|_{L^2(\Gamma)\otimes \boldsymbol{V}_0^{h\prime}} = \sup_{\boldsymbol{v}\in L^2(\Gamma)\otimes \boldsymbol{V}_0^h} \dfrac{E[(\boldsymbol{f}, \boldsymbol{v})]}{\|\boldsymbol{v}\|_{L^2(\Gamma)\otimes \boldsymbol{V}_0^h}}$.

According to the definition of the norm $\|\cdot\|_{L^2(\Gamma)\otimes \boldsymbol{V}_0^h}$ and the bilinear operators, it is straightforward to show the continuity and coercivity of the bilinear form $A_h(\cdot,\cdot)$ and the continuity of $B(\cdot,\cdot)$. Hence, to prove Theorem 4.2.2, it is sufficient to show the following inf-sup condition:

Lemma 4.2.1. *For any $q_{m,h}(\xi, x) \in Y^m \otimes W_0^h$, there exists a $\boldsymbol{v}_{m,h}(\xi, x) \in Y^m \otimes \boldsymbol{V}_0^h$, such that*

$$\mathrm{div}\, \boldsymbol{v}_{m,h} = q_{m,h}, \;\; \textit{and} \;\; \|\boldsymbol{v}_{m,h}\|_{L^2(\Gamma)\otimes \boldsymbol{V}_0^h} \lesssim \|q_{m,h}\|_{L^2(\Gamma)\otimes L_0^2(D)}.$$

Proof. Using the deterministic result in [66] that for any $q(x) \in W_0^h$, there exists $\boldsymbol{v}(x) \in \boldsymbol{V}_0^h$, such that

$$\mathrm{div}\, \boldsymbol{v}(x) = q(x) \;\text{ and }\; \|\boldsymbol{v}(x)\|_{\boldsymbol{V}_0^h} \le \tilde{c}\|q(x)\|,$$

where $\tilde{c} > 0$, $\|\boldsymbol{v}\|^2_{\boldsymbol{V}_0^h} = (\mathrm{rot}_h\, \boldsymbol{v}, \mathrm{rot}_h\, \boldsymbol{v}) + (\mathrm{div}\, \boldsymbol{v}, \mathrm{div}\, \boldsymbol{v})$, and following the proof of Lemma 4.1.1, we can obtain the desired result. $\square$ $\square$

4.3 Error Analysis

In this section, we prove that, on mildly structured meshes, the solution of the discrete problem (4.2.1) can achieve the optimal first-order convergence on the spacial approximation, and the optimal order on the stochastic approximation.

Let us introduce the gPC orthogonal projection operator

$$\mathcal{R}_n : L^2(\Gamma) \to Y^{n-1}, \quad \mathcal{R}_n f = \sum_{k=1}^{n} f^k \Psi_k(\xi), \quad f^k = E[f \Psi_k(\xi)],$$

and the L^2 projection operator

$$Q_h : L^2(D) \to \Sigma^h, \quad (Q_h f, \tau) = (f, \tau) \quad \text{for all } \tau \in \Sigma^h,$$

We present analyses of these interpolations and projections, which will be used in the error estimates of the stochastic Stokes equations, as the following three lemmas.

Lemma 4.3.1. *(Chen, Wang, and Zhong [66]) Assume that $\boldsymbol{v} \in \boldsymbol{W}^{2,\infty}(D) \bigcap \boldsymbol{H}_0^1(D)$, $\mathrm{div}\, \boldsymbol{v} = 0$, and the triangulation is $\mathcal{O}(h^2)$ irregular. We have the error estimate:*

$$\|\, \mathrm{rot}\, \boldsymbol{v} - \mathrm{rot}_h \Pi_{\boldsymbol{V}_0^h} \boldsymbol{v}\| \lesssim h |\log h|^{1/2} \|\boldsymbol{v}\|_{2,\infty}.$$

Lemma 4.3.2. *The R_n projection holds the optimality:*

$$\|f - R_n f\|_{L^2(\Gamma)} = \inf_{g \in P_{n-1}(\Gamma)} \|f - g\|_{L^2(\Gamma)},$$

where $P_{n-1}(D)$ is the linear space of all polynomials of Γ of degrees up to $n-1$.

Remark 4.3.1. *In Lemma 4.3.2, the convergence rate depends on the smoothness of the function, e.g., if* $f(x) \in H^p[-1,1],\ p \geqslant 0$, *then* $\|f - R_n f\|_{L^2(\Gamma)} \lesssim (n-1)^{-p}\|f\|_{H^p[-1,1]}$ *(see [71]). This optimality is also valid on smaller tensor spaces, such as* $L^2(\Gamma) \otimes H^1(D)$ *and* $L^2(\Gamma) \otimes \boldsymbol{H}^2(D)$.

Hereafter, we use the following notation:

$$\begin{aligned}
&\boldsymbol{u}(\xi,x) = \sum_{i=1}^{\infty} \boldsymbol{u}^i(x)\Psi_i(\xi), \quad \boldsymbol{u}_I(\xi,x) = \sum_{i=1}^{\infty} \Pi_{\boldsymbol{V}_0^h} u^i(x)\Psi_i(\xi) := \sum_{i=1}^{\infty} u_I^i(x)\Psi_i(\xi),\\
&p(\xi,x) = \sum_{i=1}^{\infty} p^i(x)\Psi_i(\xi), \quad p_I(\xi,x) = \sum_{i=1}^{\infty} \Pi_{W_0^h} p^i(x)\Psi_i(\xi) := \sum_{i=1}^{\infty} p_I^i(x)\Psi_i(\xi),\\
&\boldsymbol{u}_{m,I} = R_m \boldsymbol{u}_I = \sum_{i=1}^{m} u_I^i(x)\Psi_i(\xi), \quad p_{m,I} = R_m p_I = \sum_{i=1}^{m} p_I^i(x)\Psi_i(\xi).
\end{aligned}$$

Theorem 4.3.2. *Assume that the solution of the stochastic Stokes equations satisfies* $\boldsymbol{u} \in L^2(\Gamma) \otimes (\boldsymbol{W}^{2,\infty}(D) \cap \boldsymbol{H}_0^1(D))$, $\operatorname{rot} \boldsymbol{u} \in L^2(\Gamma) \otimes \boldsymbol{H}_0^1(D)$, $p \in L^2(\Gamma) \otimes (H^1(D) \bigcap L_0^2(D))$. *Assume the triangulation is* $\mathcal{O}(h^2)$ *irregular. Let* $(\boldsymbol{u}_I, p_I)$ *be the canonical interpolation of* $(\boldsymbol{u}, p)$, *and* $(\boldsymbol{u}_{m,h}, p_{m,h})$ *be the solution to the discrete problem* (4.2.1). *We have:*

$$\begin{aligned}
&\|\boldsymbol{u}_I - \boldsymbol{u}_{m,h}\|_{L^2(\Gamma)\otimes \boldsymbol{V}_0^h} + \|p_I - p_{m,h}\|_{L^2(\Gamma)\otimes L^2(D)}\\
&\lesssim h|\log h|^{1/2}\|\boldsymbol{u}\|_{L^2(\Gamma)\otimes \boldsymbol{W}^{2,\infty}(\Omega)} + h\|\operatorname{rot} \boldsymbol{u}\|_{L^2(\Gamma)\otimes \boldsymbol{H}^2(D)} + h\|p\|_{L^2(\Gamma)\otimes H^1(D)}\\
&+ \inf_{\boldsymbol{v}\in P_{m-1}(\Gamma)\otimes \boldsymbol{H}^2(D)} \|\boldsymbol{v} - \operatorname{rot} \boldsymbol{u}\|_{L^2(\Gamma)\otimes L_0^2(D)} + \inf_{q\in P_{m-1}(\Gamma)\otimes L_0^2(D)} \|q - p\|_{L^2(\Gamma)\otimes L_0^2(D)}.
\end{aligned}$$

Proof. We expand the solution $\boldsymbol{u}_{m,h}$ and $p_{m,h}$ as:

$$\boldsymbol{u}_{m,h}(\xi,x) = \sum_{i=1}^{m} \boldsymbol{u}_{m,h}^i(x)\Psi_i(\xi), \quad p_{m,h}(\xi,x) = \sum_{i=1}^{m} p_{m,h}^i(x)\Psi_i(\xi).$$

According to the definitions and the boundedness of $\nu(\xi)$, we obtain:

$$
\begin{aligned}
& A_h(\boldsymbol{u}_{m,h} - \boldsymbol{u}_{m,I}, \boldsymbol{v}_{m,h}) \\
=& E[(\boldsymbol{f}, \boldsymbol{v}_{m,h})] - B(\boldsymbol{v}_{m,h}, p_{m,h}) - A_h(\boldsymbol{u}_{m,I}, \boldsymbol{v}_{m,h}) \\
=& E[\nu(\xi) \cdot (\operatorname{curl} \operatorname{rot} \boldsymbol{u}, \boldsymbol{v}_{m,h})] \\
& - E[\nu(\xi) \cdot (\operatorname{rot}_h \boldsymbol{u}_{m,I}, \operatorname{rot}_h \boldsymbol{v}_{m,h})] - E[(p - p_{m,h}, \operatorname{div} \boldsymbol{v}_{m,h})] \\
=& E[\nu(\xi) \cdot (\operatorname{rot} \boldsymbol{u} - \operatorname{rot}_h \boldsymbol{u}_{m,I}, \operatorname{rot}_h \boldsymbol{v}_{m,h})] \\
& + E[\nu(\xi) \cdot (\operatorname{curl}(I - Q_h) \operatorname{rot} \boldsymbol{u}, \boldsymbol{v}_{m,h})] - E[(p - p_{m,h}, \operatorname{div} \boldsymbol{v}_{m,h})] \\
\leq& \nu_{max} E[(\operatorname{rot} \boldsymbol{u} - \operatorname{rot}_h \boldsymbol{u}_{m,I}, \operatorname{rot}_h \boldsymbol{v}_{m,h})] \\
& + \nu_{max} E[(\operatorname{curl}(I - Q_h) \operatorname{rot} \boldsymbol{u}, \boldsymbol{v}_{m,h})] - E[(p - p_{m,h}, \operatorname{div} \boldsymbol{v}_{m,h})] \\
:=& \nu_{max} I_1 + \nu_{max} I_2 + I_3.
\end{aligned}
$$

To estimate the first part, we apply Lemma 4.3.1 and have:

$$
\begin{aligned}
I_1 &= E[(\operatorname{rot} \boldsymbol{u} - \operatorname{rot}_h \boldsymbol{u}_{m,I}, \operatorname{rot}_h \boldsymbol{v}_{m,h})] \\
&= \sum_{i=1}^{m} (\operatorname{rot} \boldsymbol{u}^i(x) - \operatorname{rot}_h \boldsymbol{u}_I^i(x), \operatorname{rot}_h \boldsymbol{v}_{m,h}^i(x)) \\
&\leq \sum_{i=1}^{m} \| \operatorname{rot} \boldsymbol{u}^i(x) - \operatorname{rot}_h \boldsymbol{u}_I^i(x) \| \| \operatorname{rot}_h \boldsymbol{v}_{m,h}^i(x) \| \\
&\lesssim h |\log h|^{1/2} \sum_{i=1}^{m} \| \boldsymbol{u}^i(x) \|_{2,\infty} \| \operatorname{rot}_h \boldsymbol{v}_{m,h}^i(x) \| \\
&\lesssim h |\log h|^{1/2} \| \boldsymbol{v}_{m,h}(x) \|_{L^2(\Gamma) \otimes \boldsymbol{V}_0^h} \sum_{i=1}^{m} \| \boldsymbol{u}^i(x) \|_{2,\infty}.
\end{aligned}
$$

Applying the standard property of the L^2 projection Q_h that

$$
\|f - Q_h f\| + h|f - Q_h f|_1 \lesssim h^2 |f|_2 \quad \text{for all} \;\; f \in H^2(D),
$$

we obtain the estimate of the second part:

$$
\begin{aligned}
I_2 = E[(\operatorname{curl}(I-Q_h)\operatorname{rot}\boldsymbol{u}, \boldsymbol{v}_{m,h})] &= \sum_{i=1}^{m}(\operatorname{curl}(I-Q_h)\operatorname{rot}\boldsymbol{u}^i(x), \boldsymbol{v}^i_{m,h}(x)) \\
\leq \sum_{i=1}^{m} \|\operatorname{curl}(I-Q_h)\operatorname{rot}\boldsymbol{u}^i(x)\| \|\boldsymbol{v}^i_{m,h}(x)\| &\lesssim h\|\boldsymbol{v}_{m,h}(x)\|_{L^2(\Gamma)\otimes \boldsymbol{V}_0^h} \sum_{i=1}^{m} \|\operatorname{rot}\boldsymbol{u}^i(x)\|_2.
\end{aligned}
$$

Let $\boldsymbol{v}_{m,h} = \boldsymbol{u}_{m,h} - \boldsymbol{u}_{m,I}$, while the differential operator div commutes with the canonical interpolations, i.e., $\Pi_{W_0^h}\operatorname{div}\boldsymbol{u} = \operatorname{div}\Pi_{\boldsymbol{V}_0^h}\boldsymbol{u} = 0$ [72]. Then it is readily verifiable that $\operatorname{div}\boldsymbol{v}_{m,h} = \operatorname{div}\boldsymbol{u}_{m,h} - \operatorname{div}\boldsymbol{u}_{m,I} = 0$, whereupon the third part I_3 disappears. Applying the coercivity of the bilinear form $A_h(\cdot,\cdot)$, and the previous estimates,

$$
\begin{aligned}
&\|\boldsymbol{u}_{m,h} - \boldsymbol{u}_{m,I}\|^2_{L^2(\Gamma)\otimes \boldsymbol{V}_0^h} \leq A_h(\boldsymbol{u}_{m,h} - \boldsymbol{u}_{m,I}, \boldsymbol{u}_{m,h} - \boldsymbol{u}_{m,I}) \\
&\lesssim \|\boldsymbol{u}_{m,h} - \boldsymbol{u}_{m,I}\|_{L^2(\Gamma)\otimes \boldsymbol{V}_0^h} \left[h|\log h|^{1/2} \sum_{i=1}^{m} \|\boldsymbol{u}^i(x)\|_{2,\infty} + h\sum_{i=1}^{m} \|\operatorname{rot}\boldsymbol{u}^i(x)\|_2 \right].
\end{aligned}
$$

From this, we obtain:

$$
\|\boldsymbol{u}_{m,h} - \boldsymbol{u}_{m,I}\|_{L^2(\Gamma)\otimes \boldsymbol{V}_0^h} \lesssim h|\log h|^{1/2} \sum_{i=1}^{m} \|\boldsymbol{u}^i(x)\|_{2,\infty} + h\sum_{i=1}^{m} \|\operatorname{rot}\boldsymbol{u}^i(x)\|_2.
$$

By the triangular inequality, we have:

$$
\|\boldsymbol{u}_{m,h} - \boldsymbol{u}_I\|_{L^2(\Gamma)\otimes \boldsymbol{V}_0^h} \leq \|\boldsymbol{u}_{m,h} - \boldsymbol{u}_{m,I}\|_{L^2(\Gamma)\otimes \boldsymbol{V}_0^h} + \|\boldsymbol{u}_{m,I} - \boldsymbol{u}_I\|_{L^2(\Gamma)\otimes \boldsymbol{V}_0^h}.
$$

To estimate the second term, we have:

$$
\begin{aligned}
\|\boldsymbol{u}_{m,I}-\boldsymbol{u}_I\|^2_{L^2(\Gamma)\otimes \boldsymbol{V}_0^h} &= \sum_{i=1}^{\infty}(\mathrm{rot}_h \boldsymbol{u}^i_{m,I}-\mathrm{rot}_h \boldsymbol{u}^i_I, \mathrm{rot}_h \boldsymbol{u}^i_{m,I}-\mathrm{rot}_h \boldsymbol{u}^i_I)\\
&= \sum_{i=m+1}^{\infty} \|\mathrm{rot}_h \boldsymbol{u}^i_I\|^2 \lesssim \sum_{i=m+1}^{\infty} (\|\operatorname{rot} \boldsymbol{u}^i - \mathrm{rot}_h \boldsymbol{u}^i_I\|^2 + \|\operatorname{rot} \boldsymbol{u}^i\|^2)\\
&\lesssim \sum_{i=m+1}^{\infty} h^2 |\log h| \|\boldsymbol{u}^i(x)\|^2_{2,\infty} + \sum_{i=m+1}^{\infty} \|\operatorname{rot} \boldsymbol{u}^i\|^2\\
&\lesssim \sum_{i=m+1}^{\infty} h^2 |\log h| \|\boldsymbol{u}^i(x)\|^2_{2,\infty} + \|(I-R_m)\operatorname{rot}\boldsymbol{u}\|^2.
\end{aligned}
$$

Combining Lemma 4.3.2, we obtain:

$$
\begin{aligned}
\|\boldsymbol{u}_{m,I}-\boldsymbol{u}_I\|_{L^2(\Gamma)\otimes \boldsymbol{V}_0^h} \lesssim & \sum_{i=m+1}^{\infty} h|\log h|^{1/2} \|\boldsymbol{u}^i(x)\|_{2,\infty}\\
&+ \inf_{\boldsymbol{v}\in P_{m-1}(\Gamma)\otimes \boldsymbol{H}^2(D)} \|\boldsymbol{v}-\operatorname{rot}\boldsymbol{u}\|_{L^2(\Gamma)\otimes L_0^2(D)}.
\end{aligned}
$$

By uniting the two parts, we obtain:

$$
\begin{aligned}
\|\boldsymbol{u}_{m,h}-\boldsymbol{u}_I\|_{L^2(\Gamma)\otimes \boldsymbol{V}_0^h} \lesssim & h|\log h|^{1/2} \|\boldsymbol{u}\|_{L^2(\Gamma)\otimes \boldsymbol{W}^{2,\infty}} + h\|\operatorname{rot}\boldsymbol{u}\|_{L^2(\Gamma)\otimes \boldsymbol{H}^2(D)}\\
&+ \inf_{\boldsymbol{v}\in P_{m-1}(\Gamma)\otimes \boldsymbol{H}^2(D)} \|\boldsymbol{v}-\operatorname{rot}\boldsymbol{u}\|_{L^2(\Gamma)\otimes L_0^2(D)}.
\end{aligned}
$$

To estimate the pressure error, using Lemma 4.2.1, we can choose $\boldsymbol{v}_{m,h} \in Y^m(\Gamma)\otimes \boldsymbol{V}_0^h$, such that

$$
-\operatorname{div}\boldsymbol{v}_{m,h} = p_{m,I}-p_{m,h}, \text{ and } \|\boldsymbol{v}_{m,h}\|_{L^2(\Gamma)\otimes \boldsymbol{V}_0^h} \lesssim \|p_{m,I}-p_{m,h}\|_{L^2(\Gamma)\otimes L_0^2(D)}.
$$

With this $\boldsymbol{v}_{m,h}$, we have:

$$
\begin{aligned}
\|p_{m,I}-p_{m,h}\|^2_{L^2(\Gamma)\otimes L^2(D)} &= B(p_{m,I}-p_{m,h}, \boldsymbol{v}_{m,h})\\
&= B(p_{m,I}, \boldsymbol{v}_{m,h}) + A_h(\boldsymbol{u}_{m,h}, \boldsymbol{v}_{m,h}) - E[(\boldsymbol{f}, \boldsymbol{v}_{m,h})]\\
&= B(p_{m,I}-p, \boldsymbol{v}_{m,h}) + \{A_h(\boldsymbol{u}_{m,h}, \boldsymbol{v}_{m,h}) - E[\nu(\xi)(\operatorname{curl}\operatorname{rot}\boldsymbol{u}, \boldsymbol{v}_{m,h})]\}\\
&:= I_4 + I_5.
\end{aligned}
$$

For the term I_4, because p_I is the L^2 projection of p to the space $L^2(\Gamma) \otimes W_0^h$, we have:

$$I_4 = E[(p_{m,I} - p, \operatorname{div} \boldsymbol{v}_{m,h})] = E[(p_{m,I} - p, p_{m,I} - p_{m,h})] = \sum_{i=1}^{m} (p_I^i - p^i, p_{m,I}^i - p_{m,h}^i) = 0.$$

For the term I_5, we obtain the following estimate by applying Lemma 4.3.1 and the error estimates in [66]:

$$\begin{aligned}
I_5 &\leqslant \nu_{max} E[(\operatorname{rot}_h \boldsymbol{u}_{m,h}, \operatorname{rot}_h \boldsymbol{v}_{m,h}) - (\operatorname{rot} \boldsymbol{u}, \operatorname{rot}_h \boldsymbol{v}_{m,h}) + (\operatorname{curl}(Q_h - I) \operatorname{rot} \boldsymbol{u}, \boldsymbol{v}_{m,h})] \\
&\leqslant \nu_{max} \sum_{i=1}^{m} (\operatorname{rot}_h \boldsymbol{u}_{m,h}^i - \operatorname{rot} \boldsymbol{u}^i, \operatorname{rot}_h \boldsymbol{v}_{m,h}^i) + \sum_{i=1}^{m} (\operatorname{curl}(Q_h - I) \operatorname{rot} \boldsymbol{u}^i, \boldsymbol{v}_{m,h}^i) \\
&\lesssim \|\boldsymbol{v}_{m,h}\|_{L^2(\Gamma)\otimes \boldsymbol{V}_0^h} \sum_{i=1}^{m} (h|\log h|^{1/2} \|u^i\|_{2,\infty} + h\|\operatorname{rot} \boldsymbol{u}^i\|_2) \\
&\lesssim \|p_{m,I} - p_{m,h}\|_{L^2(\Gamma)\otimes L_0^2(D)} \sum_{i=1}^{m} (h|\log h|^{1/2} \|u^i\|_{2,\infty} + h\|\operatorname{rot} \boldsymbol{u}^i\|_2).
\end{aligned}$$

For the third inequality featured in the preceding estimate, we use the standard property of the L^2 projection Q_h.

Combining both I_4 and I_5 leads to:

$$\|p_{m,I} - p_{m,h}\|_{L^2(\Gamma)\otimes L^2(D)} \lesssim h|\log h|^{1/2} \|\boldsymbol{u}\|_{L^2(\Gamma)\otimes \boldsymbol{W}^{2,\infty}} + h\|\operatorname{rot} \boldsymbol{u}\|_{L^2(\Gamma)\otimes \boldsymbol{H}^2(D)}.$$

Using the triangular inequality, we have:

$$\begin{aligned}
\|p_I - p_{m,h}\|_{L^2(\Gamma)\otimes L^2(D)} &\leq \|p_{m,I} - p_{m,h}\|_{L^2(\Gamma)\otimes L^2(D)} + \|p_I - p_{m,I}\|_{L^2(\Gamma)\otimes L^2(D)} \\
&\lesssim \|p_{m,I} - p_{m,h}\|_{L^2(\Gamma)\otimes L^2(D)} + \sum_{i=m+1}^{\infty} (\|p^i - p_I^i\| + \|p^i\|) \\
&\lesssim \|p_{m,I} - p_{m,h}\|_{L^2(\Gamma)\otimes L^2(D)} + \sum_{i=m+1}^{\infty} (h\|p^i\|_1 + \|p^i\|) \\
&\lesssim h|\log h|^{1/2} \|\boldsymbol{u}\|_{L^2(\Gamma)\otimes \boldsymbol{W}^{2,\infty}} + h\|\operatorname{rot} \boldsymbol{u}\|_{L^2(\Gamma)\otimes \boldsymbol{H}^2(D)} \\
&+ h\|p\|_{L^2(\Gamma)\otimes H^1(D)} + \inf_{q\in P_{m-1}(\Gamma)\otimes L_0^2(D)} \|q - p\|.
\end{aligned}$$

□ □

4.4 Efficient Solvers of Stochastic Stokes Equations

In this section, we construct preconditioners and multigrid solvers for the coupled block linear systems (4.2.2). We first reorganize the linear systems and make them more solver-friendly. In fact, after reorganization, each diagonal block corresponds to a deterministic Stokes problem. Based on fast solvers for the deterministic Stokes system developed in [68], we construct block-diagonal and block-triangular preconditioners for use with Krylov subspace iterative methods, such as GMRes and BiCGStab. In addition, we introduce multigrid methods with block Jacobi and block Gauss-Seidel smoothers to solve stochastic Stokes systems.

4.4.1 Reorganization of the Linear System.

Let

$$\begin{aligned}
\vec{U}_i &= (U_{(i-1)N_u+1}, \cdots, U_{iN_u})^t, \\
\vec{P}_i &= (P_{(i-1)N_p+1}, \cdots, P_{iN_p})^t, \\
\vec{F}_i &= (F_{(i-1)N_p+1}, \cdots, F_{iN_p})^t.
\end{aligned}$$

By grouping the velocity gPC coefficients $\vec{U}_i$ with the corresponding pressure gPC coefficients $\vec{P}_i$, (4.2.2) can be reorganized as the following linear system:

$$\tilde{L} := G_1 \otimes \begin{pmatrix} K & 0 \\ 0 & 0 \end{pmatrix} + G_0 \otimes \begin{pmatrix} 0 & W' \\ 0 & 0 \end{pmatrix} + G_0 \otimes \begin{pmatrix} 0 & 0 \\ W & 0 \end{pmatrix},$$

$$
\tilde{L}\begin{pmatrix} \vec{U}_1 \\ \vec{P}_1 \\ \vdots \\ \vec{U}_{N_\xi} \\ \vec{P}_{N_\xi} \end{pmatrix} = \begin{pmatrix} \vec{F}_1 \\ \vec{0} \\ \vdots \\ \vec{F}_{N_\xi} \\ \vec{0} \end{pmatrix}. \tag{4.4.1}
$$

Figure 4.1 and 4.2 compare the different structures of L and $\tilde{L}$.

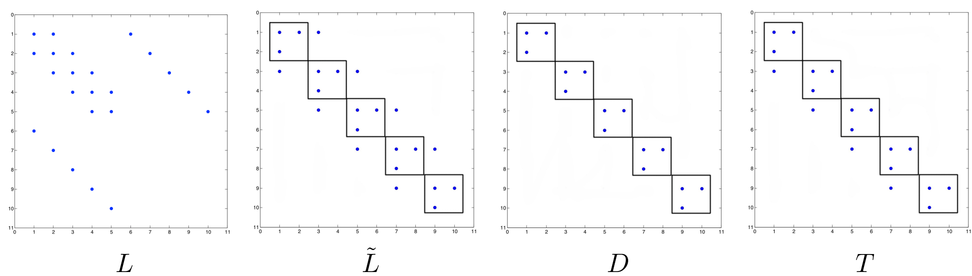

Figure 4.1: The structure of matrices when $N_\xi = 5$, $\nu(\xi) = 1 + 0.5\xi$, where $\xi \sim U(-1, 1)$.

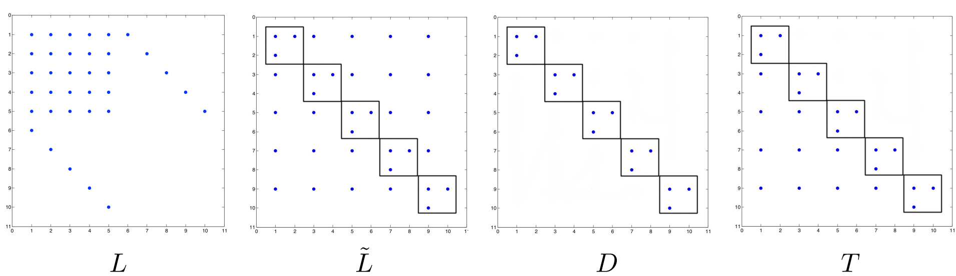

Figure 4.2: The structure of matrices when $N_\xi = 5$, $\nu(\xi) = 1 + e^{1+\xi}$, where $\xi \sim N(0, 1)$.

4.4.2 Block Preconditioners.

Block preconditioners have been shown to perform well for elliptic-type SPDEs [53, 63, 51, 65, 52, 54]. In the following, we propose two block preconditioners for the stochastic Stokes equations. Their efficiency and robustness are demonstrated numerically in Section 4.5.

Block-diagonal Preconditioner.

The block-diagonal part of the reorganized system $\tilde{L}$ is given by:

$$D := \text{diag}\,(G_1) \otimes \begin{pmatrix} K & 0 \\ 0 & 0 \end{pmatrix} + G_0 \otimes \begin{pmatrix} 0 & W' \\ W & 0 \end{pmatrix},$$

where the matrix diag(G_1) is the diagonal part of G_1. Clearly, each 2×2 block corresponds to a discrete deterministic Stokes system (see Figure 4.1 and 4.2). Because these 2×2 block systems are completely decoupled, they can be solved in parallel by existing fast solvers for deterministic Stokes problems. In our study, we apply the optimal multigrid solver using a distributive Gauss-Seidel smoother (see [68]).

Theorem 4.4.1. *The eigenvalues of $D^{-1}\tilde{L}$ are positive real numbers, which belong to the interval*

$$\left[\frac{\min\{\nu_{min}, 1\}}{\max\{\nu_{max}, 1\}}, \frac{\max\{\nu_{max}, 1\}}{\min\{\nu_{min}, 1\}}\right].$$

Proof. Let λ be the eigenvalue, $[\boldsymbol{v}, q]^t$ be the corresponding eigenvector. We have

$$\tilde{L}\begin{pmatrix} \boldsymbol{v} \\ q \end{pmatrix} = \lambda \begin{pmatrix} \boldsymbol{v} \\ q \end{pmatrix},$$

i.e.,

$$\begin{aligned} &\left(G_1 \otimes \begin{pmatrix} K & 0 \\ 0 & 0 \end{pmatrix} + G_0 \otimes \begin{pmatrix} 0 & W' \\ W & 0 \end{pmatrix}\right)\begin{pmatrix} \boldsymbol{v} \\ q \end{pmatrix} \\ &= \lambda\left(\text{diag}\,(G_1) \otimes \begin{pmatrix} K & 0 \\ 0 & 0 \end{pmatrix} + G_0 \otimes \begin{pmatrix} 0 & W' \\ W & 0 \end{pmatrix}\right)\begin{pmatrix} \boldsymbol{v} \\ q \end{pmatrix}. \end{aligned}$$

We can rewrite the above system as following

$$\left((G_1 - G_0) \otimes \begin{pmatrix} K & 0 \\ 0 & 0 \end{pmatrix} + G_0 \otimes \begin{pmatrix} K & W' \\ W & 0 \end{pmatrix}\right) \begin{pmatrix} \boldsymbol{v} \\ q \end{pmatrix}$$
$$= \lambda \left((\text{diag}\,(G_1) - G_0) \otimes \begin{pmatrix} K & 0 \\ 0 & 0 \end{pmatrix} + G_0 \otimes \begin{pmatrix} K & W' \\ W & 0 \end{pmatrix}\right) \begin{pmatrix} \boldsymbol{v} \\ q \end{pmatrix}.$$

Applying $G_0^{-1} \otimes \begin{pmatrix} K & W' \\ W & 0 \end{pmatrix}^{-1}$ on both sides, we have

$$\left(G_0^{-1}(G_1 - G_0) \otimes \begin{pmatrix} K & W' \\ W & 0 \end{pmatrix}^{-1} \begin{pmatrix} K & 0 \\ 0 & 0 \end{pmatrix} + I\right) \begin{pmatrix} \boldsymbol{v} \\ q \end{pmatrix}$$
$$= \lambda \left(G_0^{-1}\,(\text{diag}\,(G_1) - G_0) \otimes \begin{pmatrix} K & W' \\ W & 0 \end{pmatrix}^{-1} \begin{pmatrix} K & 0 \\ 0 & 0 \end{pmatrix} + I\right) \begin{pmatrix} \boldsymbol{v} \\ q \end{pmatrix}.$$

It is easy to verify that the eigenvalues of $\begin{pmatrix} K & W' \\ W & 0 \end{pmatrix}^{-1} \begin{pmatrix} K & 0 \\ 0 & 0 \end{pmatrix}$ is either 1 or 0.

For any $x \in R^{N_\xi}$, we define a function $\varphi(y) = \sum x_i \Psi_i(y)$, then

$$x^t G_1 x = \int_\Gamma \nu(y)\varphi(y)\varphi(y)\rho_\xi(y)dy \geq \nu_{min} \int_\Gamma \varphi(y)\varphi(y)\rho_\xi(y)dy = \nu_{min} x^t G_0 x.$$

$$x^t G_1 x = \int_\Gamma \nu(y)\varphi(y)\varphi(y)\rho_\xi(y)dy \leq \nu_{max} \int_\Gamma \varphi(y)\varphi(y)\rho_\xi(y)dy = \nu_{max} x^t G_0 x,$$

The eigenvalues of diag (G_1) is also bounded by ν_{max} and ν_{min}, because

$$G_1^{(i,i)} = \int_\Gamma \nu(y)\Psi_i(y)\Psi_i(y)\rho_\xi(y)dy \geq \nu_{min} \int_\Gamma \Psi_i(y)\Psi_i(y)\rho_\xi(y)dy = \nu_{min}, \quad \forall i,$$

$$G_1^{(i,i)} = \int_\Gamma \nu(y)\Psi_i(y)\Psi_i(y)\rho_\xi(y)dy \leq \nu_{max} \int_\Gamma \Psi_i(y)\Psi_i(y)\rho_\xi(y)dy = \nu_{max}, \quad \forall i.$$

While the normalized orthogonal polynomials are used, we have $G_0 = I$.

All together, we have

$$\frac{1+\min\{\nu_{min}-1,0\}}{1+\max\{\nu_{max}-1,0\}} \leq \lambda \leq \frac{1+\max\{\nu_{max}-1,0\}}{1+\min\{\nu_{min}-1,0\}}.$$

$\square$

Block-triangluar Preconditioner.

The block-triangular preconditioner T is defined as:

$$T := \text{tril}\,(G_1) \otimes \begin{pmatrix} K & 0 \\ 0 & 0 \end{pmatrix} + G_0 \otimes \begin{pmatrix} 0 & W' \\ W & 0 \end{pmatrix},$$

where the matrix tril(G_1) denotes the lower triangular of G_1. The block-triangular preconditioner system can be solved efficiently by applying blockwise forward substitution and using a fast deterministic Stokes solver to approximately solve each diagonal 2×2 block system.

Theorem 4.4.2. *The eigenvalues of $T^{-1}\tilde{L}$ are positive real numbers, which belong to the interval*

$$\left[\frac{\min\{\nu_{min},1\}}{\max\{\nu_{max},1\}}, \frac{\max\{\nu_{max},1\}}{\min\{\nu_{min},1\}}\right].$$

Proof. The proof is very similar to Theorem 4.4.1, noticing that the eigenvalues of D are the same with those of T. $\square$

4.4.3 Multigrid Method.

In the following, we present a multigrid method using block Jacobi and block Gauss-Seidel smoothers for the stochastic Stokes systems.

We first describe the block Jacobi and block Gauss-Seidel iterations for the system $\tilde{L}\boldsymbol{x} = \boldsymbol{b}$ as follows: let $\boldsymbol{x}_k$ be the previous solution, then $\boldsymbol{x}_{k+1}$ can be computed by

- block Jacobi: $D\boldsymbol{x}_{k+1} = \boldsymbol{b} - (\tilde{L} - D)\boldsymbol{x}_k$
- block Gauss-Seidel: $T\boldsymbol{x}_{k+1} = \boldsymbol{b} - (\tilde{L} - T)\boldsymbol{x}_k$.

The multigrid V-cycle is depicted by the following procedure.

$\boldsymbol{x} \leftarrow Vcycle(\mu_1, \mu_2, \boldsymbol{x}, \boldsymbol{b})$

---

1. Relax μ_1 times on $\tilde{L}\boldsymbol{x} = \boldsymbol{b}$ by block Jacobi or block Gauss-Seidel iteration.
2. Form the fine space residual

$$\boldsymbol{r} = \boldsymbol{b} - \tilde{L}\boldsymbol{x}$$

and restrict the residual to the coarse grid $\boldsymbol{r}^H = Res^H \boldsymbol{r}$.
3. Solve the coarse residual equation

$$\tilde{L}\boldsymbol{e}^H = \boldsymbol{r}^H$$

with one multigrid V-cycle procedure, i.e., $\boldsymbol{e}^H \leftarrow Vcycle(\mu_1, \mu_2, \mathbf{0}, \boldsymbol{r}^H)$.
4. Interpolate the coarse grid correction to the fine grid $\boldsymbol{e} = Pro^H \boldsymbol{e}^H$, and update the fine grid approximation

$$\boldsymbol{x} \leftarrow \boldsymbol{x} + \boldsymbol{e}.$$

5. Relax μ_2 times on $\tilde{L}\boldsymbol{x} = \boldsymbol{b}$ by block Jacobi or block Gauss-Seidel iteration.

4.5 Numerical Experiments

This section demonstrates the performance of the proposed block preconditioners and the multigrid methods with block smoothers applied to the discrete stochastic Stokes equations with random viscosity. All computations are done in the MATLAB package iFEM [13] on a laptop with a 2.4 GHz Intel Core 2 Duo processor and 4 GB of memory. In the following, we select the spacial domain to be the unite square $(0,1) \times (0,1)$. The triangular meshes used in our experiments are obtained by uniform (red) refinement on an initial three-directional structured grid. We consider the following two examples with random viscosity satisfies uniform or lognormal distribution.

Example 1. Let $\nu(\xi) = 2 + \xi$, where ξ is a uniformly distributed random variable, i.e., $\xi \sim U(-1,1)$. The exact solution is given by:

$$\boldsymbol{u}(\xi,x,y) = \begin{pmatrix} -\dfrac{2^8}{2+\xi}(x^2-2x^3+x^4)(2y-6y^2+4y^3)+200xy^3 \\ \dfrac{2^8}{2+\xi}(2x-6x^2+4x^3)(y^2-2y^3+y^4)+50x^4-50y^4 \end{pmatrix},$$

$$p(\xi,x,y) = 10\xi(60x^2y-20y^3-5) - 2^8(2-12x+12x^2)(y^2-2y^3+y^4).$$

Example 2. Let $\nu(\xi) = 1 + e^{\xi}$, where $\xi \sim N(0,1)$ is a normal random variable. The exact solution is given by:

$$\boldsymbol{u}(\xi,x,y) = \begin{pmatrix} 200xy^3 \\ 50x^4-50y^4 \end{pmatrix},$$

$$p(\xi,x,y) = e^{\xi}(60x^2y-20y^3-5).$$

In this case, the pressure p is a random function, but the velocity $\boldsymbol{u}$ is deterministic.

In the following, we first verify the convergence rate of the stochastic Galerkin discretization for the Stokes equations with random viscosity. Then, we demonstrate the efficiency and robustness of the proposed preconditioners and multigrid solver with respect to the discretization parameters (e.g., mesh size h, gPC order m) and the variance of the random viscosity. Finally, a benchmark lid-driven cavity problem is examined to show the propagation of uncertainty from random viscosity to the velocity and pressure fields.

4.5.1 Spatial and Stochastic Convergence.

Uniform Distributed Viscosity.

In Figures 4.3 and 4.4, the convergence of the errors of the mean value and variance with respect to the mesh size h is shown when the gPC expansion order is fixed as $m = 4$. The convergence of the errors of the mean velocity in norm $\|\cdot\|_{\boldsymbol{V}_0^h}$ and the mean pressure in L^2 norm are both higher than first order, which is better than the theoretical result in Theorem 4.3.2. Figure 4.4 shows the first order accuracy for the variances of both velocity and pressure in the L^2 norm. We also compute the errors in other different norms for completeness. It is worth noting that the maximum norm of the pressure error does not converge.

To check the error convergence in stochastic space, we fix a small mesh size $h = 1/128$ and observe that before the spatial discretization error starts to dominate the overall error, the solution errors decay exponentially with respect to the gPC expansion order m (see Figure 4.5).

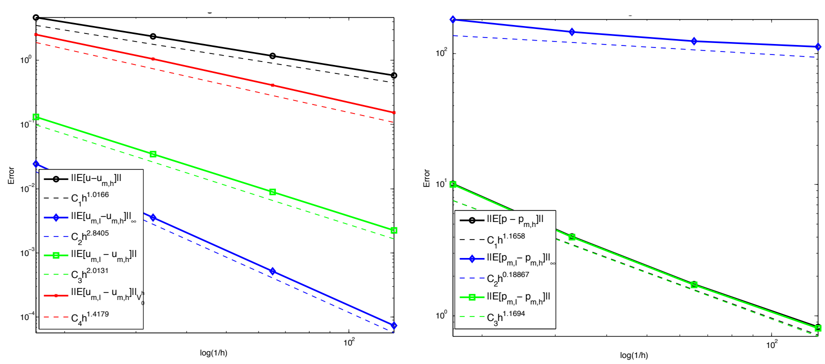

(A) mean value of velocity (B) mean value of pressure

Figure 4.3: The convergence of the mean error with respect to mesh size h ($m = 4$).

Lognormal Distributed Viscosity.

Lognormal random variables are unbounded. Hence, Theorem 4.3.2 does not apply in this case. However, the error convergence rates are similar to those using uniform distributed viscosity (see Figures 4.6, 4.7, and 4.8). Notice that Figure 4.7 shows that velocity variance error is close to the

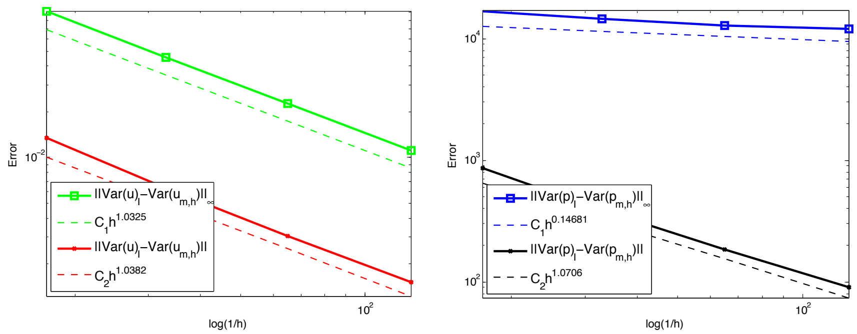

(A) variance of velocity (B) variance of pressure

Figure 4.4: The convergence of the variance error with respect to mesh size h ($m = 4$).

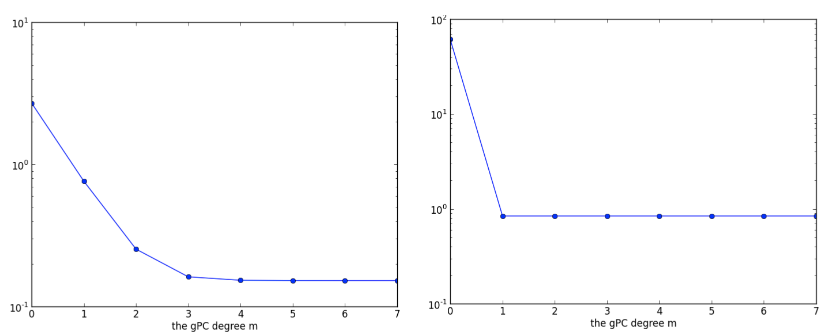

(A) semi-log of $\|\boldsymbol{u}_{m,h} - \boldsymbol{u}_I\|_{L^2_\Gamma \otimes \boldsymbol{V}_0^h}$ (B) semi-log of $\|p_{m,h} - p_I\|_{L^2_\Gamma \otimes \boldsymbol{V}_0^h}$

Figure 4.5: The convergence of the velocity and pressure error with respect to gPC degree m.

machine precision 10^{-16}, and the horizontal line in Figure 4.8 indicates there is no stochastic error for the velocity. These observations are consistent with the fact that velocity is deterministic.

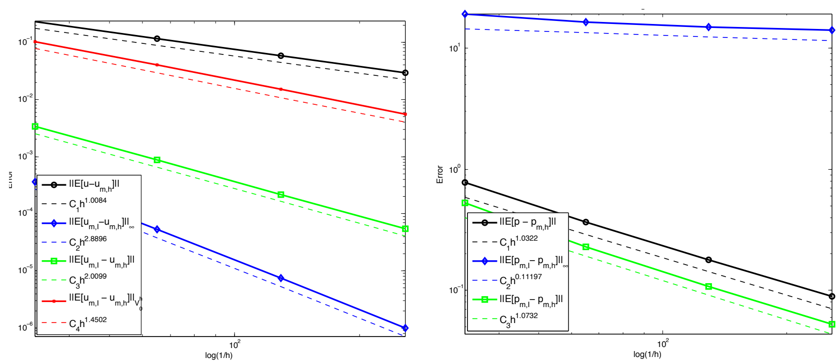

(A) mean value of velocity (B) mean value of pressure

Figure 4.6: Convergence of the mean value with respect to the spatial parameter h.

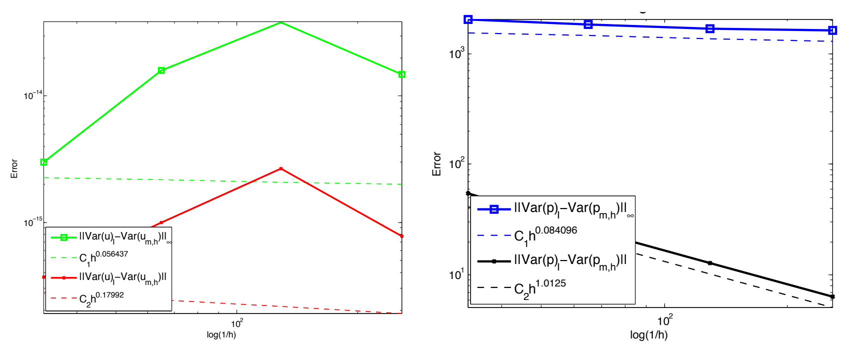

(A) variance of velocity (B) variance of pressure

Figure 4.7: Convergence of the variance with respect to the spatial parameter h.

4.5.2 The Solver Parameters.

We use the preconditioned, preconditioned BiCGStab, and V-cycle multigrid methods to solve the discrete stochastic Stokes systems. The block preconditioner systems and block smoothers are solved approximately using a deterministic W-cycle distributive Gauss-Seidel (DGS) multgird method. Hence, a balance between the inner and outer iterations through the choice of parameters (e.g., tolerance, number of smoothing steps) is important for achieving good overall performance.

In Tables 4.1 and 4.2, we list outer iteration counts, inner iteration counts for solving each block, and the total CPU time for each given inner tolerance ranging from 10^{-1} to 10^{-8}. The star $*$

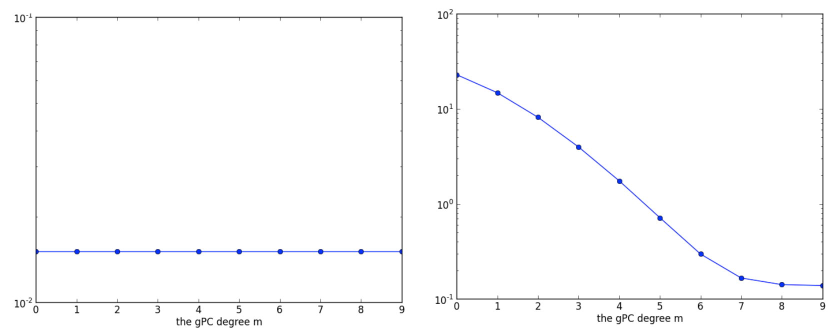

(A) semi-log of $\|\boldsymbol{u}_{m,h} - \boldsymbol{u}_I\|_{L^2_\Gamma \otimes \boldsymbol{V}^h_0}$ (B) semi-log of $\|p_{m,h} - p_I\|_{L^2_\Gamma \otimes \boldsymbol{V}^h_0}$

Figure 4.8: Convergence of velocity and pressure with respect to the gPC degree m.

	inner tol	10^{-1}	10^{-2}	10^{-4}	10^{-8}
M_1	BD	13 2 9.92s	* * *	7 6 9.78s	5 12 10.09s
	BT	7 6 6.48s	* * *	3 6 6.20s	2 12 6.17s
M_2	BD	7.52 9.75s	6.54 10.20s	5 6 9.95s	4.512 15.76s
	BT	4 2 6.12s	3 4 5.46s	2.56 5.64s	0.512 2.07s
M_3	BJ(1)	27 2 28.56s	31 4 43.90s	31 6 79.07s	31 12 143.03s
	BJ(2)	7 2 14.20s	7 4 21.81s	7 6 35.37s	7 12 68.21s
	BJ(3)	7 2 21.78s	5 4 22.56s	4 6 29.21s	4 12 57.18s
	BGS(1)	7 2 8.42s	5 4 8.17s	4 6 10.03s	1 12 5.56s
	BGS(2)	7 2 15.17s	4 4 13.60s	3 6 15.42s	1 12 10.20s

Table 4.1: Legendre polynomial to degree m=4. $h = 1/64$. $\nu(\xi) = 1 + 0.5\xi,\ \xi \sim U(-1, 1)$. M_1: GMRes, M_2: BiCGStab, M_3: V-cycle multigrid.

means the solver diverges or does not reach the tolerance within a maximum number of 100 iterations. The results in these two tables suggest using a relatively large inner tolerance for the block-diagonal preconditioner and block Jacobi smoother, but smaller inner tolerance is better for the block-triangular preconditioner and block Gauss-Seidel smoother. Notice that preconditioned GMRes may fail to converge for certain inner tolerance. The divergence of the V-cycle multigrid with block-Jacobi smoother is mainly due to the large variance of the random variable (addressed in the subsection that follows). We also test the weighted block Jacobi smoother with an under- or over-relaxation parameter, which also fails for the same testing case as in Table 4.2.

	inner tol	10^{-1}	10^{-2}	10^{-4}	10^{-8}
M_1	BD	$*$ $*$ $*$	$*$ $*$ $*$	9 6 12.66 s	7 12 18.64s
	BT	13 2 9.45s	$*$ $*$ $*$	3 6 6.02s	2 12 6.50s
M_2	BD	20 2 22.26s	28 4 43.83 s	14 6 32.20 s	7.5 12 28.97 s
	BT	8 2 9.89s	6 4 9.67s	4 6 9.42s	0.5 12 2.11s
M_3	BJ	$*$ $*$ $*$	$*$ $*$ $*$	$*$ $*$ $*$	$*$ $*$ $*$
	BGS(1)	$*$ $*$ $*$	$*$ $*$ $*$	$*$ $*$ $*$	1 12 5.33s
	BGS(2)	28 2 56.53s	89 4 256.23s	19 6 99.42s	1 12 10.48s
	BGS(3)	9 2 27.70s	7 4 32.23s	4 6 31.94s	1 12 15.36s

Table 4.2: Hermite polynomial to degree m=4. $h = 1/64$. $\nu(\xi) = 1 + e^{\xi}$, $\xi \sim N(0, 1)$. M_1: GMRes, M_2: BiCGStab, M_3: V-cycle multigrid.

4.5.3 Robustness with respect to Discretization Parameters and Variance of Viscosity.

Herein, we investigate the robustness of the two block preconditioners used with the GMRes and BiCGStab methods and the multigrid method with block smoothers in terms of discretization parameters (e.g., spatial mesh size h, gPC degree m) and the variance of $\nu(\xi)$. The outer iterations of these solvers are terminated when the relative error reaches the tolerance 10^{-8}.

Mesh size h.

At each level of the outer multigrid V-cycle, the equations are relaxed twice for the block Jacobi, and once for the block Gauss-Seidel. During the block Jacobi and block Gauss-Seidel iterations, each diagonal block is solved to reach a tolerance of 10^{-1} and 10^{-8}, respectively. This fixed solver parameter setting may not be the best choice for all testing cases. However, we retain the same setting for a clean and tidy presentation.

We fix the gPC expansion order to be $m = 4$. Two different types of random variables, i.e., uniform and lognormal distributed, are tested and presented in Tables 4.3 and 4.4, respectively. The outer iteration counts, the inner iteration counts for solving each block, and the CPU time are listed for each given mesh size. As illustrated by Tables 4.3 and 4.4, the results are robust with respect to h.

	h	1/16	1/32	1/64	1/128
M_1	BD	5 12 2.23s	5 12 3.56s	5 12 9.82s	5 12 32.32s
	BT	1 12 1.60s	2 12 2.25s	2 12 6.31s	1 12 12.50s
M_2	BD	4.5 12 2.78s	4.5 12 5.17s	4.5 12 15.45s	4.5 12 47.82s
	BT	0.5 12 1.43s	0.5 12 0.96s	0.5 12 2.01s	0.5 12 6.53s
M_3	BJ	7 2 2.54s	7 2 4.54s	7 2 14.00s	7 2 44.10s
	BGS	1 12 1.79s	1 12 1.81 s	1 12 5.17 s	1 12 16.15 s

Table 4.3: Legendre polynomial to degree m=4. $\nu(\xi) = 1 + 0.5\xi,\ \xi \sim U(-1, 1)$. M_1: GMRes, M_2: BiCGStab, M_3: V-cycle multigrid.

gPC expansion order m

To investigate the performance of the proposed iterative solvers with respect to the gPC expansion order m, we fix $h = 1/32$. In Table 4.5, the outer iteration counts are listed. The inner iteration counts in this table are ignored because they are similar to those in Table 4.1 $\sim$ 4.4. Clearly, the block-triangular preconditioned GMRes, BiCGStab, and the multigrid solvers are robust with respect to m. As m increases, the outer iteration numbers of the diagonally preconditioned GMRes and BiCGStab increase at the beginning and quickly reach a uniform upper bound.

Variance of viscosity.

Here, we fix both m and h, the mean value of $\nu(\xi)$, and change the variance of $\nu(\xi)$ by changing the parameter a. From Table 4.6, the block-triangular preconditioned GMRes, BiCGStab, and the multigrid solver with block Gauss-Seidel relaxation method are quite robust with respect to the variance of $\nu(\xi)$. The outer iteration numbers of the block-diagonal preconditioned GMRes and BiCGStab also are quite robust in a. However, the multigrid with block Jacobi fails for large a.

According to Tables 4.3$\sim$4.6, the triangluar preconditioner is more robust and efficient than the diagonal preconditioner. Compared to the block Jacobi smoother, the block Gauss-Seidel smoother has better performance in both robustness and efficiency.

	h	1/16	1/32	1/64	1/128
M_1	BD	12 12 4.18s	7 12 6.06s	7 12 16.68s	7 12 54.62s
	BT	1 12 0.578s	2 12 2.29s	2 12 6.07s	2 12 19.56s
M_2	BD	8 12 3.35s	7.5 12 9.65s	7.5 12 29.07s	7.5 12 85.57s
	BT	0.5 12 0.42s	0.5 12 0.67s	0.5 12 2.14s	0.5 12 6.96s
M_3	BJ	* * *	* * *	* * *	* * *
	BGS	1 12 0.68s	1 12 1.87s	1 12 5.26s	1 12 16.34s

Table 4.4: Hermite polynomial to degree m=4. $\nu(\xi) = 1 + e^{\xi}$, $\xi \sim N(0,1)$. M_1: GMRes, M_2: BiCGStab, M_3: V-cycle multigrid.

		$\nu(\xi_1) = 1 + 0.5\xi_1$						$\nu(\xi_2) = 1 + e^{\xi_2}$					
	m	4	6	8	10	12	14	4	6	8	10	12	14
M_1	BD	5	7	9	9	9	9	7	8	12	19	19	19
	BT	2	2	2	2	2	2	2	2	2	2	2	2
M_2	BD	4.5	6.5	8	8.5	8.5	8.5	4	4.5	5.5	6	6.5	7.5
	BT	0.5	0.5	0.5	0.5	0.5	0.5	0.5	0.5	0.5	0.5	0.5	0.5
M_3	BJ	7	7	7	7	7	7	*	*	*	*	*	*
	BGS	1	1	1	1	1	1	1	1	1	1	1	1

Table 4.5: The mesh size $h = 1/32$. $\xi_1 \sim U(-1,1)$. $\xi_2 \sim N(0,1)$. M_1: GMRes, M_2: BiCGStab, M_3: V-cycle multigrid.

.

		$\nu(\xi_1) = 1 + a\xi_1$						$\nu(\xi_2) = 1 + e^{a\xi_2}$					
	a	0.1	0.2	0.4	0.6	0.8	1.0	0.1	0.2	0.4	0.6	0.8	1.0
M_1	BD	5	7	7	7	7	7	5	6	6	6	6	8
	BT	2	2	2	2	2	2	2	2	2	2	2	2
M_2	BD	3.5	4.5	4.5	4.5	4.5	5	7.5	13	21	7.5	7.5	7.5
	BT	0.5	0.5	0.5	0.5	0.5	0.5	0.5	0.5	0.5	0.5	0.5	0.5
M_3	BJ	6	7	7	10	47	*	6	7	23	*	*	*
	BGS	1	1	1	1	1	1	1	1	1	1	1	1

Table 4.6: The gPC order to $m = 4$, the mesh size $h = 1/32$. $\xi_1 \sim U(-1,1)$. $\xi_2 \sim N(0,1)$. M_1: GMRes, M_2: BiCGStab, M_3: V-cycle multigrid.

4.5.4 Lid-driven Cavity Flow Problem.

The classical lid-driven cavity flow problem has been used as a benchmark to test many numerical methods for fluid dynamics. It models incompressible flow in a square domain driven by the motion of the upper lid. In [59], a stochastic lid-driven cavity flow with random boundary condition (i.e., the lid velocity) and fixed constant viscosity is investigated, and the effect of uncertainty on flow fields is demonstrated. Here, we study the stochastic Stokes flow in a lid-driven cavity with random viscosity and deterministic lid velocity.

The computational domain is the unite square $[0, 1] \times [0, 1]$, and the external force is set at zero. The boundary condition for the velocity is $\boldsymbol{u} = (1, 0)^t$ on the top lid and zero everywhere else. The random viscosity is set to be $\nu(\xi) = \nu_0 + \nu_1\xi$, where $\xi \sim U(-1, 1)$ and ν_0, ν_1 are positive numbers chosen such that $\nu(\xi) > 0$. For the spatial discretization, we use the $RT_0 - P_0$ pair on a uniform triangular mesh size $h = 1/128$, and for the stochastic discretization, we use Legendre polynomials of degree $k = 5$. The resulting saddle-point linear systems are solved using the iterative solvers proposed in the previous sections.

For the stochastic Stokes flow with random viscosity ν, and deterministic boundary conditions, the flow velocity field $\boldsymbol{u}$ does not depend on ν and the pressure p depends linearly on ν [62]. Our numerical experiments demonstrate this fact. The variance of the computed velocity field $\boldsymbol{u}$ scales around 10^{-19}, and the mean of the velocity field (Figure 4.9) is the same as the deterministic velocity field obtained by solving Stokes equations with mean viscosity. Moreover, the mean of p depends linearly on ν_0, and the standard deviation of p depends linearly on ν_1 (see Figures 4.11-4.13). Figure 4.10 plots the mean streamline contours for the velocity field, which shows the main eddy in the center and two small Moffatt eddies in the corners.

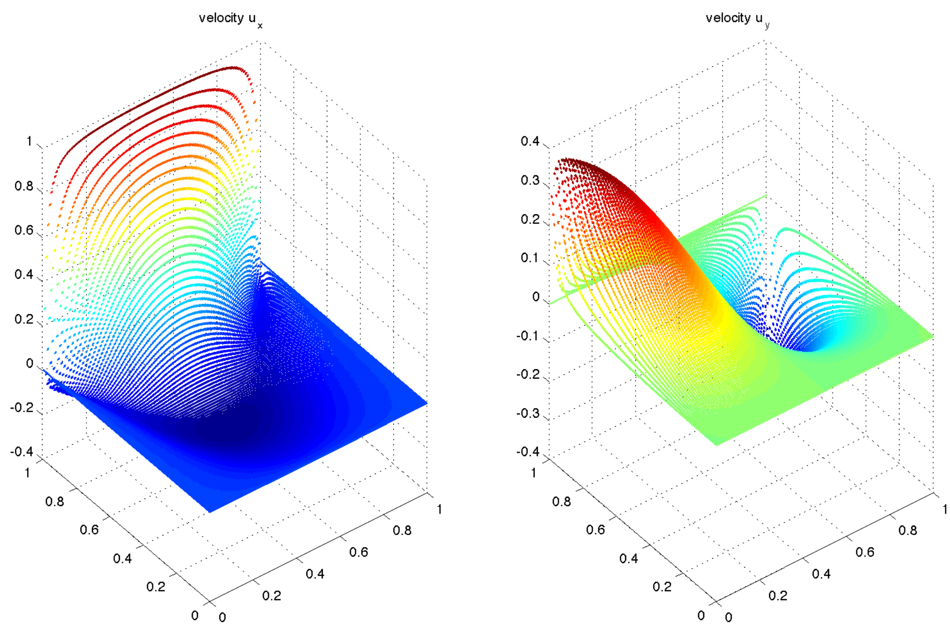

Figure 4.9: The mean value of the numerical velocity.

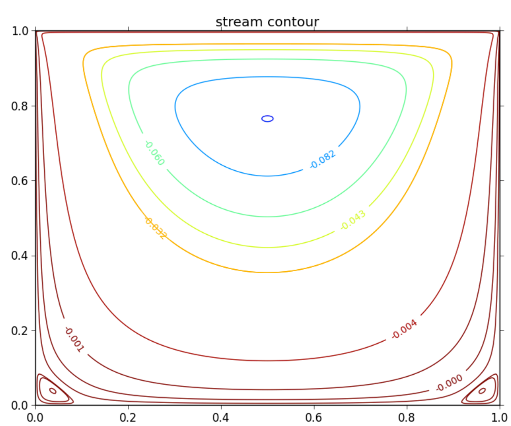

Figure 4.10: The contour of the streamlines.

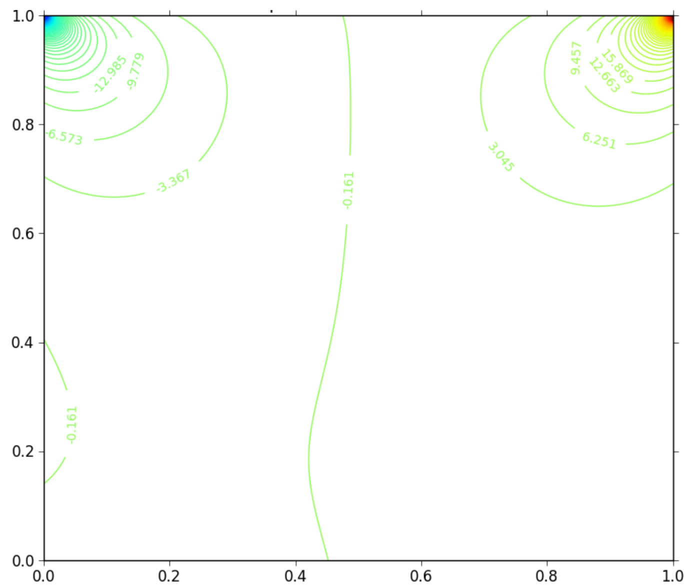

(A) pressure mean

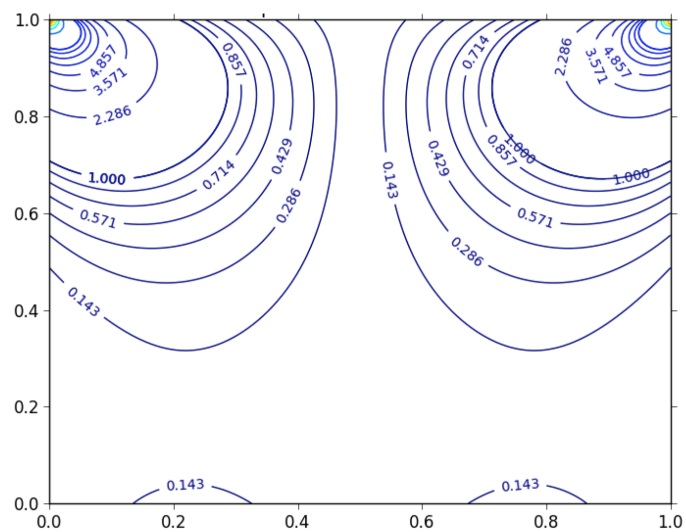

(B) pressure deviation

Figure 4.11: Contours of pressure mean and pressure deviation when $\nu(\xi) = 1 + 0.5\xi$, where $\xi \sim U(-1, 1)$.

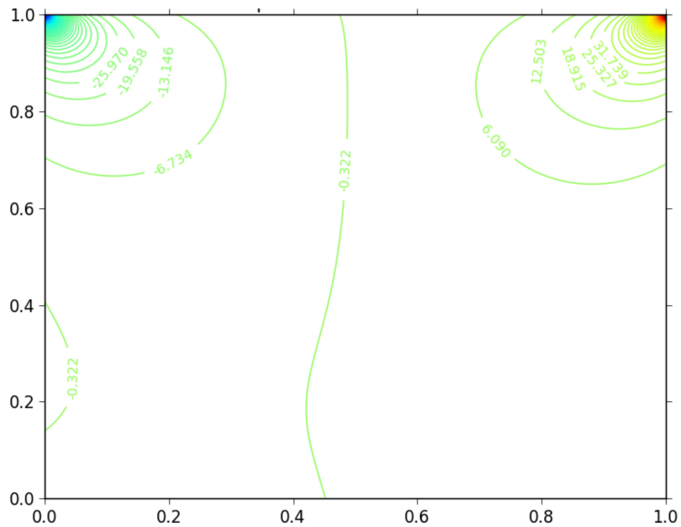

(A) pressure mean

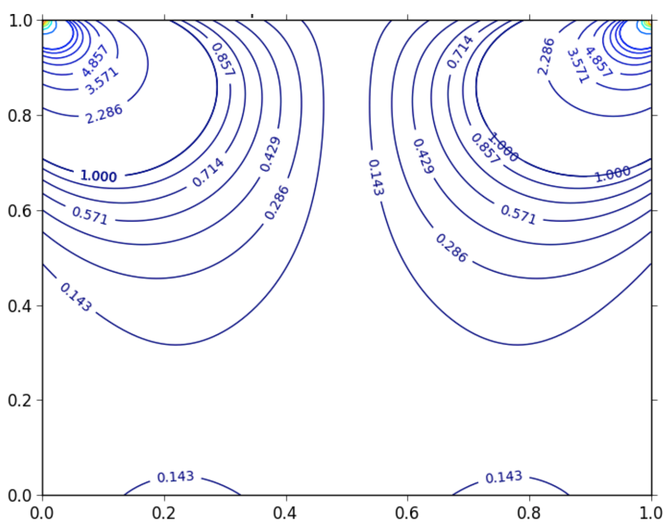

(B) pressure deviation

Figure 4.12: Contours of pressure mean and pressure deviation when $\nu(\xi) = 2 + 0.5\xi$, where $\xi \sim U(-1, 1)$.

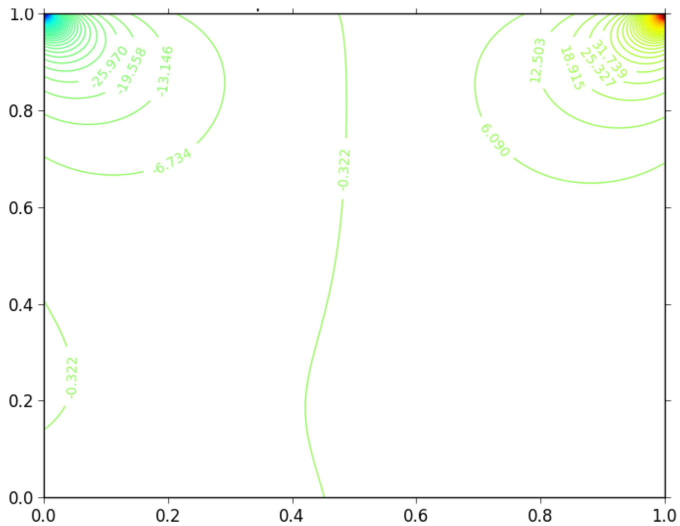

(A) pressure mean

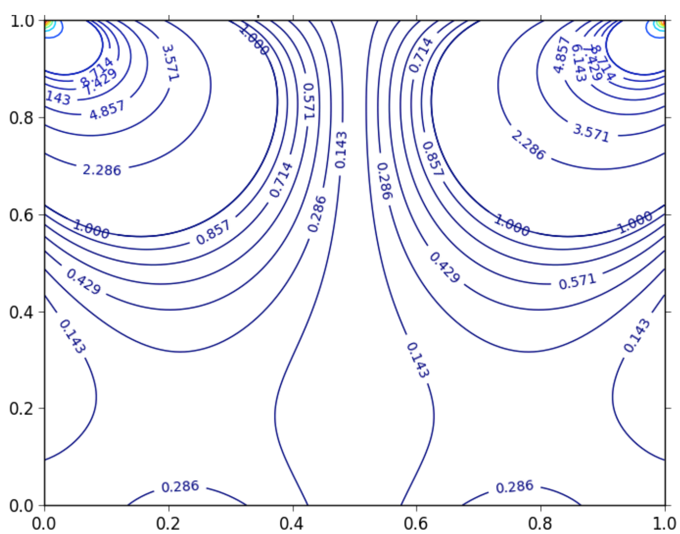

(B) pressure deviation

Figure 4.13: Contours of pressure mean and pressure deviation when $\nu(\xi) = 2 + \xi$, where $\xi \sim U(-1, 1)$.

Bibliography

[1] I. Babuska, J. Osborn, and J. Pitkaranta. Analysis of Mixed Methods Using Mesh Dependent Norms. Mathematics of Computation, 35(152):1039, oct 1980.

[2] D. Arnold, R. Falk, and R. Winther. Finite element exterior calculus, homological techniques, and applications. Acta numerica, 15:1–155, 2006.

[3] D. N. Arnold, R. S. Falk, and R. Winther. Multigrid in H(div) and H(curl). Numer. Math., 85:197–218, 2000.

[4] D. N. Arnold, R. S. Falk, and R. Winther. Finite element exterior calculus: from Hodge theory to numerical stability. Bulletin of the American Mathematical Society, 47(2):281–354, Jan. 2010.

[5] D. N. Arnold, R. S. Falk, and J. Gopalakrishnan. Mixed finite element approximation of the vector Laplacian with Dirichlet boundary conditions. Mathematical Models and Methods in Applied Sciences, 22(09), 2012.

[6] D. N. Arnold, R. S. Falk, J. Guzmán, and G. Tsogtgerel. On the consistency of the combinatorial codifferential. To appear in Transactions of the American Mathematical Society, 2013.

[7] R. E. Bank and J. Xu. Asymptotically exact a posteriori error estimators, part I: Grids with superconvergence. SIAM Journal on Numerical Analysis, 41(6):2294–2312, 2003.

[8] J. H. Bramble, J. E. Pasciak, and J. Xu. The analysis of multigrid algorithms with nonnested spaces or noninherited quadratic forms. Math. Comp., 56:1–34, 1991.

[9] J. H. Bramble, and J. E. Pasciak. The analysis of smoothers for multigrid algorithms.. Math. Comp., 58:467–488, 1992.

[10] F. Brezzi, J. Douglas, R. Duran, and M. Fortin. Mixed finite elements for second order elliptic problems in three variables. Numer. Math., 51:237–250, 1987.

[11] F. Brezzi, J. Douglas, and L. D. Marini. Two families of mixed finite elements for second order elliptic problems. Numer. Math., 47(2):217–235, 1985.

[12] F. Brezzi and M. Fortin. Mixed and hybrid finite element methods. Springer-Verlag, 1991.

[13] L. Chen. iFEM: An integrated finite element methods package in matlab. Technical report, University of California at Irvine, 2009.

[14] L. Chen. Deriving the X-Z Identity from Auxiliary Space Method. In Y. Huang, R. Kornhuber, O. Widlund, and J. Xu, editors, Domain Decomposition Methods in Science and Engineering XIX, pages 309–316. Springer Berlin Heidelberg, 2010.

[15] L. Chen, Y. Wu, L. Zhong, and J. Zhou. MultiGrid Preconditioners for Mixed Finite Element Methods of Vector Laplacian. Submitted for publication.

[16] E. Chow and Y. Saad. Approximate Inverse Preconditioners via Sparse-Sparse Iterations. SIAM Journal on Scientific Computing, 19(3):995–1023, May 1998.

[17] M. Costabel and A. McIntosh. On Bogovskii and regularized Poincare integral operators for de Rham complexes on Lipschitz domains. *Mathematische Zeitschrift*, 265(2):297–320, 2010.

[18] R. G. Duran. An elementary proof of the continunity from L^2_0(Omega) to H_0^1(Omega)^n of Bogovskiis right inverse of the divergence. *REVISTA DE LA UNION MATEM ATICA ARGENTINA*, 2(2):59–78, 2012.

[19] M. Fortin and R. Glowinski. Augmented Lagrangian Methods. Applications to the numerical solution of boundary value problems, North-Holland Publishing Co., Amsterdam, 1983.

[20] R. Hiptmair. Multigrid method for H(div) in Three Dimensions. Electronic Transactions on Numerical Analysis, 6:133–152, 1997.

[21] R. Hiptmair. Multigrid method for Maxwell's equations. SIAM J. Numer. Anal., 36(1):204–225, 1999.

[22] R. Hiptmair. Finite elements in computational electromagnetism. Acta Numer., 11:237–339, 2002.

[23] R. Hiptmair and J. Xu. Nodal Auxiliary Space Preconditioning in H(curl) and H(div) Spaces. SIAM J. Numer. Anal., 45(6):2483–2509, 2007.

[24] K. A. Mardal and R. Winther. Uniform preconditioners for the time dependent Stokes problem. Numerische Mathematik, 98:305–327, 2004.

[25] P. Monk. Finite Element Methods for Maxwell's Equations. Oxford University Press, 2003.

[26] J. C. Nédélec. Mixed finite elements in R^3. Numer. Math., 35:315–341, 1980.

[27] J. C. Nédélec. A new family of mixed finite elements in R^3. Numer. Math., 50:57–81, 1986.

[28] P. A. Raviart and J. Thomas. A mixed finite element method fo 2-nd order elliptic problems. In I. Galligani and E. Magenes, editors, Mathematical aspects of the Finite Elements Method, Lectures Notes in Math. 606, pages 292–315. Springer, Berlin, 1977.

[29] J. Xu. Iterative methods by space decomposition and subspace correction. SIAM Rev., 34:581–613, 1992.

[30] J. Xu and L. Zikatanov. The Method of Alternating Projections and the Method of Subspace Corrections in Hilbert Space. J. Amer. Math. Soc., 15:573–597, 2002.

[31] R. Ghanem, Probabilistic characterization of transport in heterogeneous media, Computer Methods in Applied Mechanics and Engineering 158 (3-4) (1998) 199–220.

[32] R. G. Ghanem, S. Dham, Stochastic finite element analysis for multiphase flow in heterogeneous porous media, Transport in Porous Media 32 (3) (1998) 239–262.

[33] X. Ma, N. Zabaras, A stochastic mixed finite element heterogeneous multiscale method for flow in porous media, Journal of Computational Physics 230 (12) (2011) 4696–4722.

[34] O. P. L. Maître, O. M. Knio, H. N. Najm, R. G. Ghanem, A stochastic projection method for fluid flow: I. basic formulation, Journal of Computational Physics 173 (2) (2001) 481–511.

[35] O. P. L. Maître, M. T. Reagan, H. N. Najm, R. G. Ghanem, O. M. Knio, A stochastic projection method for fluid flow: Ii. random process, Journal of Computational Physics 181 (1) (2002) 9–44.

[36] D. Xiu, D. Lucor, C.-H. Su, G. E. Karniadakis, Stochastic modeling of flow-structure interactions using generalized polynomial chaos, Journal of Fluids Engineering 124 (1) (2001) 51–59.

[37] S. M. Ross, Simulation, 4th Edition, Academic Press, 2006.

[38] M. A. Tatang, W. Pan, R. G. Prinn, G. J. McRae, An efficient method for parametric uncertainty analysis of numerical geophysical models, Journal of Geophysical Research 102 (D18) (1997) 21925–21932.

[39] L. Mathelin, M. Y. Hussaini, T. A. Zang, Stochastic approaches to uncertainty quantification in CFD simulations, Numerical Algorithms 38 (1-3) (2005) 209–236.

[40] I. M. Babuška, F. Nobile, R. Tempone, A stochastic collocation method for elliptic partial differential equations with random input data, SIAM Journal on Numerical Analysis 45 (3) (2007) 1005–1034.

[41] R. G. Ghanem, P. D. Spanos, Stochastic Finite Element: A Spectral Approach, Springer, 1991.

[42] M. K. Deb, I. M. Babuška, J. T. Oden, Solution of stochastic partial differential equations using Galerkin finite element techniques, Comput. Methods Appl. Engrg. 190 (48) (2001) 6359–6372.

[43] I. M. Babuška, R. Tempone, G. E. Zouraris, Galerkin finite element approximations of stochastic elliptic partial differential equations, SIAM Journal on Numerical Analysis 42 (2) (2004) 800–825.

[44] I. M. Babuška, R. Tempone, G. E. Zouraris, Solving elliptic boundary value problems with uncertain coefficients by the finite element method: the stochastic formulation, Computer Methods in Applied Mechanics and Engineering 194 (12-16) (2005) 1251–1294.

[45] J. Bäck, F. Nobile, L. Tamellini, R. Tempone, Stochastic spectral Galerkin and collocation methods for PDEs with random coefficients: a numerical comparison, in: Proceedings of the ICOSAHOM '09 Conference, Vol. 76 of Lecture Notes in Computational Science and Engineering, Springer, Berlin, 2011, pp. 43–62.

[46] H. Elman, C. W. Miller, E. T. Phipps, R. S. Tuminaro, Assessment of collocation and Galerkin approaches to linear diffusion equations with random data, International Journal for Uncertainty Quantification 1 (2011) 19–33.

[47] M. F. Pellissetti, R. G. Ghanem, Iterative solution of systems of linear equations arising in the context of stochastic finite elements, Advances in Engineering Software 31 (2000) 607–616.

[48] H. Elman, D. Furnival, Solving the stochastic steady-state diffusion problem using multigrid, IMA Journal of Numerical Analysis 27 (2007) 675–688.

[49] B. Seynaeve, B. N. E. Rosseel, S. Vandewalle, Fourier mode analysis of multigrid methods for partial differential equations with random coefficients, Journal of Computational Physics 224 (2007) 132–149.

[50] E. Rosseel, T. Boonen, S. Vandewalle, Algebraic multigrid for stationary and time-dependent partial differential equations with stochastic coefficients, Numer. Linear Algebra Appl. 15 (2008) 141–163.

[51] E. Rosseel, S. Vandewalle, Iterative solvers for the stochastic finite element method, SIAM J. Sci. Comput. 32 (2010) 372–397.

[52] B. Sousedík, R. G. Ghanem, E. T. Phipps, Hierarchical Schur complement preconditioner for the stochastic Galerkin finite element methods, preprint (2012).

[53] C. E. Powell, H. C. Elman, Block-diagonal preconditioning for spectral stochastic finite-element systems, IMA Journal of Numerical Analysis 29 (2009) 350–375.

[54] B. Zheng, G. Lin, J. Xu, Block triangular preconditioning for stochastic Galerkin method, http://arxiv.org/abs/1304.1755 (2012).

[55] O. P. L. Maître, A Newton method for the resolution of steady stochastic Navier-Stokes equations, Computers and Fluids 38 (8) (2009) 1566–1579.

[56] O. P. L. Maître, O. M. Knio, Spectral Methods for Uncertainty Quantification: with Applications to Computational Fluid Dynamics, Springer, New York, 2010.

[57] H. Manouzi, T. Theting, Numerical analysis of the stochastic stokes equations of wick type, Numerical Methods for Partial Differential Equations 23 (1) (2007) 73–92.

[58] D. Xiu, G. E. Karniadakis, Modeling uncertainty in flow simulations via generalized polynomial chaos, Journal of Computational Physics 187 (2003) 137–167.

[59] V. A. B. Narayanan, N. Zabaras, Variational multiscale stabilized FEM formulations for transport equations: stochastic advection–diffusion and incompressible stochastic Navier–Stokes equations, Journal of Computational Physics 202 (1) (2005) 94–133.

[60] H. N. Najm, Uncertainty quantification and polynomial chaos techniques in computational fluid dynamics, Annual Review of Fluid Mechanics 41 (2009) 35–52.

[61] D. Qu, C. Xu, Generalized polynomial chaos decomposition and spectral methods for the stochastic Stokes equations, Computer and Fluids 71 (2013) 250–260.

[62] C. E. Powell, D. J. Silvester, Preconditioning steady-state Navier-Stokes equations with random data, SIAM Journal on Scientific Computing 34 (5) (2012) A2482–A2506.

[63] O. G. Ernst, C. E. Powell, D. J. Silvester, E. Ullmann, Efficient solvers for a linear stochastic galerkin mixed formulation of diffusion problems with random data, SIAM Journal on Scientific Computing 31 (2) (2009) 1424–1447.

[64] H. Elman, D. Furnival, C. Powell, H(div) preconditioning for a mixed finite element formulation of the diffusion problem with random data, Mathematics of Computation 79 (270) (2010) 733–760.

[65] C. E. Powell, E. Ullmann, Preconditioning stochastic Galerkin saddle point systems, SIAM Journal on Matrix Analysis and Applications 31 (5) (2010) 2813–2840.

[66] L. Chen, M. Wang, and L. Zhong. ”Convergence Analysis of Triangular MAC Schemes for Two Dimensional Stokes Equations.” Journal of Scientific Computing 63.3 (2014): 716-744.

[67] D. Xiu, G. E. Karniadakis, The Wiener-Askey polynomial chaos for stochastic differential equations, SIAM J. Sci. Comput. 24 (2002) 619–644.

[68] M. Wang, L. Chen, Multigrid methods for the stokes equations using distributive Gauss–Seidel relaxations based on the least squares commutator, Journal of Scientific Computing (2013) 1–23.

[69] B. Øksendal, Stochastic Differential Equations: An Introduction with Applications, 5th Edition, Springer, Berlin, 1998.

[70] V. Girault, H. Lopez, Finite-element error estimates for the mac scheme, IMA journal of numerical analysis 16 (3) (1996) 347–379.

[71] D. Xiu, Numerical methods for stochastic computations: a spectral method approach, Princeton University Press, 2010.

[72] R. Hiptmair, Finite elements in computational electromagnetism, Acta Numerica 11 (0) (2002) 237–339.

[73] Mardal, Kent Andre, Xue-Cheng Tai, and Ragnar Winther. ”A robust finite element method for Darcy–Stokes flow.” SIAM Journal on Numerical Analysis 40.5 (2002): 1605-1631.

[74] Whitaker, Stephen. ”Flow in porous media I: A theoretical derivation of Darcy’s law.” Transport in porous media 1.1 (1986): 3-25.

[75] Haug, Einar, Torgeir Rusten, and Hvard J. Thevik. ”A mathematical model of macrosegregation formation in binary alloy solidification.” Numerical Methods and Software Tools in Industrial Mathematics. Birkhuser Boston, 1997. 157-176.

[76] G. Kanschat and B. Rivière. A strongly conservative finite element method for the coupling of Stokes and Darcy flow. Journal of Computational Physics, 229(17):5933–5943, 2010.

[77] Schoeberl, Joachim. ”Commuting quasi-interpolation operators for mixed finite elements.” (2001).

[78] K. A. Mardal, X.-C. Tai, and R. Winther. A robust finite element method for darcystokes flow. SIAM J. Numerical Analysis, 40(5):1605–1631, 2002.

[79] K. A. Mardal and R. Winther. Uniform preconditioners for the time dependent Stokes problem. Numer. Math., 98:305–327, 2004.

[80] K. Mardal and R. Winther. Preconditioning discretizations of systems of partial differential equations. Numerical Linear Algebra with Applications, 18:1–40, 2011.

[81] K. A. Mardal, J. Schberl, and R. Winther. A uniform inf–sup condition with applications to preconditioning. arXiv preprint arXiv,1201.1513 (2012).

[82] M. A. Olshanskii, J. Peters, and A. Reusken, Uniform preconditioners for a parameter dependent saddle point problem with application to generalized Stokes interface equations. Numerische Mathematik, 105.1 (2006): 159-191.

[83] M. A. Olshanskii. Multigrid analysis for the time dependent Stokes problem. Mathematics of Computation, 5718:1–23, 2011.

[84] X. Xie, J. Xu, and G. Xue. Uniformly-stable finite element methods for Darcy-Stokes-Brinkman models. Journal of Computational Mathematics, 26(3):437–455, 2008.

[85] G. Cohen, P. Joly, J. E. Roberts, and N. Tordjman. Higher Order Triangular Finite Elements with Mass Lumping for the Wave Equation. SIAM J. Numer. Anal., 38(6):2047–2078, 2001.